Republic of Iraq

Ministry of Higher Education

and Scientific Research

University of Babylon

Effect of Geometry on Stability of Diaphragm Cellular Cofferdams

A Thesis

Submitted to the College of Engineering

of the University of Babylon in Partial

Fulfillment of the Requirements

for the Degree of Master

in Water Resources

Engineering

By

Sarmad Hameed Majeed Al-rmmahi

(B.Sc. Civil Engineering)

May 2009

جمهورية العراق

وزارة التعليم العالي

والبحث العلمي

جامعة بابل

تأثيرالخواص الهندسية على استقرارية السدود الخلوية الحجابية

رسالة

مقدمة الى كلية الهندسة-جامعة بابل

كجزء من متطلبات نيل شهادة الماجستير

في هندسة الموارد المائيه

من قبل

سرمد حميد مجيد الرماحي

(بكالوريوس هندسة مدنية)

أيار 2009

بسم الله الرحمن الرحيم

وَمِنْ آيَاتِهِ أَنَّكَ تَرَى الْأَرْضَ خَاشِعَةً فَإِذَا أَنزَلْنَا
اهْتَزَّتْ وَرَبَتْ إِنَّ الَّذِي أَحْيَاهَا لَمُحْيِي الْمَوْتَى إِنَّهُ
عَلَى كُلِّ شَيْءٍ قَدِيرٌ

صدق الله العلي العظيم

- سورة فُصِّلَتْ - الآية (36)

REFERENCES

APPENDIX (A)

الخلاصة

في هذه الدراسة تمت دراسة استقرارية السدود الخلوية الحاجزةباستخدام طريقتين هي الفحص المختبري وبرنامج (PLAXIS).حيث تم اجراء سلسلة من الفحوصات المختبرية على نماذج خلايا حجابية ثنائية (Diaphragm) وبنسب عرض/ ارتفاع مختلفة (0.75, 0.85, 1.0) تضمنت هذه الفحوصات دراسة العوامل التي تؤثر على استقرارية السدود الخلوية وهي: تأثير العرض والارتفاع وخواص التربة وكذلك عمق الدفن تحت سطح الارض, ويكون عمق الغرز حسب نسبة الارتفاع/ عمق الغرز والتي هي (0.15 ,0.3, 0.45) وتم ذلك بأستخدام اربعة انواع من الترب وهي السبيس و الرمل المار من غربال رقم 4 و الرمل النهري و الطين الرملي.

وبعد ذللك تم الاعتماد على النتائج التي حصلنا عليها من المختبربطريقة التحليل الاحصائي للحصول على اربعة معادلات تمثل العلاقة بين التشوهات (الازاحة) وعمق الغرز بعد تسليط الاحمال على النموذج.

ثم تم تحليل النماذج بطريقة العناصر المتناهية بأستخدام برنامج (PLAXIS) لحساب التشوهات والاجهادات والنفعال داخل جسم السد والاساس, ومن ثم مقارنة النتائج التي حصلنا عليها من البرنامج وتلك النتائج التي حصلنا عليها من الفحوصات المختبرية.

من الاستنتاجات التي تم التوصل اليها في هذه الدراسة هي ان مقدار التحمل في حالة الانقلاب اكبر من مقدار التحمل في حالة الانزلاق, وان الزيادة في عمق الغرز وخواص التربة وجدت انها تؤثر على استقرارية المنشاءات الخلوية, حيث ان قيمة الازاحة في السدود الخلوية الموضوعة على سطح الارض تساوي 3.72 ملم من الفحص المختبري وان قيمة التشوه من خلال البرنامج (PLAXIS) هي تساوي 3.22 ملم , والازاحة للسدود الخلوية في حالة غرز السد في التربة هي 3.21 ملم من الفحص المختبري وان قيمة التشوه من خلال البرنامج (PLAXIS) هي 2.61 ملم , ان الفرق بمقدار الازاحة بين الطريقتين قليل وعليه يمكن الاعتماد على نتائج البرنامج (PLAXIS) للحصول على قيم التشوهات.

Examining Committee Certificate

We certify that we have read this thesis entitled **"Effect of Geometry on Stability of Diaphragm Cellular Cofferdams",** and as an examining committee, examined the student **"Sarmad Hameed Majeed Al-Rammahi"** in its contents and what related to it, and that in our opinion it meets the standard of a thesis for the degree of Master of Science in Civil Engineering in field of specialization is **Water Resources Engineering**.

Signature:

Name: **Asst. Prof. Dr. Jaafar S. Maatooq**
(Member)
Date: / /2009

Signature:

Name: **Asst. Prof. Dr. Abdul-Hassan K. Al-Shukur**
(Member)
Date: / /2009

Signature:

Name: **Asst. Prof. Kadhim N. Al-Ta'ee**
(supervisor)
Date: / /2009

Signature:

Name: **Asst. Prof. Dr. Kareem R. Al-Murshidi**
(Chairman)
Date: / /2009

Approval of Civil Engineering Department

Signature :

Name: Prof. Dr. Ammar Y. Ali
Head of the Civil Engineering Department.
Date: / /2009

Approval of Deanery of the College of Engineering.

Signature :

Name: Prof. Dr. Adil A. Alwan
Dean of the College of Engineering.
Date: / /2009

Appendix A

Table (A-1): Comparison of the deformation observed and PLAXIS software, with (b/H) =1.0

Soil type	Applied load KN/m	Effective stresses KN/m²	Shear stress KN/m²	Horizontal stress KN/m²	Shear strain %
Subbase	0.94	-22.6	7.17	-10.46	5.4
Sand passing No.4	0.77	-20.04	4.7	-13.14	1.2
River sand	0.63	-16.78	3.9	-11.14	1.04
Sandy clay	0.56	-13.9	2.95	-8.6	1.08

Table (A-2): Comparison of the deformation observed and PLAXIS software, with (b/H) =0.85

soil type	Applied load KN/m	Effective stresses KN/m²	Shear stress KN/m²	Horizontal stress KN/m²	Shear strain %
Subbase	0.68	-19.13	5.12	-8.7	3.23
Sand passing No.4	0.56	-16.97	4.17	-15.03	1.27
River sand	0.44	-14.6	3.73	-13.22	1.01
Sandy clay	0.48	-13.29	4	-10.07	0.85

Table (A-3): Comparison of the deformation observed and PLAXIS software, with D/H=0.3

soil type	Applied load KN/m	Effective stresses KN/m²	Shear stress KN/m²	Horizontal stress KN/m²	Shear strain %
Subbase	0.75	-23.4	11.4	-21.97	2.38
Sand passing No.4	0.69	-20.55	9.9	-19.02	2.6
River sand	0.55	-16.97	8.03	-15.82	2.22
Sandy clay	0.62	-17.37	7.44	-14.20	3.66

Table (A-4): Comparison of the deformation observed and PLAXIS software, with D/H=0.15

soil type	Applied load KN/m	Effective stresses KN/m²	Shear stress KN/m²	Horizontal stress KN/m²	Shear strain %
Subbase	0.62	-19.8	10.8	-16.26	3.32
Sand passing No.4	0.58	-18.4	9.5	-16.3	3.2
River sand	0.43	-14.6	7.2	-13	2.63
Sandy clay	0.51	-14.22	7.6	-12.3	4.24

List of References

*** Al-Chalabi, K. T. [1959]:** "Stability of cellular cofferdams". Ph. D.Thesis, College of Engineering, University of Michigan, U.S.A.

*** Al-Khyatt, H.S. [2009]:** "Design sheet pile cellular structures cofferdams and retaining structures". M. Sc. thesis, College of Engineering, University of Babylon.

*** Alizadeh, M. M. [1973]:** "Circular land cofferdam for deep excavation". J. Construction, ASCE, Vol. 99, No.GT1, pp. 11-20.

*** Al-Taee, K.N. [1990]:** "Effect of geometry on stability of cellular cofferdams". M. Sc. thesis, College of Engineering, University of Baghdad.

*** Bowles, J. E. [1997]:** "Foundation analysis and design". McGraw-Hill, New York, U.S.A.

*** Brinkgreve, R.B.J, and Vermeer, P.A.[2008**] " Plaxis-finite element code for soil and rock analysis-Version 8.2, A.A. Balkema Publishers, Netherlands.

*** Burki, Naveed K. and Richards, R. Jr. [1975]:** "Photoelastic analysis of a cofferdam". J. Geotech., ASCE, Vol. 101, No. GT2, pp.129-145.

*** Cummings, E. M. [1957]:** "Cellular cofferdams and docks". Proceedings, ASCE, Vol. 83, No. WW3, pp. 13-45.

*** Dismuke, T. D. [1975]:** "Foundation engineering handbook". Litton educational publishing Inc., New York, U.S.A.

*** Esrig, M. I. [1970]:** " Stability of cellular cofferdams against vertical shear". J. Soil Mechanics and foundation, ASCE, Vol. 96, No. 6, pp. 1853-1862.

*** Horiuchi, S. , Taketsuka, M. , Takuro, O., and Kawasaki, H. [1992]:** "Fly-Ash slurry island: I. theoretical and experimental investigations". J. Materials. ASCE, Vol. 4, Paper No.2, pp. 117-133.

* **Kelly, P. B. [1969]:** "Design and evaluation of a foundation model testing device". M. Sc. Thesis, Oregon State University,U.S.A.

* **Krynine, D. P. [1945]:** "Discussion of stability and stiffness of cellular cofferdams". ASCE, Vol. 110, Paper No.2253, pp. 1175-1178.

* **Lacroix, Y., Esrig, M. I., and Lusher, U. [1970]:** "Design, construction, and performance of cellular cofferdams". ASCE, pp. 271-328.

* **Maitland, J. K., and Schroeder, W. L. [1979]:** "Model study of circular sheetpile cells". J. Geotech. Div., ASCE, Vol. 105, Paper No. GT7, pp. 805-821

* **Ovesen, N.K. [1962]:** "Cellular cofferdams, calculation methods and model tests". The Danish geotechnical institute, Copenhagen.

* **Polivka, J. J. [1945]:** "Discussion of stability and stiffness of cellular cofferdams by K. Terzaghi". Transactions, ASCE, Vol. 110, pp. 1170-1187.

* **Rossow, Mark P. [1984]:** "Sheetpile interlock tension in cellular cofferdams". J. Geotech., ASCE, Vol. 110, No. GT10, pp. 1446-1458.

* **Schroeder, W. L. Marker. D. K. and Khuayjarempanishk, T. [1977]:** "Performance of a cellular wharf". J. Geotech. Eng. Div., ASCE, Vol. 103, No. GT3, pp. 153-168.

* **Schroeder, W. L. and Maitland, J. K. [1979]:** "Cellular bulkhead and cofferdams". J. Geotech, ASCE, Vol. 105, No. GT7, pp. 823-837.

* **Sorota, Max. D. and Kinner, Edward B. [1981]:** "Cellular cofferdam for trident drydock: Design". J. Geotech. Div., ASCE, Vol. 107, No. GT12, pp. 1643-1655.

* **Swatek, E. P. [1967]:** "Cellular cofferdams design and practice". J. Wtrwys. and Hrbrs. Div., ASCE, Vol. 93, pp. 109-132.

* **Thomas, Harry E., Speaker, John J., and Miller, Eugene J. [1975]:** "Difficult dam problems - Cofferdam failure". J. Geotech, ASCE, Vol.45, No.GT8, pp. 66-70.

* **Teng, W. C. [1962]:** "Foundation design". Prentic hall, Inc., Englewood cliffs N. J. .

* **Terzaghi, K. [1945]:** "Stability and stiffness of cellular cofferdams". Transactions, ASCE, Vol. 110, pp. 1083-1202.

* **TVA (Tennesse Valley Authority) [2003]:** "Steel sheetpile cellular cofferdams on rock". Technical monograph 75, Pilebuck edition, U.S.A.

* **USACE (U.S.Army Corps of Engineers) [1989]:** "Design of sheetpile cellular structures". Engineering manual No. 1110-2-2503, Department of the army, Washington.

* **USS (United State Steel). [1970]:** "USS sheetpiling design manual". www.eng-tips.com**.**

* **White, A. , Cheney, J. A. , and Duke, M. [1963]:** "Field study of cellular bulkhead". Transactions, ASCE, Vol. 128, pp. 463-508.

* **الدكتور ابراهيم عبيدو, 1985.** " هندسة الموانئ والمنشآت البحرية" دار الراتب الجامعية, بيروت, لبنان

List of Contents

List of Figures

Supervisor Certificate

I certify that the preparation of this thesis entitled **"Effect of Width to Depth Ratio on Stability of Cellular Cofferdams"** was prepared by **"Sarmad Hameed Majeed Al-Rammahi"** under my supervision at Babylon University in partial fulfillment of the requirements for the degree of Master of Science in Civil Engineering with field of specialization in Water Resources Engineering.

Signature:

Name: **Asst. Prof. Kadhim Naief Kadhim Al-Ta'ee**

(Supervisor)

Date: / /2009

List of Symbols

symbols	***Notations***	***units***
b	Equivalent Width of the Cell	mm
C1,C2	Coefficient	-
C3	Coefficient	mm/KN
d	Driving depth of cellular	mm
D	Embedment Depth	m
E	Young's Modules	KN/m2
E1,E2	External Earth Pressure	KN/m2
F	Load Failure	KN
F1,F2	External Earth Pressure	KN/m2
F.S	Factor of Safety	-
f	Coefficient of Friction of Cell Fill	-
f_{ss}	The Coefficient of Friction of Steel on Steel	-
H	Height of the Cell	m
ha	Height of the Active Side	m
h	Height of Cellular cofferdam	mm
k	Coefficient of Lateral Earth Pressure	-
K_a	Active Earth Pressure	-
L	Length of the Cellular Cofferdam	mm
M	Moment Due to External Force	KN.m
M_{max}	Maximum Resisting Moment	N.m/m

Symbols	***Notations***	***Units***
M_r	Resisting Moment	KN.m
M_o	Overturning Moment	KN.m
M_t	Total Resisting Moment	KN.m
N	Component (Normal to the Chord)of Internal Forces in Rupture-Circle	KN
N_s	Stability Number	-
P	Lateral Load	N
P_a	Active Pressure	N/m2
P_p	Passive Pressure	N/m2
q	Distance from Foot of Wall to line of Action of Exterior Force on Cellular Cofferdam	m
R	Radius of Diaphragm and Cloverleaf Cell	mm
r	Radius of Circular Cell	mm
R^2	Square Regression	-
S_1, S_2	Shearing Resistance Along the Center of the Cell	N/m
T	Component (parallel to the chord) of Internal Forces in Rupture-Circle	KN
t	Interlock Tension	N/m2
t_{max}	Maximum Interlock Tension	N/m2
V	Variance Explained	-
V_{max}	Maximum Vertical Shear stress	N
y	height of Lateral Load Above the Ground Surface	m

Symbols	***Notations***	***Units***
y_{cr}	Critical Height	m
W	Effective Weight of Cell Fill	N
γ	Unit Weight of the Soil	N/m3
δ	Friction Angle Between the Fill and the Sheetpile	degree
△	Deformation in Cofferdam	mm
ø	Angle of Internal Friction of Soil	degree

List of Tables

Dedication

To my wife

To my family

To my real friends

To all people who love me and all that I love deeply

ACKNOWLEDGEMENT

"In The Name of ALLAH, the Compassionate, the Merciful"

Many thanks and praise are due first of all and above all to my Creator, almighty **ALLAH,** most beneficent, most gracious and most merciful who gave me the ability and the desire to complete this research work despite of all the hurdles and constraints in the way of its completion.

Special thanks are presented for my country, **IRAQ,** with deepest wishes for a greatest land and greatest people to stay in peace forever.

I wish to express my cordial thanks and deepest gratitude towards my supervisor, **Asst. Prof. Kadhim N. Al-Ta'ee,** for his appreciated guidance, encouragement, valuable advice, inspiration, and constant help.

I am indebted to the laboratory of soil mechanics in engineering college in Babylon University for helping me to achieve my work in this search.

Sincere thanks are expressed to **Bauhaus-University Weimar** in Germany especially for **Prof. Dr. Tom Schanz** in helping me in software work.

Sincere thanks are presented to my family for their patience and support. Finally, a special acknowledgment is expressed to all my friends who helped, encouraged and supported me.

Sarmad Hameed Al-Rammahi

2009

ABSTRACT

In this study the stability of cellular cofferdams is studied by using two methods; test models and software which is known Plaxis. Series of laboratory tests have been carried out on two diaphragm cells of different width to depth ratios (0.75, 0.85, and 1). The tests include the following factors. These factors are effect of width, height, properties of soil and embedment depth to height ratios (0.15, 0.3, and 0.45). Four type of soil ware used. These types are subbase, sand passing sieve No.4, and river sand and sandy clay soil.

Reliability of results which obtained from experimental tests have been conducted using statistical analysis to formulate these results by four functions are created to computes the deformations. The functions represent the relation between the deformations and the embedment depths that occurred after applied load.

Then, the analysis of cellular cofferdam by software PLAXIS finite element code was done to compute the deformations, stresses, and strain in the body of cofferdam and foundation. The results have been compared between the laboratory tests and these which resulting from PLAXIS.

The load capacity in overturning failure has been found greater than sliding failure. The, increasing of the embedment depth and properties of good soil has been found more affecting the stability of cells. Thus, the displacement for the cellular cofferdam placed on ground surface in the laboratory test is equal to 3.72mm and the displacement obtained from PLAXIS is equal to 3.22mm. The displacement of cofferdam with embedment depth in laboratory test is equal to 3.21mm and the displacement from software PLAXIS is equal to 2.61mm. Therefore, the different between two methods is very small and PLAXIS software prediction of lateral displacement for cellular cofferdam acceptable as compared with laboratory test.

CHAPTER ONE

INTRODUCTION

CHAPTER TWO

LITERATURE REVIEW

CHAPTER THREE

TYPES OF THE CELLULAR COFFERDAM, APPARATUS, MATERIALS, TESTING PROCEDURE AND PROGRAM

CHAPTER FOUR

RESULTS AND DISCUSSION

CHAPTER FIVE

ANALYSIS OF CELLULAR COFFERDAM BY PLAXIS

CHAPTER SIX

CONCLUSIONS AND RECOMMENDATION

Chapter one
Introduction

1.1- General

There are many construction projects are executed inside the water such as piers of bridges or weirs, and close to water such as docks. Such execution is relatively difficult because of the expected seepage of water unless the area of construction is protected against the water.

There are many ways of such a protection. One of these ways is by using a temporary structure, called cofferdam. A cofferdam serves through surrounding the area of construction to prevent the water from access. One of the most type of cofferdams is the cellular cofferdam.

A cellular cofferdam is a gravity retaining structure formed from the series of interconnected straight web steel sheet pile cells filled with soil usually sand, gravel or clay. The interconnection provides water-tightness and self-stability against the lateral pressure of water and earth **[Bowles, (1997)]**.

The purpose of the cofferdam is to retain a hydrostatic head of water or to provide a lateral support to the mass of soil behind it. However, the cofferdam is subjected to unbalanced lateral forces acting at different heights. These unbalanced forces will tend to produce a resultant moment which tends to overturn the cofferdam or to produce a resultant force which tends to slide the cofferdam on its base. The resisting forces and moments against the sliding and overturning vary in magnitude from soil to soil depending on the unit weight, the coefficient of friction of the soil, Young's Modulus of elasticity, poison's ratio, and cohesion **[Bowles, (1997)]**.

The cellular cofferdam was first developed as a temporary structure to exclude water from an excavation and allow construction in the dry. It is now used with increasing frequency as either a temporary or permanent structure

retaining soil, water, or both. Cellular cofferdams are used lie of earth or rock fill cofferdams when the width of the structure must be small, when a vertical face is required, or when stability against scour is required. Permanent cellular cofferdams are performing well as dock walls, piers, and retaining walls **[Bowles, (1997)]**.

Meanwhile, a cellular cofferdam is usually constructed of steel sheet piles and used primarily as a water-retaining structure. However, its stability depends on the interaction of the soil used to fill the cell and the steel sheet piling, whereas either material, if used alone, would be unsatisfactory. Both materials in combination provide a satisfactory means to develop a dry work area in water-covered sites such as construction projects areas close to ocean, lakefront, or a river. One of the most common shapes of a cellular cofferdam is the diaphragm.

1.2- Objective of the Present Study

The main objective of this study is to design a more stable diaphragm cellular cofferdam (materials and dimensions) to withstand sliding and overturning, analysis of the same cellular cofferdam by software PLAXIS and using Statistica software to create equation deal with three variables are (D) , (F) and (δ), embedment depth , load failure and deformation respectively.

1.3- Methodology of the Research

The methodology of research can be summarized as follows:

1- The laboratory tests have been conducted to diaphragm cellular cofferdams with different width to depth ratio.

2- The tested models were built with different types of soil**,** to finding the best case which offers the more resistance against sliding and overturning forces will be found.

3- Determination the effect ratio of embedment depth to height on stability of cofferdam.

4- By using the statistical analysis, the reliabilities of the laboratory results may be presented.

5- Analysis of the same cellular cofferdam by software PLAXIS and the comparison of the results between laboratory testing and PLAXIS will be done.

Chapter Two
Literature Review

2.1- General

A cellular cofferdam is a structure built in place, consisting of a series of cells connected to each other, made of steel sheet-piles, filled with soil to furnish stability, for the purpose of retaining a hydrostatic head of water or to provide a lateral support to the mass of soil behind it. It could be used either as a temporary or permanent structure.**[Al-Chalabi, (1959)].**

Cellular cofferdams are made of steel sheet-pile driven into the soil in the form of an enclosure of cells. These cells are connected to each other forming a continuous line of cells. The cells are filled with soil material which should be well consolidation.

Cofferdams, in their simplest form, were found in ancient times. The Mesopotamian Rivers, for example, were edged in many places with wooden box cofferdams filled with soil to protect the land from the floods. Beside the simplicity of the structure they were basically functioning to retain a hydrostatic head of water. **[Al-Chalabi, (1959)].**

The first cellular cofferdam was built in the United States of America in 1908-1909 at Black Rock Harbor, Buffalo, New York. This cofferdam was a rectangular type and it consisted of 70 cells of (9×9 m). It was built on rock foundation. The outer and inner walls of this cofferdam bulged. This idea led Major-General Harley B. Ferguson, Corps of Engineers, U.S. Army to use the circular cells in constructing the cofferdam for raising the battleship; **[Al-Chalabi, (1959)].**

The first circular cofferdam was built in 1910 for raising the battleship Maine in the harbor of Havana, Cuba. This cofferdam was the circular type. The

cells were filled with clay and rested on a stratum of soft silt and clay. Under this stratum was a stratum of medium clay.

The first diaphragm type cellular cofferdam was built Troy, New York. It was built for constructing Troy´s Dam and Lock. In this cofferdam the inner and outer walls of the cofferdam were arcs; **[Al-Chalabi, (1959)].**

Then fourteen cofferdams were built by the Tennessee Valley Authority (TVA) for their various projects. The first of these projects requiring cellular cofferdams was the Pickwick Landing Dam. In this case a circular type was used, it was successful and economical, since then the circular type was adopted by the TVA in all the Tennessee River projects; **[TVA, (2003)].**

2.2-Theoretical Studies

Pennoyer, (1934) attempted to solve the design problems of cofferdams theoretically from calculation method was intended primarily for safety against total overturning or sliding of the cofferdam. For this purpose the cofferdam was regarded as a rigid box, which, when acted upon by its gravity force and an external force , will either turn about its lower rear edge or slide along its base. Pennoyer also advanced methods for calculation of the internal stability, i.e. for calculation of the tensile stresses in the cofferdam's sheet walls.

Pennoyer´s methods were subsequently further developed by Jacoby and Davies (1941).

Terzaghi, (1945) introduced an entirely new calculation method. He pointed out that before a cellular cofferdam fails by overturning or sliding, it will probably have failed already because of a shear rupture in the central vertical plane of the fill. Terzaghi determined accordingly the factor of safety as the ratio of the shear resistance in the central plane to the shear force in the same plane . The shear resistance here was due to the fill and the transverse sheet wall, and the sheer force was due to the external water pressure. He found that

reasonable agreement between his theory and practical experience was obtained when the earth pressure factor in the vertical central plane was assumed to be (0.4 – 0.5).

Hansen, J. Brinch, (1958) introduced a calculation method based on rupture-figure which, unlike all formerly applied rupture-figure, is kinematically and statically possible. He assumed the formation of a circular was either convex or concave, line-rupture between the feet of the sheet walls. In the state of failure the whole mass of earth above the circle was rotate about the center of the circle as one rigid body. The cofferdam´s stability problem was solved by calculation according to either the equilibrium method, using all three conditions of equilibrium for the earth (including the walls) above the rupture-circle, or the extreme-method by which the rupture-line was approximated by a logarithmic spiral.

2.3- Laboratory Studies

A popular approach to investigate the behavior of cellular structures has been explained through model studies. In general, these studies have consisted of relatively small scale models loaded to failure. Cell stability, i.e., determination of the force or moment required for failure, has been of primary concern.

Polivka, (1945) involved a series of tests on a five-cell model of cofferdam during Polivka preliminary investigation on cellular cofferdams in the Kaiser shipyards at Richmond, California. The testing set-up consisted of five circular cells, (75mm, 100mm, 125mm, 150mm, and 175 mm) in diameter, (150 mm) high and arranged in an arc shaped wall. The cell walls consisted of a continuous cylinder, made from (0.1 mm) thick sheet metal. In this study, Polivka attempted to correlate the model test results with field data and Terzaghi’s theory of vertical shear. The auther found that the coefficient of earth

pressure decreased with an increase of H/R ratio, where H is the height and R is the radius of the cell, and the total resistance against slippage increased with increasing the radius.

Cummings, (1957) contained the results of Cummings model studies of cofferdams on rock. It is probably the best known model study and forms the basis for his theory of internal cell failure by horizontal shear. Cummings' model consisted of (612.5 mm) diameter, (600 mm) high circular cells and equivalent rectangular cells with (487.5 mm× 612.5 mm). Wood staves, (7.8 mm× 37.5 mm), were used as model sheetpiles. These staves were held together by a thin wire threaded through screw-eyes located at the top, middle, and bottom of the sheetpiles. Each cell was threaded together loosely, with little contact between the wood staves, so that very little friction could be developed between model sheetpiles. All the cells rested on a rough concrete base (25 mm) thick. The fill consisted of crushed rock. Lateral loads were applied by a wire loop at (⅓ H) [where (H) is the height of the cell]. Cable loads were measured with proving rings. Cummings was also concerned with the change in the state of stress in the fill resulting from lateral loads. Pullout tests of wood staves buried in the cell fill were conducted before and after application of the lateral load to provide data for calculation of the aforementioned stresses in the fill.

The author found that pullout tests conducted on laterally loaded cells indicated an increase in lateral pressure occurred within the cell fill at the loaded side of the cell, he found that the plane of rupture goes from the top of the pressure side to the bottom inner corner (toe of cofferdam). The cell fill in the rupture region acts essentially as a surcharge and only the soil below the failure plane will develop shear resistance, as shown in Fig. (2-1).

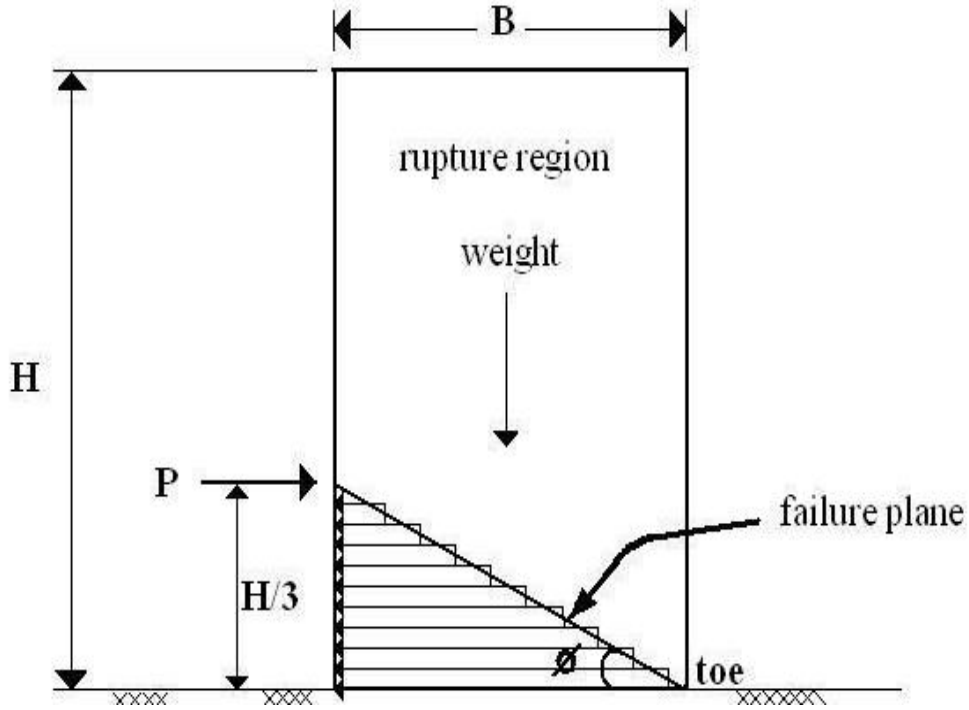

Fig. (2-1): Cell fill resistance to lateral force (After Cummings, 1957)

Ovesen, (1962) has made model tests for determination of the rupture-loads and deformations of cellular cofferdams were carried out in two different model setups, called the large and small model . Most of the tests (in a number of about 70) were made with cellular cofferdams in the small model, the rest(about) were made the cellular cofferdams in the large model . In the large model the cofferdam is built up of three circular cells with a diameter of (72cm), in the small of four circular cells with a diameter of (20cm). The tests with cellular cofferdams constructed on a layer of soil proved that the rupture-load and the deformations varied with the fill´s density, the cofferdam´s width-height ratio, and its driving depth. The tests with cellular cofferdams constructed on rock surface proved that the rupture-load and the deformations varied with fill´s density and the cofferdam´s width height ratio. The model tests of cellular

cofferdams were supplemented by a series of tests of double sheet-wall structure in a two-dimensional mechanical-analogy model.

Burki et al., (1975) developed a method to determine elastic stresses inside the soil mass of a cofferdam by using photoelastic technique. A cofferdam model was fabricated simulating the soil mass with gelatin and the steel sheet piles with urethane rubber. This model was tested in a state of plain strain, and, from the photoelastic data, elastic stresses within the fill material were found due to both gravity loading and water pressure. In the gravity loading case, normal stresses agreed with the standard theory of soil mechanics for geostatic stresses. Water pressure introducing bending was found to affect the stresses appreciably causing a nonlinear distribution of stresses and pressure on the base of the cofferdam. Contrary to many theories, shear stresses were found to be higher near the sheet pile walls than the midplane. New failure surfaces, in accordance with the elastic stress state, were postulated.

Maitland and Schroeder, (1979) performed a series of model tests. The process involved four large model circular cells and three smaller cells. The larger models consisted of a single circular cell (1225 mm) in diameter and constructed of 58 interlocking sheet piles and two connecting arcs (525 mm) in diameter, each constructed with 12 sheet piles. Total sheet piles lengths from (1200 mm to 1800 mm) with embedment depth below the dredgeline ranging from (0 mm to 600 mm). The smaller cells were (600 mm) in diameter. The proportions of embedment depth to cell height corresponded to those used for the larger cells.

Uniformly graded sub angular sand was used during the study. Loads were applied incrementally and continued until large cell deflections had occurred by a steel cable loop (200*100 mm). Timber was used as a loading yoke. Deflections of the front sheets, sheet pile strains, and cable force were monitored throughout cell failure. The model test results were related to field

data and with Terzaghi's theory of vertical shear. Terzaghi found that the ultimate overturning capacity of the model cellular structures was best predicted by:

$$M\max = \tfrac{1}{3}\gamma * b * k * H^2 * (\tan\phi + f) \qquad (2\text{-}1)$$

Where:

$M\max =$ maximum resisting moment, $(\frac{N.m}{m})$

$\gamma =$ weighted effective unit weight of cell fill, $(\frac{N}{m^3})$

$b =$ equivalent width of cell, (m)

$k =$ coefficient of lateral earth pressure,

$H =$ height of cell, (m)

$\phi =$ angle of internal friction of cell fill, and

$f =$ coefficient of interlock friction for sheetpiles.

Al-Taee, (1990) studied the design and construction of cellular cofferdams through test models to observe their stability. Series of laboratory tests have been carried out on one, two, and three diaphragm cells of different width to depth ratios, as well as a rectangular and an isolated circular cell. The tests included the study of the following factors: effect of height, width, length, embedment depth, and loading height, additional tests were carried out on an instrumented diaphragm cell to determine the distribution of the bending moments and hoop tensions.

Many conclusions had been drawn from this study. Among these were the sliding resistance dose not affected by the length of cell while the length is pronounsly alters the overturning resistance.

Horiuchi et al., (1992) studied the construction of a man-made island using a cofferdam and fill which problems are often encountered, such as sliding failures of a soft seabed or ruptures of the cofferdam. A new filling method,

underwater placement of light and self hardening slurry, presents great advantages that were confirmed by theoretical analysis. Appropriate slurry for this new method, containing fly ash, volcanic ash, and a small amount of cement, was developed from experimental investigations. This light, self-hardening slurry greatly reduces the earth pressure and increases the safety factor of the island, and it also makes subsequent construction work easier. Strength development of the slurry is inhibited by low temperature, but this can be compensated for by a small increase in the cement content. Practical slurry compositions were also proposed based on laboratory studies, which included test-tank tests. It was concluded that underwater placement of fly-ash slurry was practical method for man-made island construction.

2.4: Field Studies

White et al., (1963) contained the results of a comprehensive field investigation of a 33- circular cell bulkhead at pier E in Long Beach Harbor, California. Tests were conducted on bulkheads (18.6 m) in diameter with connecting arcs (4.87 m) in radius and retain a (16.5 m) height of fine silty sand fill. Sheet piles were instrumented to measure hoop stress in the steel. Piezometers and settlement plates were used to observe the generation of pore water pressure and settlements in the fill. The deflections of sheet piles were measured by a drift meter. The free water level in the cell and tidal fluctuations were also monitored. From this study it was found that the maximum hoop tension occurred at level 4 as shown in Fig. (2-2), approximately at the original ground level. The coefficient of lateral earth pressure was found to be equal to (0.66) during the filling of the cell, dropped to (0.54) shortly after the cell was filled, and to (0.53) two years after construction; the soil in the cell required 10 days after completion of filling to reach approximately (90%) consolidation.

Schroeder et al., (1977) performed investigation on 12-cell wharf at Terminal No.4 along the Willamette River in Portland, Oregon. Fig. (2-3), shows the general layout of the project. Individual cells are (19.74 m) in diameter, spaced (25.74 m) center to center, a freestanding height of (20.1 m), and connecting arcs which have a radius of (4.32 m). Vibrating wire strain gages were used to monitor strains at four elevations on eight different sheet piles as Shown in Fig. (2-3). besides, inclinometer casings were attached to the outside Instrumented sheet piles to measure horizontal deformations, while land-based surveys measured cell crest movement and sheet pile settlement during construction. The free water level in the cell was also monitored and compared with the adjacent river level. From this study it was found that the maximum interlock force in the cell was also near the dredge line and the lateral earth pressure values recommended by Terzaghi are adequate for design.

Sorota and Kinner, (1981) presented a description of design of a steel sheet pile cellular cofferdam that was required for construction of a graving dry-dock. The cofferdam was constructed approximately (168 m) offshore within the Hood Canal of Washington State and was required to retain (24 m) of water after basin dewatering. Interlock tensions associated with the required cell diameter in this deep water location resulted in one of the first United States cofferdam applications of high strength steel sheet piling and extruded wye connections. Much of the cofferdam was designed to be permanent to provide in-service laydown areas adjacent to the completed drylock. Items discussed include the need for two pumped dewatering systems, the need for vibratory probe compaction of the cell fills, site soil conditions, dredging, and steel sheet pile corrosion protection.

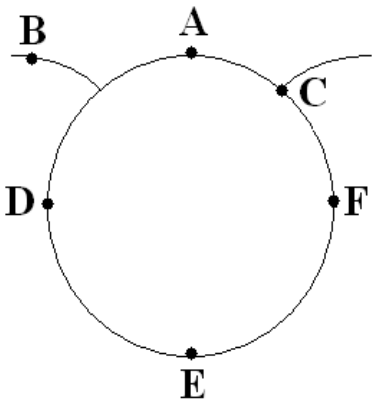

(a) Location of instrumented sheetpiles

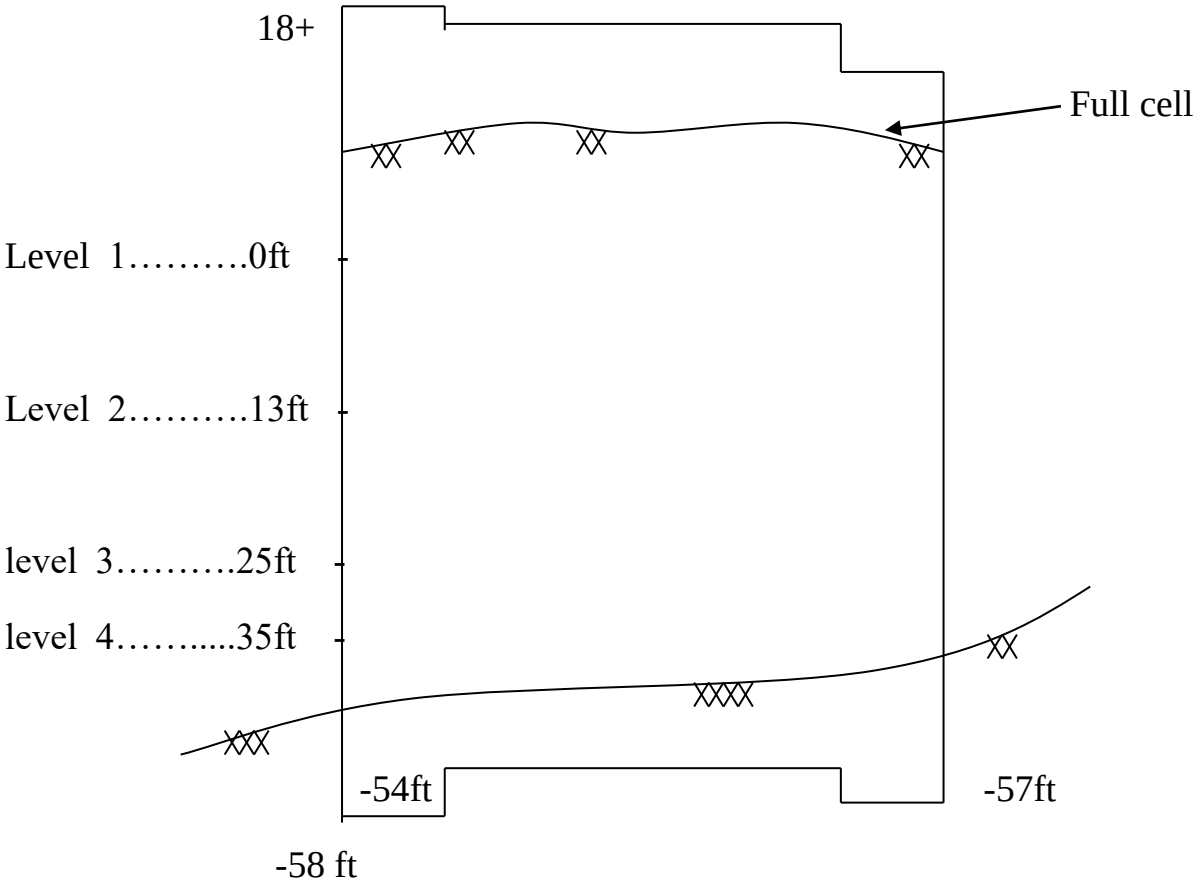

(b) Cell profile

Fig. (2-2): Long beach cell [After White et at., (1963)]

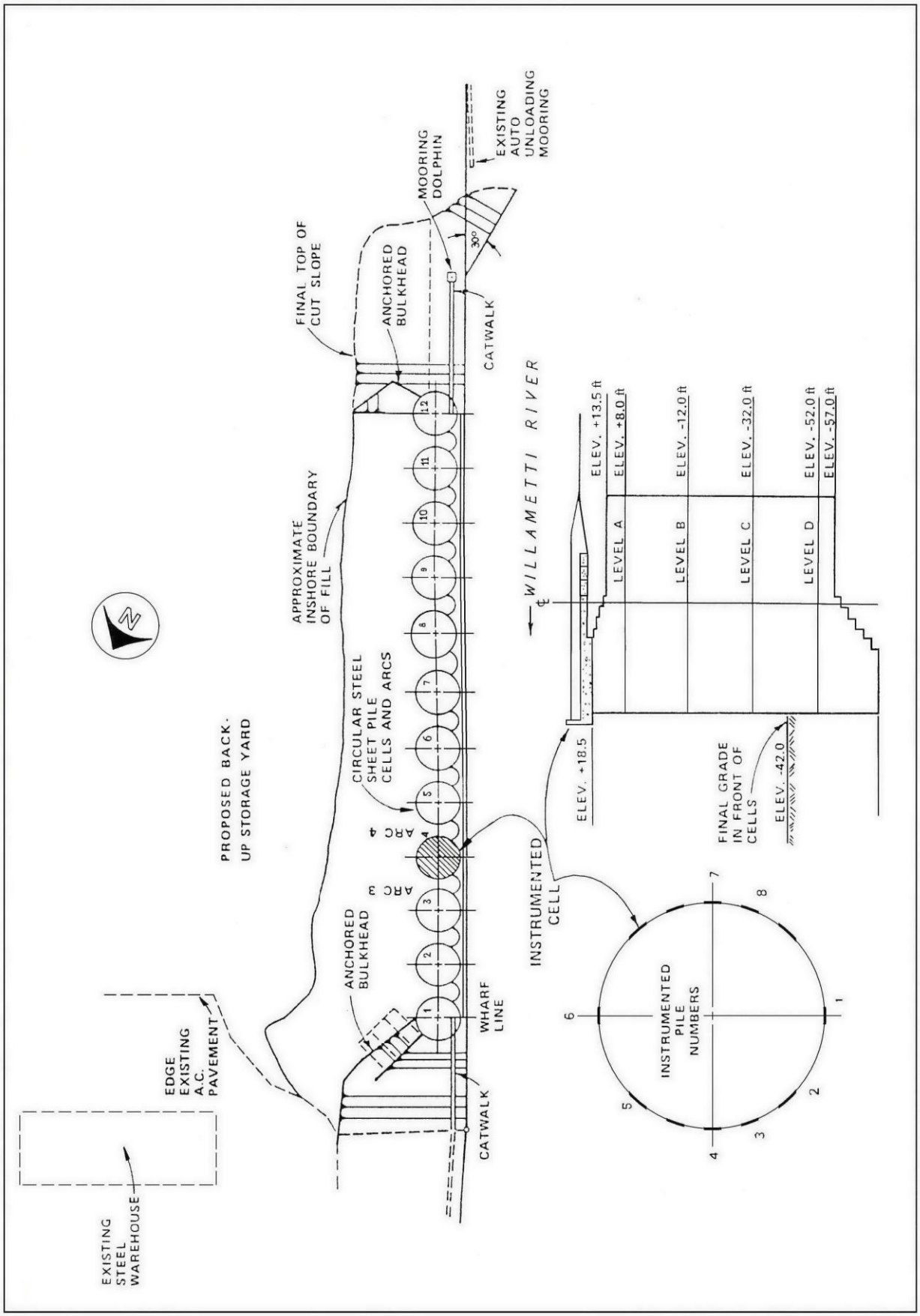

Fig. (2-3): Terminal No.4 [After Schroeder et al., (1977)]

Schroeder and Maitland, (1979) made field and laboratory research on cellular sheet pile structures. Design for both internal stability and overall stability were considered. It was proposed that for cellular bulkheads embedded in sands, neither sliding nor overturning can occur before a cell fails by tilting in the vertical shear mode. Guides for interlock force analysis and selection of lateral earth pressure coefficients for a newly proposed vertical shear model were given.

Thomas et al., (1975) studied the failure that happened in the cofferdam around the Uniontown locks and dam on the Ohio River, ten days after dewatering the project area during a rising river period. The configuration of the failure in the highly faulted shale foundation occurred as a block transition, sliding horizontally on relatively soft underclay. There were no relief drains within the cofferdam nor piezometers to monitor uplift forces. The design of the pier foundation was changed from open cut on three shales to drilled caissons on the most competent of the three shales.

Chapter Three

Types of the Cellular Cofferdams, Apparatus, Materials, Testing Procedure and program

3.1: General

The cellular cofferdams depend for stability on the interaction of the soil used to fill the cell and the steel-sheet-piling. Either material used alone is unsatisfactory; both materials in combination provide a satisfactory means to develop a dry work area in water-covered sites such as ocean or lakefront or river area construction projects.

3.2: Types of the Cellular Cofferdams

There are three general types of cellular cofferdams, each depends on the weight and strength of the fill for its stability, the typical arrangement of the three type of cells, shown in Fig. (3-1).

3.2.1: Circular cells

This type consists of a series of complete circular cells connected by shorter arcs, these generally intercept the cells at a point making an angle of 30 or 45 degrees with the longitudinal axis of the cofferdam. The circular type cell with connecting arcs was adopted for the first steel sheet pile cellular cofferdam built by TVA at Pickwick Dam in 1935, the same type was also used for all subsequent cofferdam construction on the main Tennessee River. The primary advantages of circular cells are that each cell is independent of the adjacent cells; it can be filled as soon as it is constructed, and it is easier to form by means of templates, **[TVA, (2003)].**

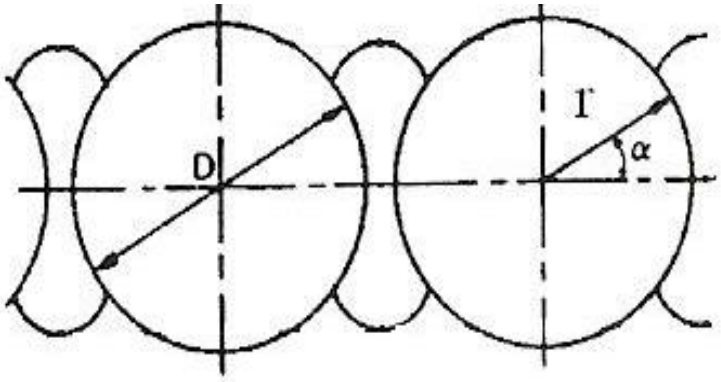

(a) CIRCULAR CELLS

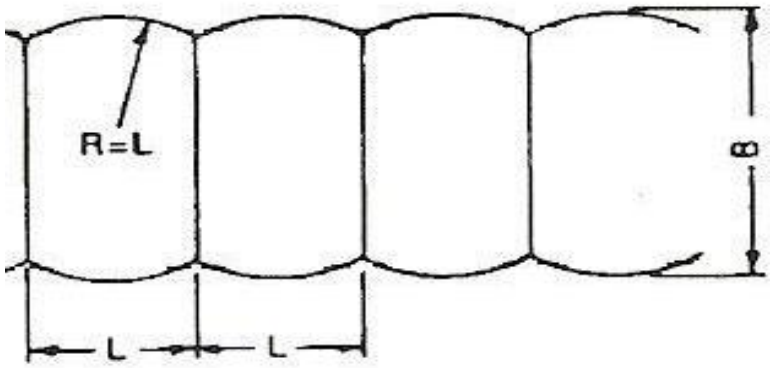

(b) DIAPHRAGM CELLS

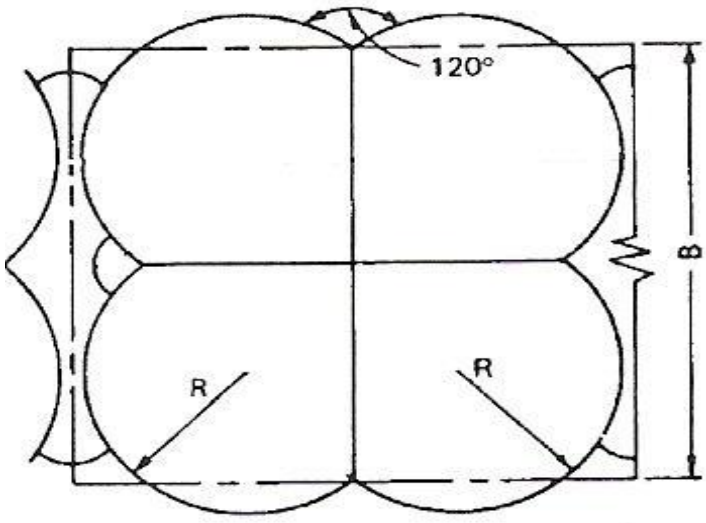

(c) CLOVERLEAF CELL

Fig. (3-1): Cellular cofferdams; [TVA, (2003)].

3.2.2: Diaphragm cells

These cells are comprised of a series of circular arcs connected by 120-degree intersection pieces or crosswalls (diaphragm). The radius of the arc is often made equal to the cell width so that these have equal tension in the arc and the diaphragm. The diaphragm cell will distort excessively unless the various units are filled essentially simultaneously with not over (1.5 meter) of differential soil height in adjacent cells. Diaphragm cells are not independently stable and failure of one cell could lead to failure of the entire cofferdam, **[TVA, (1989)]**.

3.2.3: Cloverleaf cells

This type of cell consists of four arc walls, within each of the four quadrants, formed by two straight diaphragm walls normal to each other, and intersecting at the center of the cell. Adjacent cells are connected by short arc walls and are proportioned so that the intersection of arcs and diaphragms form three angles of 120 degrees. The cloverleaf is used when a large cell width is required for stability against a high head of water. This type has the advantage of stability over the individual cells, but has the disadvantage of being difficult to form by means of templates. An additional drawback is the requirement that the separate compartments be filled so that differential soil height does not exceed (1.5 meter), **[TVA, (1989)]**.

3.2.4: Modified types

In a few cases where stability is not a problem, it may be possible to eliminate or change certain arcs in the circular or diaphragm arrangements, **[Bowles, (1997)].** As shown in Fig. (3-2),

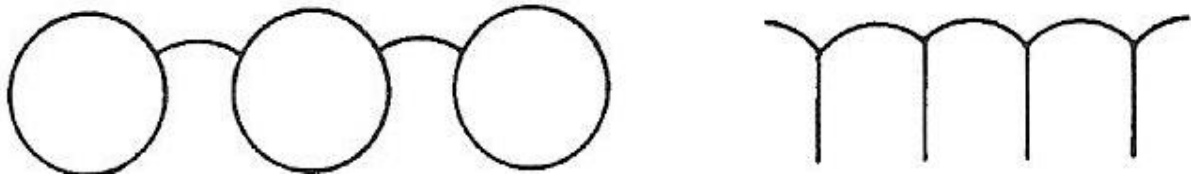

(a) Modified circular type. (b) Modified diaphragm type

Fig. (3-2): Modified cellular cofferdams; [after Bowles, (1997)].

3.3: Geometry of Cellular Cofferdam

For design analysis, a cellular cofferdam is generally replaced by an equivalent fictitious rectangular cofferdam as shown in Fig.(3-3). The width, b , of the fictitious cofferdam has either the same plan area or the same section modulus as the actual cofferdam. The calculation of the width, b , by equal area is easier and is generally justified. TVA (Tennessee Valley Authority) engineers in 1957 have found that the results of analyses by the two methods are almost identical. The average width by the method of equal areas generally is about six percent than that by the method of equal section modulii. No general statement about the conservation of either approach may be made, since the width of the cofferdam is controlled by both maximum and minimum radii, depending upon the potential failure mode being analyzed.

The relationship between the average width, b , and the radius, r , of a cell used by TVA engineers (1957) are as follows:

b= 1.57 r …… with 90 degree T connection (3-1)

b= 1.75 r …… with 60 degree T connection (3-2)

However, Terzaghi recommended:

b= 1.7 r …… for circular cells (3-3)

b= 1.8 r …… for diaphragm cells (3-4)

The height of the cofferdam must be established from flood records so that its top is at least at the level of the anticipated high water plus free board during the life of the cofferdam. The width of a cellular cofferdam is often

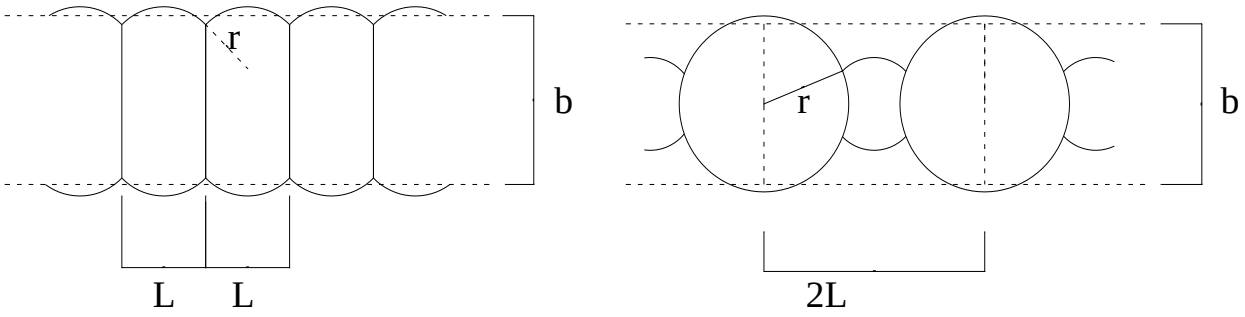

a) Diaphragm b) Circular

Fig. (3-3): Typical configuration of cellular cofferdams

determined to provide a factor of safety against overturning of at least three, **[lacroix, et at. (1970)].**

Using this width, the stability conditions with respect to sliding on the base and internal stability are checked. However, the later condition usually are not controlling. The type of cofferdam cell chosen is based on the required height and width to provide a factor of safety against excessive interlock tension of two or slightly smaller.

If sufficient space is available, a soil to increase the stability against sliding on the base and overturning. The berm also serves to lengthen the path of seepage and decrease the upward seepage pressure on the unloaded side. A berm of riprap material may be constructed on the loaded side to protect against scour. In some cases, struts have been used to increase the stability with respect to sliding and overturning. **Al-Taee, (1990)**

Experience has show that cellular cofferdams will prove to be stable with ratios of effective width "b" to height "H" between (1-0.75). The available experience data are summarized in Fig. (3-4), from which it can be seen that indicate that for ratios less than about (0.75), special geometry, berms, struts, or tiebacks have generally been used to increase stability, **[lacroix, et at (1970)].**

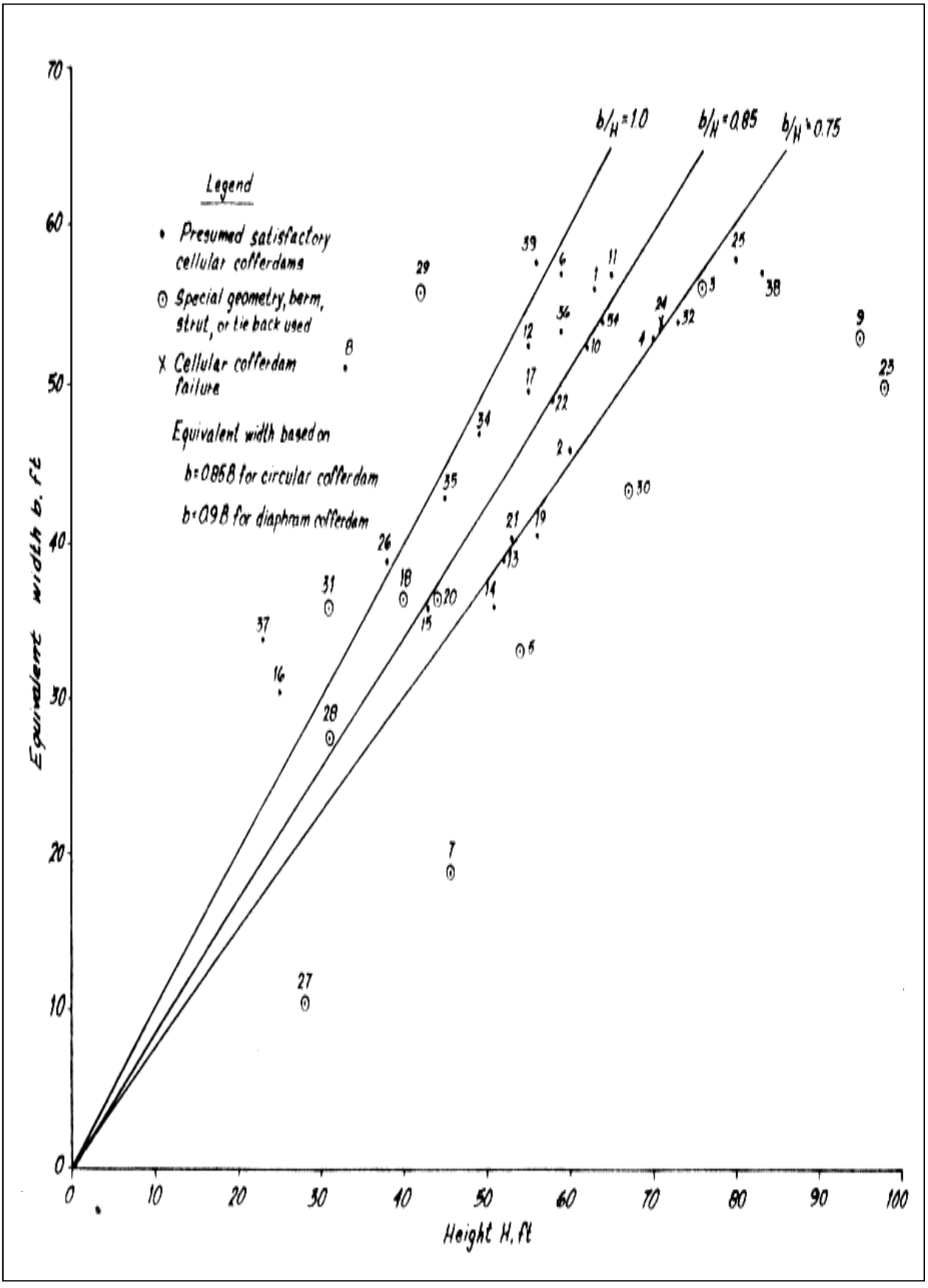

Fig. (3-4): Equivalent width to height of actual cellular cofferdams

The recommended factor of safety against overturning is ranged between (3-3.5), and consideration of accepted values of (b/H = 0.85), **[Terzaghi, (1945)],** and (b/H = 0.95), **[Swatek, (1967)].** Based on experience, taking internal stability into account.

3.4: Connection Types in Cofferdams

The major components of cellular cofferdams are the steel sheet piling for the cells, the cell fill, and the earth berms (that are often used to increase stability).

Straight sheet pile sections permit a maximum deflection angle of (10) degrees. When larger deflection angles are required for small diameter cells, standard bent piles are available as shown in Fig. (3-4-a). Junction points in cellular cofferdams require special prefabricated pieces, commonly (90) degree (T's), (30) and (120) degree (Y's). These standard connections are also shown in Fig. (3-5), (b, c, and d), **[USS, (1970)].**

3.5: Cell Fill

It is highly desirable that the cell fill material be taken from the immediate vicinity of the cofferdam. This is often done, and as a result the fill material will be found to vary widely from project to project. If no suitable fill material can be found within a radius from which it can be transported economically, then it may be advisable to use another type of cofferdam. The cell fill material should have certain inherent qualities, which must not be ignored. For projects where the cell is small these qualities may be determined by using sound judgment and past reports. For large cells, however, it becomes increasingly important that the fill material be subjected to laboratory or practical field tests in order to determine its characteristics and suitability. The cell fill material can be divided into four types of soil:

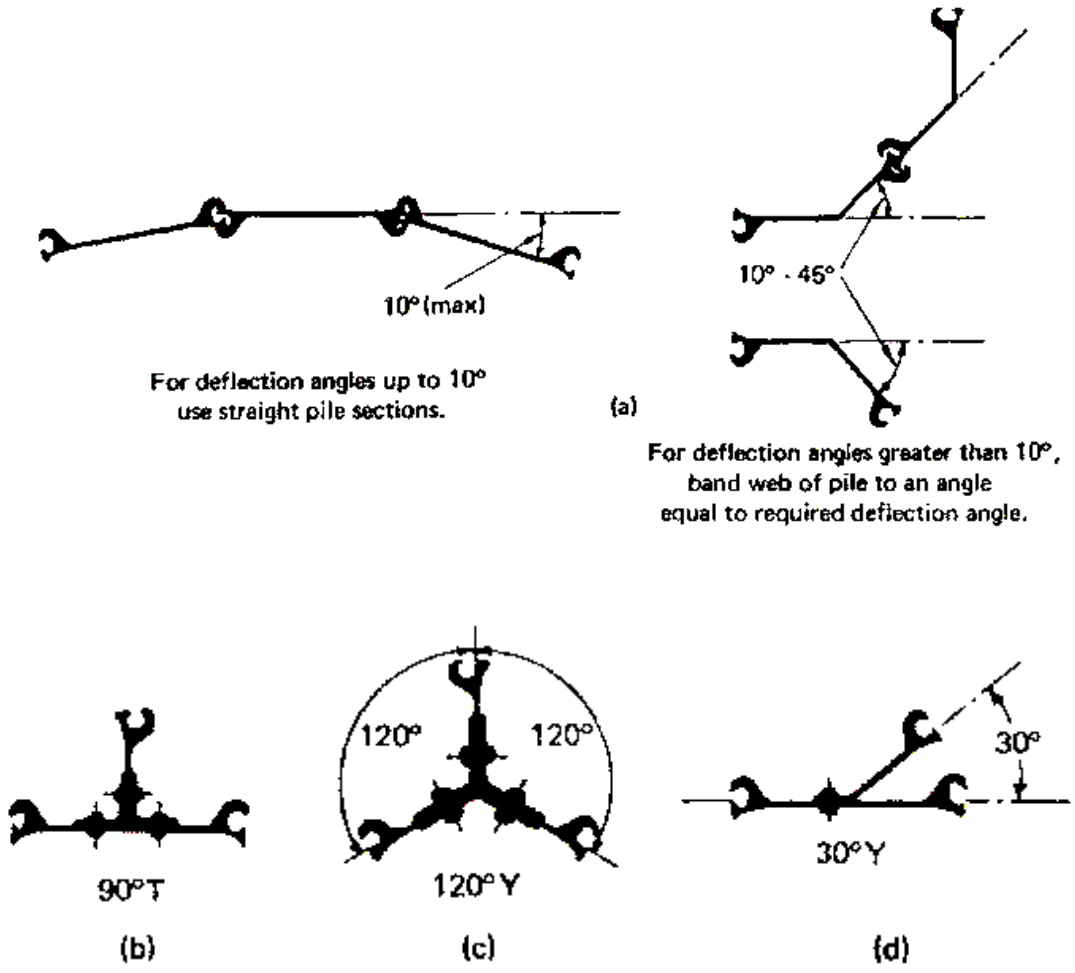

Fig. (3-5): Types of steel –sheet-pile and connections for cellular cofferdams; [after USS, (1970)].

3.5.1: Silt Soil

Silt offers resistance to leakage but no resistance to scour and little resistance to internal shear. Such a fill, unless covered with a layer of scour-resistance material, will suffer heavily in the event that the cells are overtopped by floodwater. High interlock stresses are also apt to develop during hydraulic filling because of the liquid nature of the material. Fill materials with fairly large silt content will tend to develop similar characteristics to that of pure silt and are, in general, to be avoided, **[TVA, (2003)].**

3.5.2: Clay Soil

Clay is material that extensively used in cofferdam construction because of its impervious qualities and resistance scour. However, it is not suitable as a cell fill material because of its low frictional value, when wet, in resisting sliding and internal shear. Where the supply of a more suitable material is limited, however, clay may be used satisfactorily for that part of the cell fill above the line of saturation, or as an aid in sealing leaks, **[TVA, (2003)].**

3.5.3: Sand Soil

Were used successfully to drain and stabilize diaphragm cells filled with marl in the construction of a ship construction basin. It is possible that this method could be used just as efficiently to increase shear resistance in cells filled with clay. The method might be too costly for temporary cofferdam construction, however. The procedure followed in this method consisted essentially of driving (3.5 meter) diameter closed end pipes to the fill depth of the completed cell fill, filling them with sand and gravel, and then pulling the pipe, leaving the sand and gravel in place. To facilitate removal, the pipes were capped and compressed air applied to force the sand gravel out as the pipe was removed, **[TVA, (2003)].**

3.5.4: Sand and Gravel

A natural mixture of sand and gravel offers one of the most satisfactory materials for cell fill and is often found along the bed of large streams where the cellular type of cofferdam is frequently used. It was available from the bed of the Tennessee River and was used, for the most part, as a fill for all of the cellular steel sheet pile cofferdams built by TVA. This type of material ideally suited to placement by hydraulic methods and was therefore the method used by TVA, **[TVA, (2003)].**

3.6: Soil Properties

The cell fill provides mass (or weight) for stability and a reduced coefficient of permeability κ for retaining water without excessive pumping. These advantages must be balanced against the lateral pressure effects of the soil-water mixture and the resulting stresses that the sheetpile interlocks must resist before rupture or cofferdam failure**[Bowles, (1997)].**.

For mass, it would be preferable to use a soil with a high density. For permeability considerations alone, clay is the best possible fill. The earth-pressure coefficient of sand with a high angle of internal friction Ø gives the minimum lateral pressure that must be resisted by hoop tension in the interlock, which usually cell design. Considering all these factor, the best cell fill:

a. Is free-draining (large coefficient of permeability, κ)
b. Has a high angle of internal friction, Ø
c. Contains small amounts of No.200 sieve material - preferably less than 5 percent
d. Is resistant to scour (nonsilty or clayey) - requires presence of some gravel

Cell fills that do not meet these criteria are sometimes used, but the closer the fill material approaches these criteria the design in terms of sheetpiling, which is usually the most expensive portion of cofferdam**[Bowles, (1997)].**.

Cell fill is often placed hydraulically; i.e., the material is obtained from the river bottom if at possible. The material is dredged and pumped through a pipe system and discharged into the cells, which are already driven, with the river level being the inside water line. This operation may substantially reduce the fines, which are often present in river-bottom material and which are temporarily suspended in the water and wash overboard. If material is not available close by, fill may have to be brought in by barge, truck, or rail. In any

case the cell fill is generally deposited under water so the angle of internal friction Ø may not be very large. It appears that this method of soil deposition seldom produces an angle of internal friction over about ($30^o \pm 2^o$).

Unless satisfactory drained triaxial tests can be performed on the soil and at the expected cell density, the Ø-angle should be limited to (28 -30º)
for design (or preliminary design). It is possible to increase the cell fill density and Ø by using some type of compaction with vibratory equipment such as the Vibroflot or Terra-probe. If this carefully done (*before any drawdown of on the basin side water on the basin side*) relative densities ***Dr*** on the order of (0.75-0.85) can be obtained with Ø-angle in the range of (35-40º), **[Bowles, (1997)].**

3.7: Failure Modes

Under lateral loads, cellular cofferdams may fail in one or more of the following modes:

1- General failure.

2- Local failure.

3.7.1: General failure

In this case the cell is assumed to behave as a unit. General failure includes:

i: Sliding failure

This failure takes place when the cofferdam is subjected to unbalanced forces due to water pressure; these forces cause the cell to slide as a unit along a horizontal plane located under the cell, as shown in Fig. (3-6). That means a shear stress at the base exceeds the shearing resistance, **[Al- Chalabi, (1959)]**.

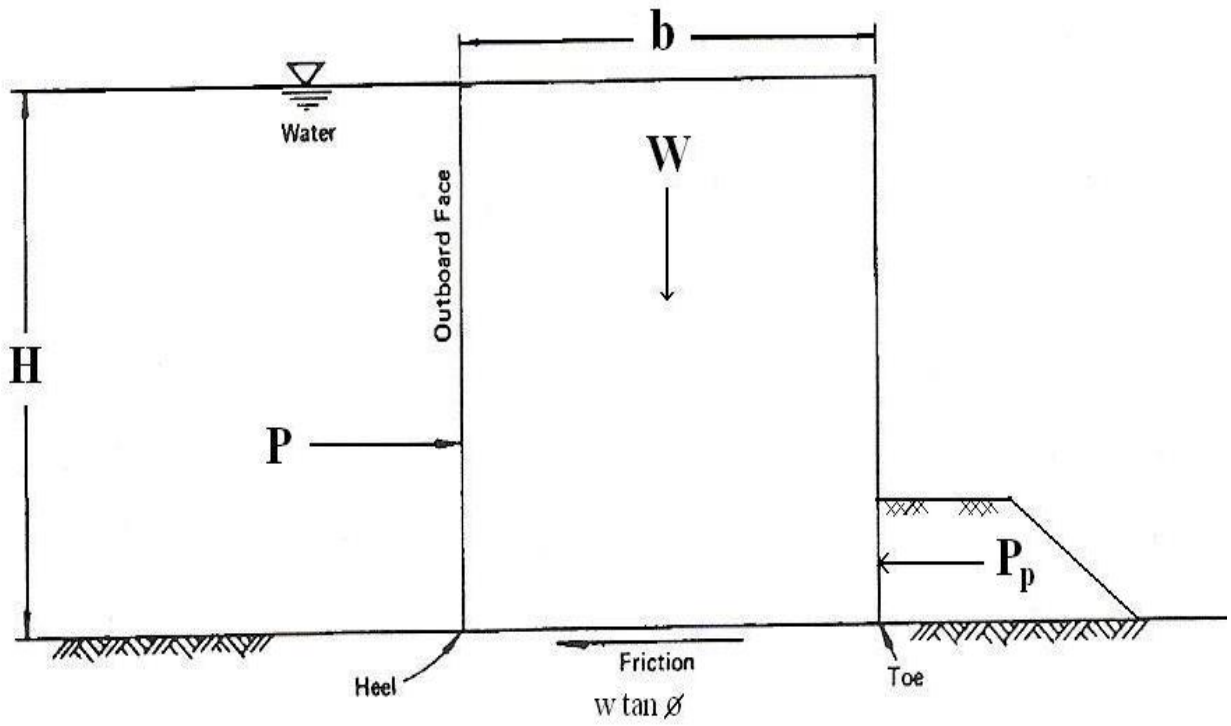

Fig. (3-6): Sliding stability of cell; [after Al-Chalabi,(1959)].

A cofferdam must provide adequate resistance to sliding on the base caused by the unbalanced hydrostatic pressure; a sliding stability number (N_s) should range between (1.10 to 1.25), **[Bowles, (1997)]**. This number is defined as the ratio of lateral force to potential resisting forces per unit length of the wall which can be calculated as:

$$N_s = \frac{f.W + P_p}{P} \qquad (3\text{-}5)$$

where: f = coefficient of friction between the cell fill and foundation at the base of the cell. This is usually taken as $\tan\phi$, where ϕ, is the friction angle of the cell fill.

W = effective weight of cell fill.

P_p = effective passive resistance which depends on the depth of embedment of sheetpiling.

P = total lateral force.

ii: Overturning failure

Usually the cofferdam is subject to unbalance lateral forces at different heights. These unbalanced forces will tend to produce a resultant moment which tends to overturn the cofferdam, **[Al-Chalabi, (1959)].**

The cell is assumed to rotate about toe. To provide the stability against overturning, the resultant normal force should be lie within the middle third of the base as shown in Fig. (3-7), **[Dismuke, (1975)]**.

The cofferdam must be stable against overturning and the number of overturning stability (N_{ot}) should range between (1.1 to 1.25), **[Bowles, (1997)]**. This number is defined as the ratio of resisting moment, (M_r), to the overturning moment, (M_o), which is calculated as follows:

$$N_{ot} = \frac{M_r}{M_o} = \frac{\frac{W * b}{2}}{\frac{P * H}{3}} \qquad (3\text{-}6)$$

where:

W= weight of cell fill.

b= width of the cell.

P= horizontal pressure, and

H= height of the cell.

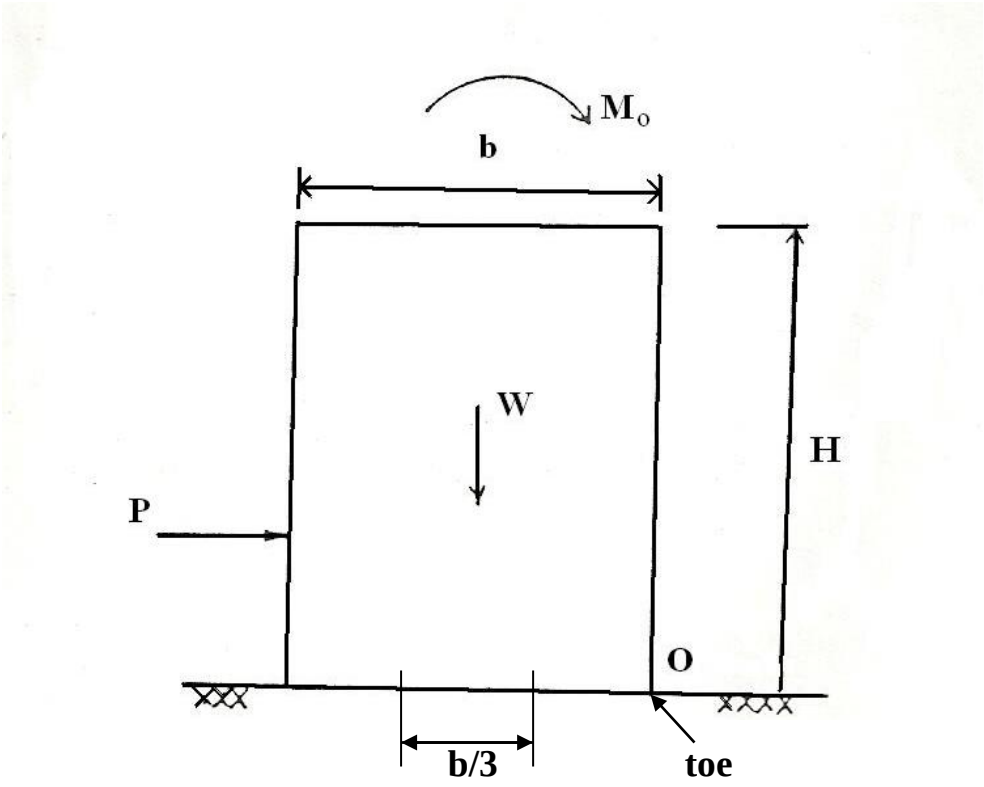

Fig. (3-7): Overturning stability of cell. [After Bowles, (1997)]

3-7-2: Local failure

In this case the failure take place in the cellular cofferdam parts during its construction or during the general failure taken, and includes:

i: Excessive interlock tension failure

A cell must be stable against bursting pressure. The pressure exerted against the sheets by the fill inside the cell must not exceed the allowable interlock tension. The interlock tension was developed in a cell as a function of the internal cell pressure. The internal horizontal pressure (P) at any depth in the cell fill is the sum of the earth and water pressures. The earth pressure is equal to the effective weight of the cell fill above that depth times the coefficient of

horizontal active earth pressure (K), its value is dependent upon the type of cell fill material, **[USACE, (1989)].**

In 1945, Terzaghi estimated that (K) must have the value between (0.4) and (0.5). He suggested the empirical value of (0.4), **[Terzaghi, (1945)].**

According to (Krynine, 1945), the following equation to determine (K), as has been suggested:

$$K = \frac{\cos \phi}{2 - \cos \phi} \tag{3-7}$$

where:

ϕ = friction angle of the soil in the cell.

The observations of the deformation of cellular cofferdams indicate that the maximum bulging of the cell occurs in a zone between ($\frac{1}{4}$ to $\frac{1}{3}$) of the height of the exposed portion of the sheetpile above the embedded part of the cell. For design purpose the maximum pressure assume occurs at a point ($\frac{1}{4}$) of the exposed height of the cell above the dredgeline, **[Lacroix et al., (1970)].**

The factor of safety (F.S) against excessive interlock tension is defined as the ratio of the interlock strength as guaranteed by the manufacturer to the maximum computed interlock tension.

Interlock tension is also proportional to the radius of the cell. The maximum interlock tension in the main cell is given by:

$$t = P * r \tag{3-8}$$

where:

P = Maximum guaranteed inboard sheeting pressure.

r = radius.

The interlock tension at the connections between the main cells and the connecting arcs is increased due to the pull of the connecting arcs, **[USACE, (1989)]**, as illustrated in Fig. (3-8), and can be approximated by**:**

$$t\max = \frac{P * L}{\cos\phi} \qquad (3\text{-}9)$$

where:

$t\max$ = interlock tension at connection.

P = maximum inboard sheeting pressure.

L = as shown in Fig. (3-8).

The factor of safety against interlock failure should be at least 2 **[USS, (1970)].**

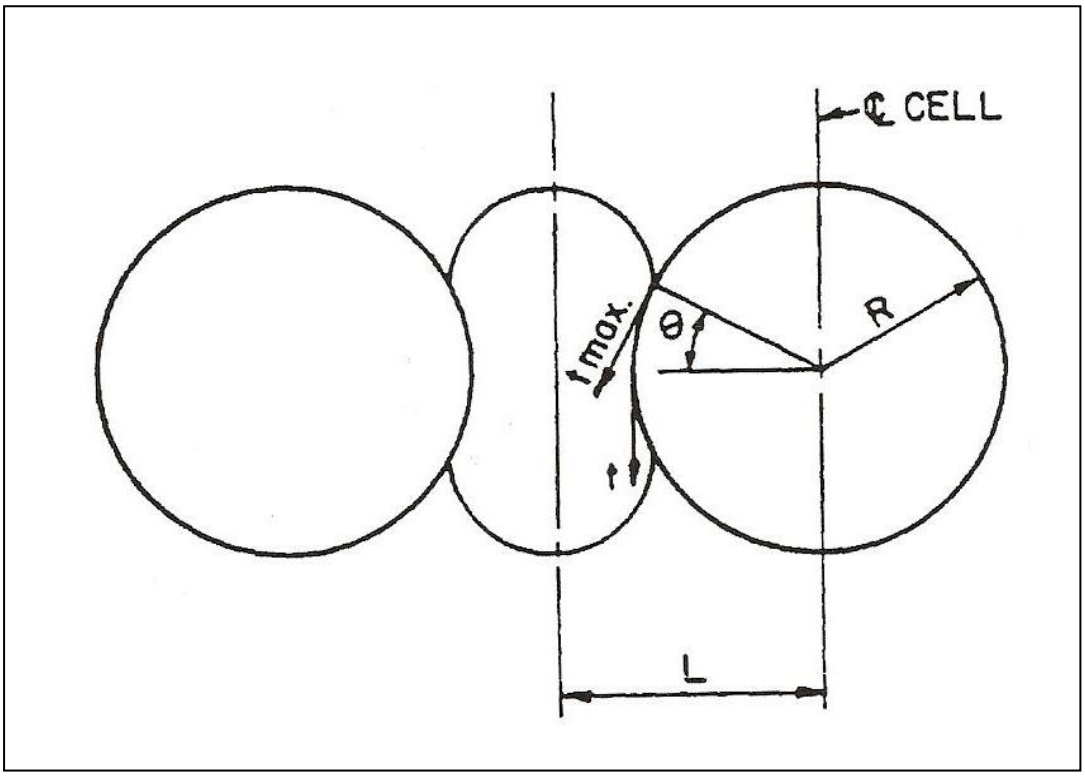

Fig. (3-8): Interlock stress at connection, **[after USACE, (1989)]**.

ii: Slipping failure between sheeting and cell fill

This mode of failure is frequently takes place between the sheetpiles and surrounding soil, when a cellular cofferdam subject to large overturning

moment, there is a tendency for the sheet sheel to rotate about the toe. As the sheet rotates, failure can occur by lifting the outboard piling and losing the cell fill as it runs out the heel of the cell. In such cases slipping occurs between the sheetpiles on the outboard face and the cell fill. The resisting moment with respect to the inboard toe is due to the frictional forces is assumed to be equal to the applied lateral load, (P), times the coefficient of friction between the cell fill and sheetpiles, as illustrated in Fig. (3-9), the factor of safety against slippage can be taken as

$$F.S. = \frac{(P \quad \tan\delta) \quad b}{P \quad (\frac{H}{3})} \tag{3-10}$$

where:

$\delta =$ friction angle between the fill and the sheetpiles.

Since slippage occurs between the cell fill and sheetpiles, the fill weight does not contribute in the resisting moment. A factor of safety against slippage of at least (1.25) has been recommended, **[Teng, (1962)]**.

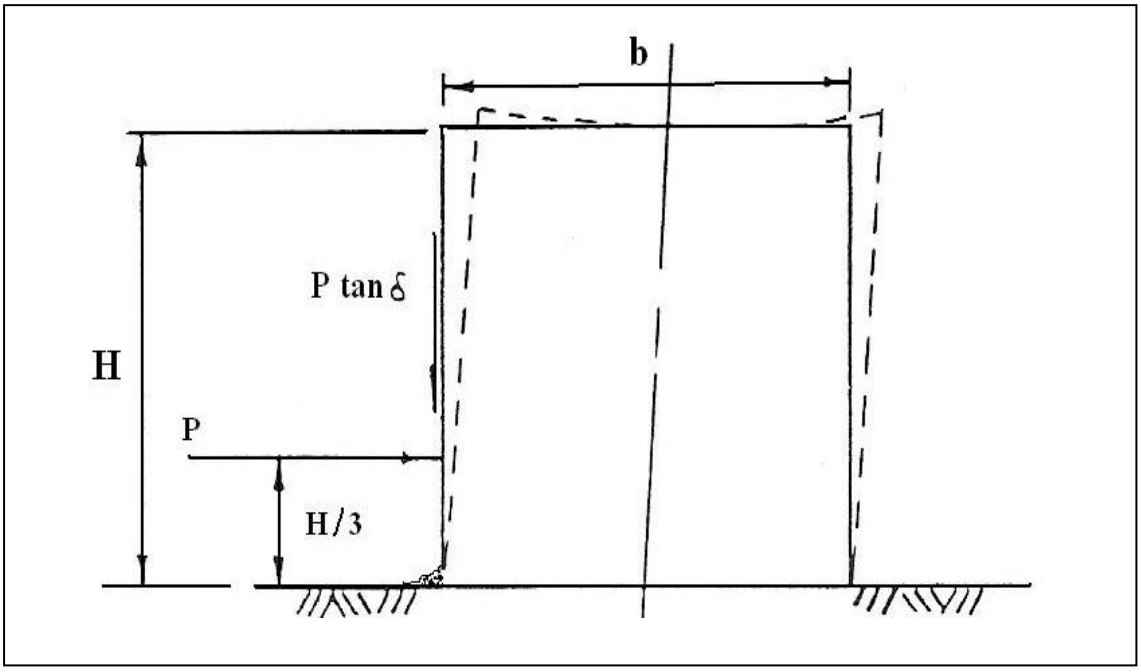

Fig. (3-9): Slipping stability of a cell, [after Teng, (1962)].

iii: Vertical shear failure

As any structural member acted upon by lateral forces, the cofferdam is subjected to shear stresses. The magnitude of this shear stress is maximum along the center of the cell, as shown in Fig. (3-10), and may be determined as follows, **[Esrig, (1970)]**.

$$V_{max} = 3/2(M/b) \quad (3\text{-}11)$$

where:

M=true moment duo to external lateral force above base (or above any horizontal section under consideration).

b=width of the cofferdam.

Shear resistance on the plane along the center of the cell is computed from the lateral, (P_a**)** as

$$S_1 = P_a \tan ø \quad (3\text{-}12)$$

where:

P_a = active horizontal pressure.

where:

ø the angle of internal friction, and

$$P_a = 1/2\ \gamma\ h_a^2\ K_a \quad (3\text{-}13)$$

where:

h_a = height of the active side, and

K_a = active earth pressure coefficient can be calculated as

$$K_a = (1-\sin ø)/(1+\sin ø) \quad (3\text{-}14)$$

Therefore

$$S_1 = 1/2(\gamma * H^2 * K_a * \tan ø) \quad (3\text{-}15)$$

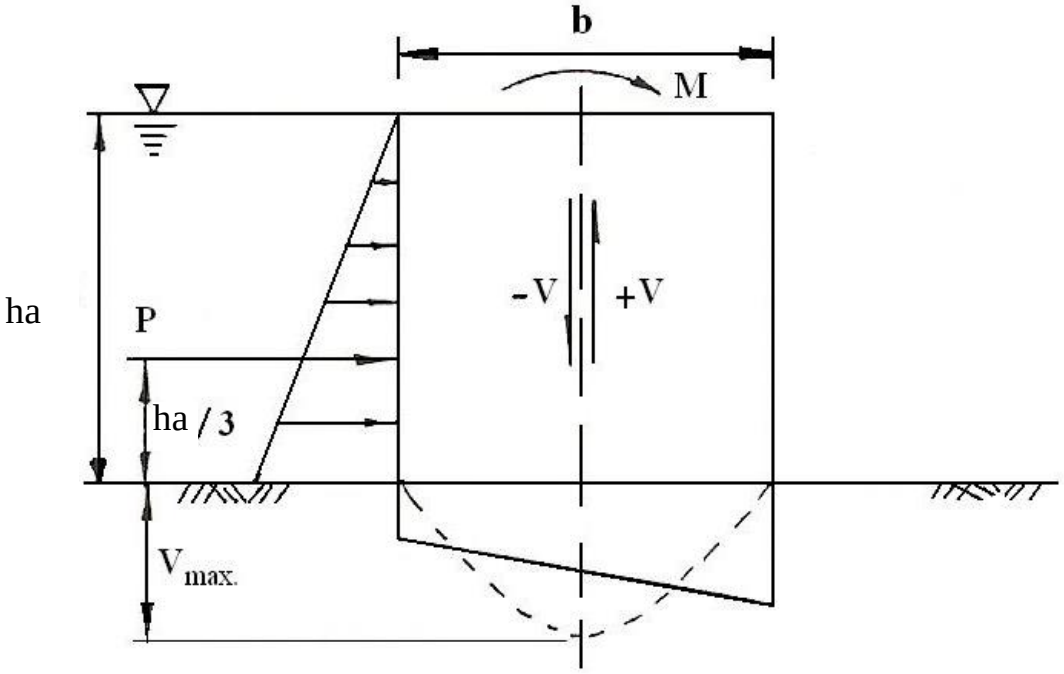

Fig. (3-10): Vertical shear in cell; [after Esring, (1970)].

In addition to this shear resistance, the friction in the sheet piles interlocks at both ends of the diameter through which the normal plane passes, also provides resistance, tension in the interlocks will be

$$t=P_a*r \qquad (3\text{-}16)$$

where:

r=radius of the cell, so the friction in the interlocks is

$$S2=P_a*r*f_{ss} \qquad (3\text{-}17)$$

where:

f_{ss} =the coefficient of friction of steel on steel.

Since there are two interlocks in a unit length, (2L) as shown in Fig.(3-3), of fictitious cell, the total available interlock friction on the neutral plane per unit length of cofferdam is

$$S2=\frac{2*\frac{1}{2}\gamma*H^2*Ka*r*fss}{2L}=\frac{\gamma*H^2*Ka*r*fss}{2L} \qquad (3\text{-}18)$$

Therefore, the total available shearing resistance per unit length is

$$S = S1 + S2 \tag{3-19}$$

The factor of safety against this type of failure is

$$F.S. = \frac{S}{V\max} \tag{3-20}$$

For temporary cofferdam structures the factor of safety against vertical shear is (1.25), and (1.5) for permanent cofferdam structures, **[USS, (1974)].**

iv: Horizontal shear failure

In 1957, Cummings proposed a method of analysis cofferdams based on his experiments on model cofferdams on rock, when the lateral force, (P), is applied to the cell, a resistance from the cell will be develop as a triangle, (hij), as shown in Fig.(3-11), forming an angle (ϕ) to the horizontal. The soil in triangle (hij) is in the passive state. The rest of the fill acts as a surcharge and stabilizes the soil in triangle (hij). This part of the fill is termed (W1). Its weight can be calculated as

$$W1 = \gamma(a + y)y \quad \cot\phi \tag{3-21}$$

The shearing resistance along the plane (gf) become

$$S1 = W1 \quad \tan\phi = \gamma(ay + y^2) \tag{3-22}$$

When $y = c,$ $S1$ is maximum

Hence

$$S1\max = \gamma(ac + c^2) \tag{3-23}$$

But

$$c = b \quad \tan\phi \tag{3-24}$$

And

$$a = H - c \tag{3-25}$$

Therefore

$$S1\max = \gamma * H * b * \tan\phi \tag{3-26}$$

From equation (3-22) (S1) can be represented by a rectangle and triangle as shown in Fig.(3-10). The resisting moment computed for (R1) and (R2) is

$$Mr = M1 + M2 = R1\frac{C}{2} + R2\frac{C}{3}$$

$$Mr = \gamma(\frac{a*C^2}{2} + \frac{C^3}{3}) \qquad (3\text{-}27)$$

If the resisting moment due to interlock friction is considered, then, the expression for the total resisting moment, (M_t), is given by

$$Mt = \gamma(\frac{a*C^2}{2} + \frac{C^3}{3}) + P*f*b \qquad (3\text{-}28)$$

The factor of safety (F.S.) against horizontal shear is defined as the ratio of resisting moment, (M_t) , to the overturning moment, ($M_\circ$), or

$$F.S. = \frac{Mt}{Mo} \qquad (3\text{-}29)$$

The factor of safety should be ranged between (1.25) and (1.5), **[Lacroix et al., (1970)].**

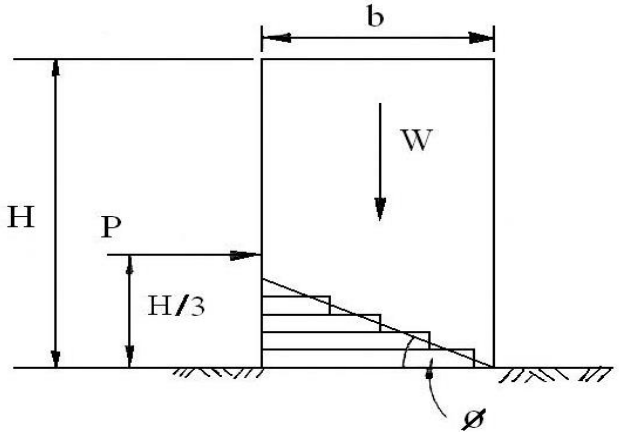

a) Cell fill resistance to lateral force

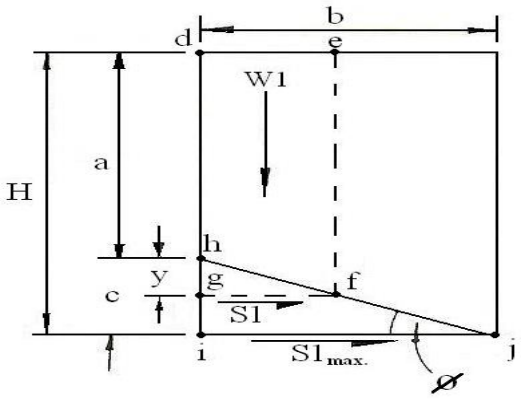

b) Forces in tilting failure mode

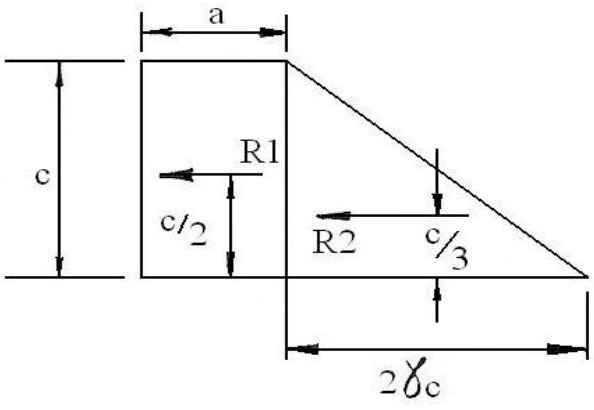

c) Pressure diagram provided by cell fill

Fig. (3-11): Tilting analysis; [after Cummings, (1957)].

3.8: Testing Apparatus:

The testing apparatus used in this research to check the general stability of cellular cofferdam and consist of:

3-8-1: Steel frame

A steel frame used to carry the soil box and its content, as illustrated in Fig. (3-12), with dimension (140 cm) length, (105 cm) width, and (80 cm) height. At the middle of its width fastened knee-braced frame, a knee-braced frame made of two angles (5*5) cm and (50 cm) length, are welded vertically, at their bottom end, to the steel frame, the upper side of the angles is connected to a steel beam of (13.5 cm) length, (5 cm) width and (0.3 cm) thickness, a space of (3.5 cm) is provided between the two angles to allowed to pass the steel cable load, on each side of knee-braced frame, two steel angles (5 *5) cm of (47 cm) length, are welded at (35 cm) height from knee-braced to support it.

In each angle, a slit-like opening with dimensions of (40 cm) height and (1.5 cm) width is made at (5 cm) height from the knee-braced base, this slit is use to fix the pulley system. The set-up described above it was designed to permit testing of the diaphragm cells under lateral loading. [**Al-Khyatt, (2009)].**

3-8-2: Loading system

The load is applied to the cell by a steel cable loop (0.4 cm) in diameter hold around the cell tightly from one end and connected to the weight holder from the other and after passing over a system as shown in Fig. (3-13), the loading system consists of:

a) The dead weight holder comprises of two parts, the first is a steal beam with dimensions (33 cm) length, and (1 cm) width with square section,

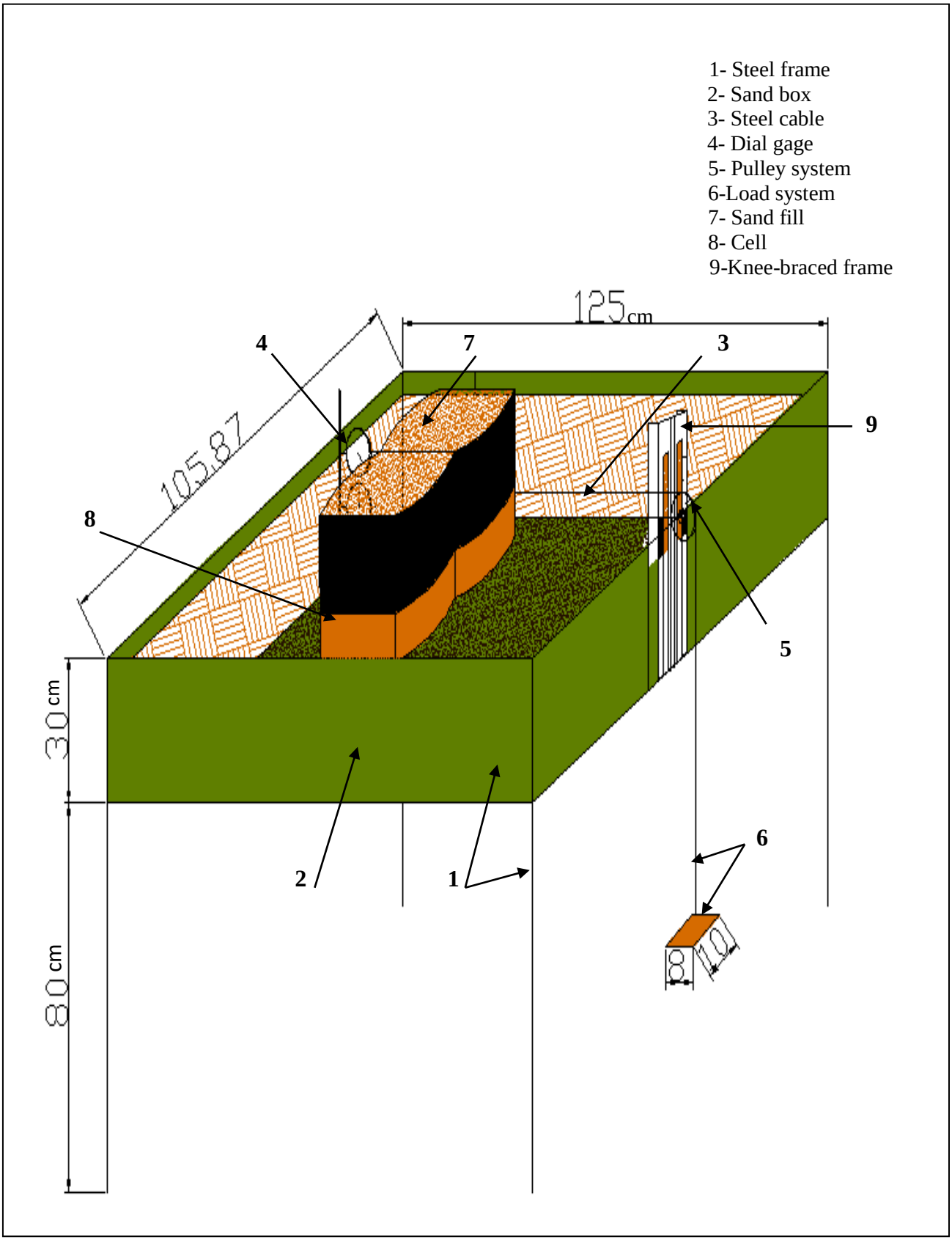

Fig. (3-12): Testing apparatus

b) the second part is a square steel plate of (10 cm) length and (0.8 cm) thickness, the first part is welded vertically to the second part.

c) The dead weight holder comprises of two parts, the first is a steal beam with dimensions (33 cm) length, and (1 cm) width with square section, the second part is a square steel plate of (10 cm) length and (0.8 cm) thickness, the first part is welded vertically to the second part.

The dead weight of (0.5, 1, 2, 4, 8, 10) kg is used as a loading units.

3-8-3: Pulley system

The pulley system as shown in figures. (3-13), and (3-14) consist of a round steel shaft (3 cm) in diameter and (20 cm) length, a pulley (5 cm) in diameter is fixed in the middle of the shaft, and two brackets each one surrounding ballbearing (6 cm) and internal diameter (3 cm), the two brackets provided with two holes that was used to fix the pulley set to the knee-braced frame.

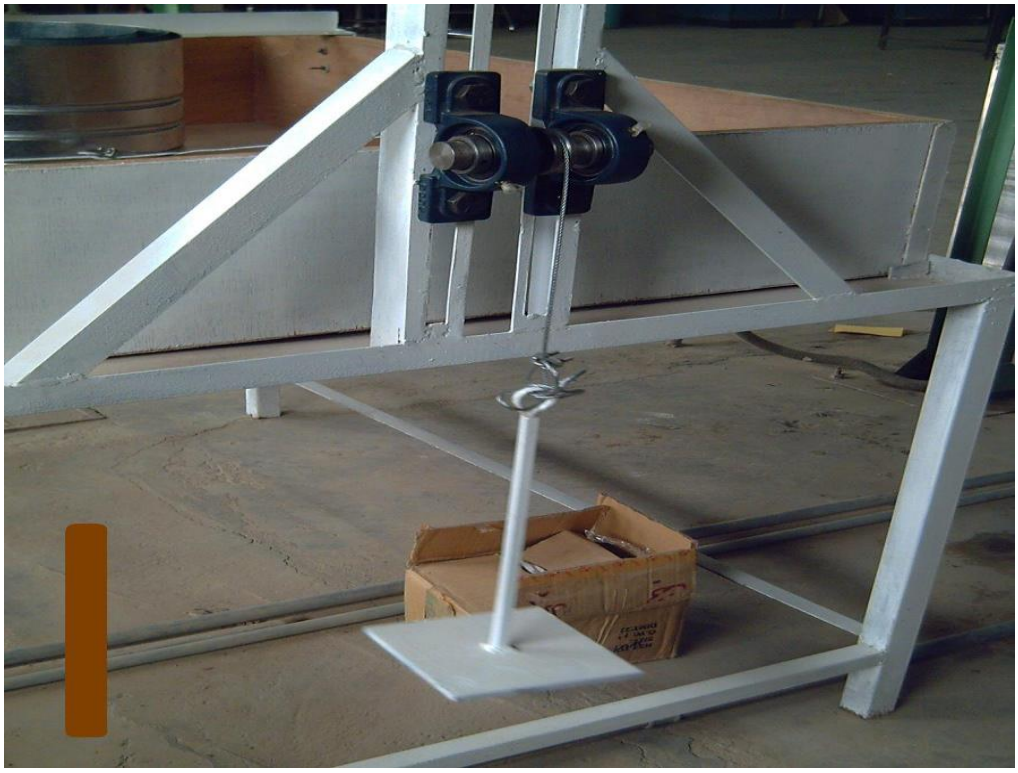

Fig. (3-13): the loading system

3-8-4: Soil box

A wooden container with inner dimensions (125 cm) length, (105.8 cm) width, and (30 cm) height, as shown in Fig. (3-12), was used as a container for a foundation to the diaphragm cells of cellular cofferdams.

At (20 cm) distance from the end of the box fastened steel angle beam of (108 cm) length, (5 cm) width and (5 cm) height by screws above the two sides of the box. There is one hole in the middle of the beam to support a steel screwed shaft, (1.5 cm) diameter, and (80 cm) length. The steel shaft was used to carry four dial gages.

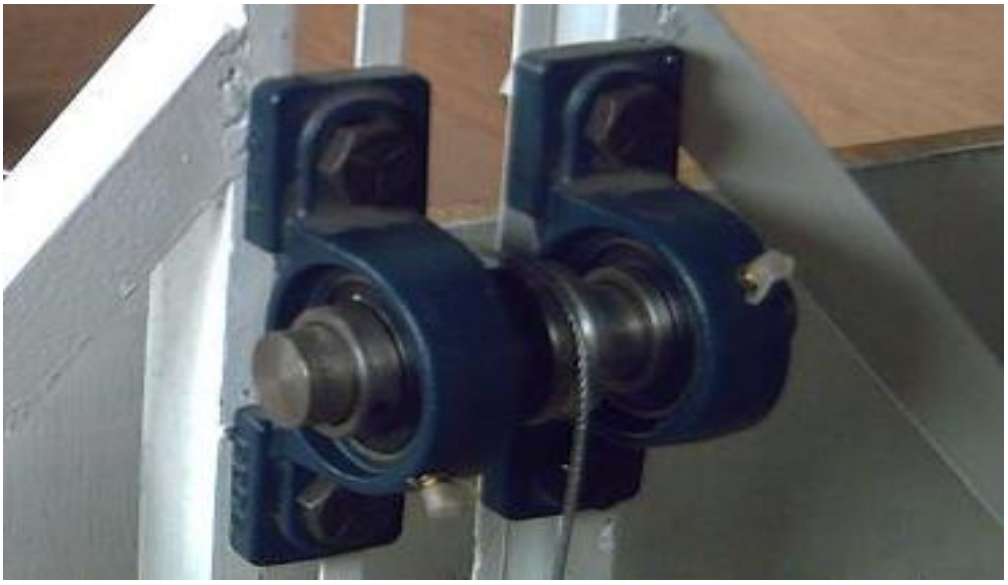

Fig. (3-14): The pulley system

3-8-4-1: General requirements for cell fill

The general requirements for a fill material for cellular steel sheetpile cofferdams, **[TVA, (1989)]**, are:

1. High coefficient of internal friction.
2. Free draining.
3. Resistance to scour. and
4. High weight in mass to resist sliding and overturning.

3-8-5: Diaphragm model cells

To construct the diaphragm model cell, the cells divided into two groups, the first group the placed on ground surface and it have a three width to depth ratios (b/h=0.75, 0.85and 1) as shown in Fig. (3-15). the second group model driven into the soil for three heights to embedment depth ratios (D/H=0.15, 0.3 and 0.45), using b/h=0.75 as shown in Fig. (3-16).

The cells, shown in Fig. (3-16), consists of two arcs connected by straight cross walls. Each arc is 20 cm in radius, 30 cm height and 0.09 cm thickness cold-rolled galvanized steel.

At each side of the cell a group of three identical straight cross walls are positioned at 3, 17, 27 cm height from the cell base. The straight cross walls has dimensions of 17.5 cm length, 3 cm width and 1mm thickness cold-rolled galvanized steel. A rubber of 30 cm height and 17.5 cm width is used to keep the soil inside the cell.

In order to hold the loading the cable tied to the cell during tests, the channel has been used at 100mm height from the base of the cell as shown in Fig. (3-17).

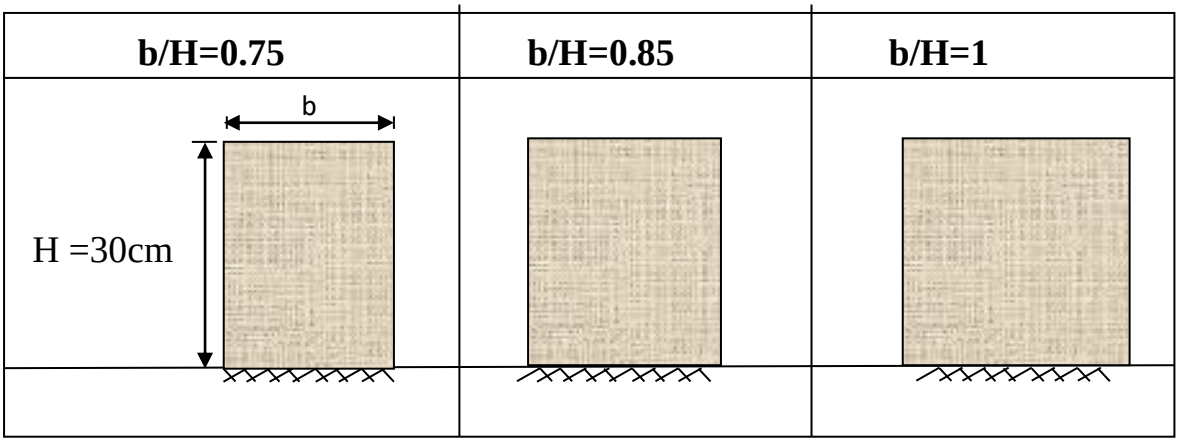

Fig. (3-15): Schematic presentation of first group testes

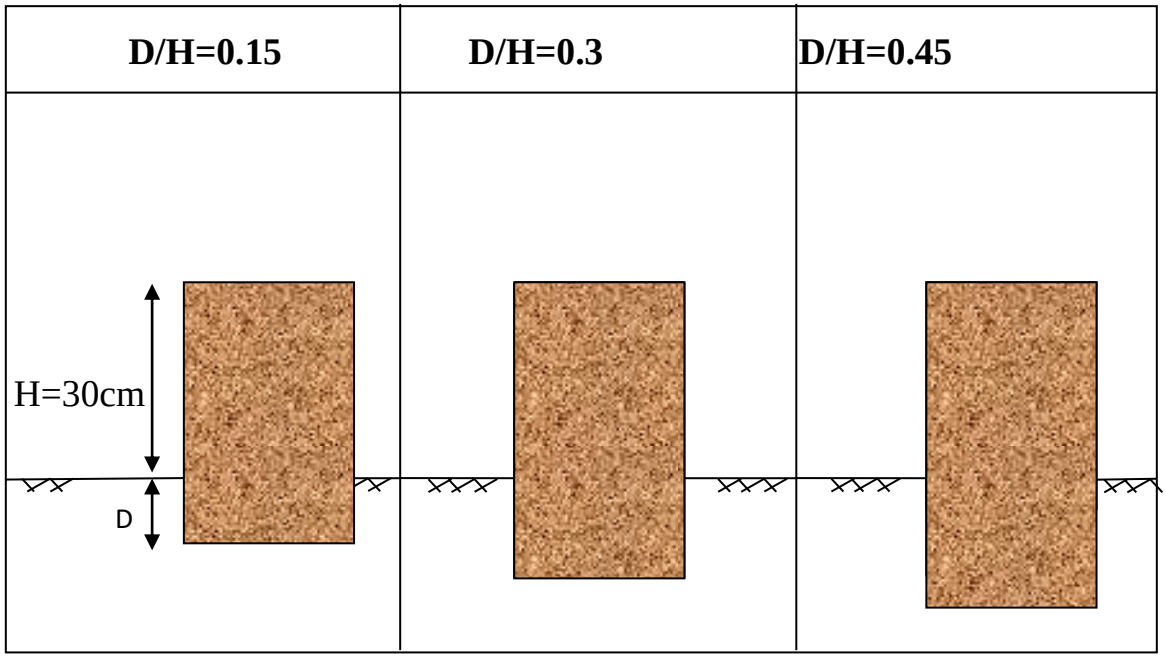

Fig. (3-16): Schematic presentation of second group testes

Fig. (3-17): Diaphragm models

3-8-6: Dial gages

Dial gages were used to monitor the displacements of models throughout the entire testing program, four dial gages of (0.01 mm) accuracy and (25 mm) travel were employed, they are mounted to vertical steel shaft as shown in Fig. (3-18), and Fig. (3-19)

Fig. (3-18): Steel shaft carry four dial gages

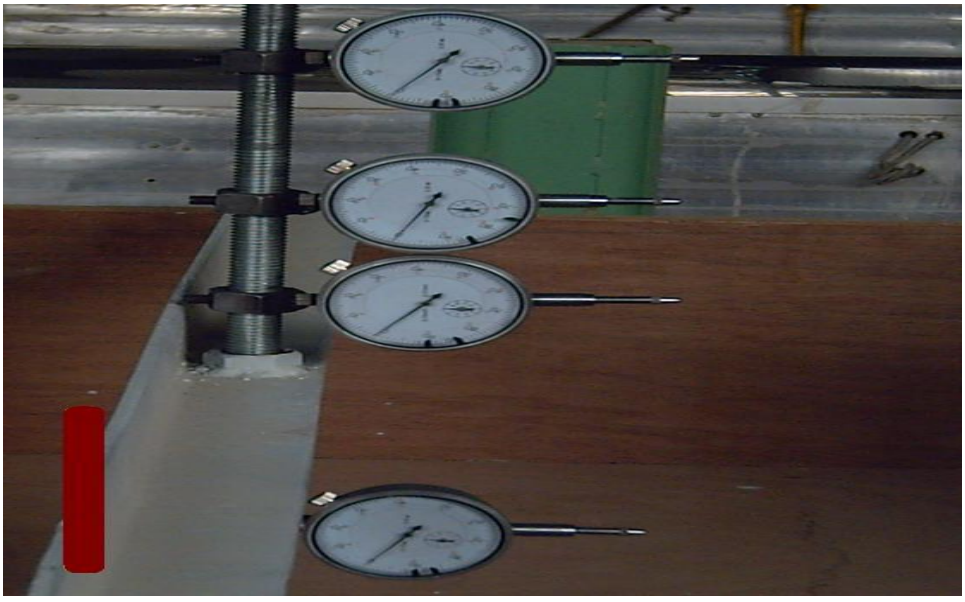

Fig. (3-19): Dial gages

3-9: The Properties of Soil

Four different types of soil used in all tests, the dry density and angle of friction for all soils which testing in laboratory are illustrated in table (3-1):

Table (3-1): the properties of the soils used in the cells fill.

Type of soil	Dry density (γ) (KN/m^3)	Angle of friction (ø)
Subbace	16.67	38
Sand sieved on No.4	17.82	33.5
River sand	14.86	31.5
Sandy clay	14.35	21

3-10: Testing Procedure

In all tests the soil bed on wooden box of (300mm) height, placed by means of raining technique. The cells then placed in the middle width of soil box at (100mm) distance from the support of dial gages. The models are then filled carefully to minimize disturbance.

The raining technique has been used successfully in providing uniformly dense soil bed for model studies, **[Kelly, (1969)].** Basically, the technique involves raining soil through a single or series of sieves with a constant height of the drop and raining intensity, weight of soil raining per unit area; the raining technique could be used to provide a uniform dense soil fill with good density control, angle of internal friction. A height of (500mm) was kept between the sieve that was used in the raining technique and the top surface of the soil. After the cell was filled, the cell level checked by handy level, the loading system and dial gages were adjusted. Then, the load is applied incrementally and continued until a failure in the model was occurred. At the end of each load increment, the dial gages recorded. The displacements of the cell, at each load level and

increment can be calculated. In all tests the same soil type was used in the cell fill and foundation.

3-11: Testing Program

The test program consists of two cases and for each case four stages of tests have been conducted. The first stage deals with testing of three diaphragm cells with different (b/H) ratio (0.75, 0.85, and 1.0), sand was sieved on No.4 used as fill and foundation for these cells, at the other stages of tests, the same cells used in tests but with different type of soils, where in the second stage the subbase was used in tests, the third stage the river sand was used, and at the last stage the sandy clay used in the test as fill and foundation, and repeated these tests with case two. On each of these cells, the load was applied at (10 cm), so that the difference between sliding and overturning failure can easily be clarified. In all tests the cells put on the ground surface and embedment depth equal to (D/H = 0.15,0.3and 0.45).

Chapter Four
Results and Discussion

4.1: Introduction

This chapter presents the results obtained experimentally according to the testing program. The tests results reported in this chapter concern of two cases, at the first case diaphragm cells placed on ground surface with width to height ratios (b/H= 0.75, 0.85, 1.0) and the second case the diaphragm cells embedded to different depths which resulting depth to height ratios, D/H = 0.15, 0.3, 0.45. It is worth mentioned that the displacement term in this study indicates both translation and rotation of the top point of cell unless otherwise is stated.

4.2: Load-Displacement Behavior

A quick survey on the load-displacement behavior of all cells that placed on ground surface have been shown that they are similar and characterized by three distinguish stages, as shown in Figs. (4-1) to (4-3). The first stage (a-b), the displacement is linearly proportional to load. After that curved relationship (b-c) was obtained, which represent the second stage, the load-displacement relationship become, again, linear (c-d) until failure but with much flatter slope compared with that of the first stage. The curve form varies from cell to others according to the (b/H) ratio and type of soil used in the filling. It is worth mention that the cell loading is incrementally increased until an overall failure is taken place. The mode of failure was found to be either translation of displacement or overturning failure as that described later in the mechanism of failure. Thus the failure loading or cell resistance may be defined as the critical loading above which a general failure in the cell is taken place.

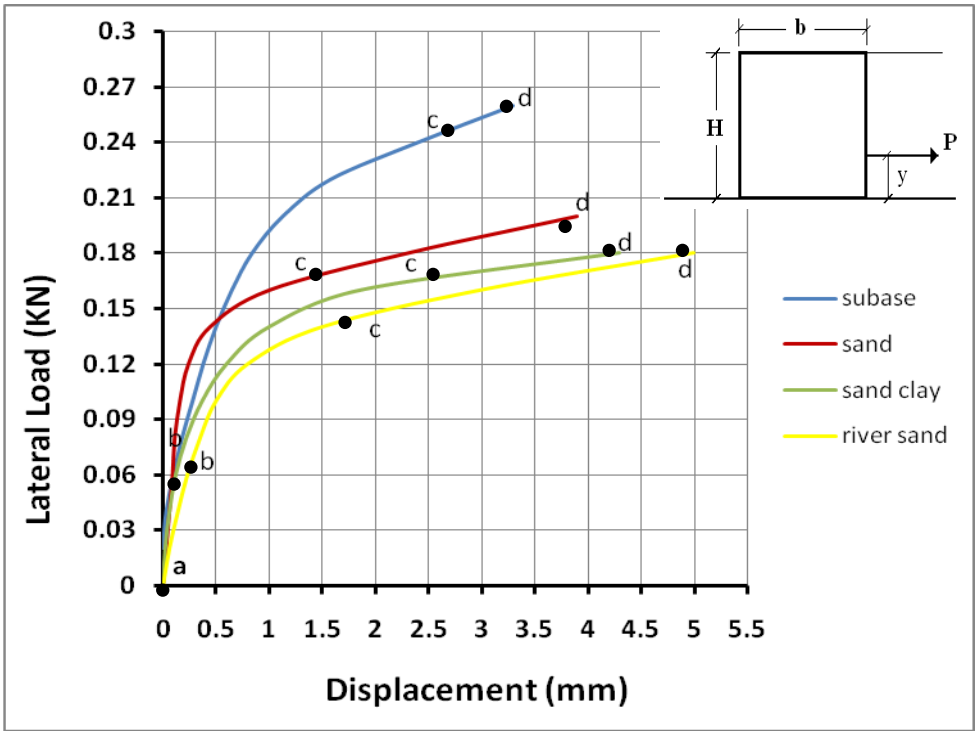

Fig. (4-1): Displacement vs. lateral load, $\frac{b}{H}$ =0.75, and y=10 cm

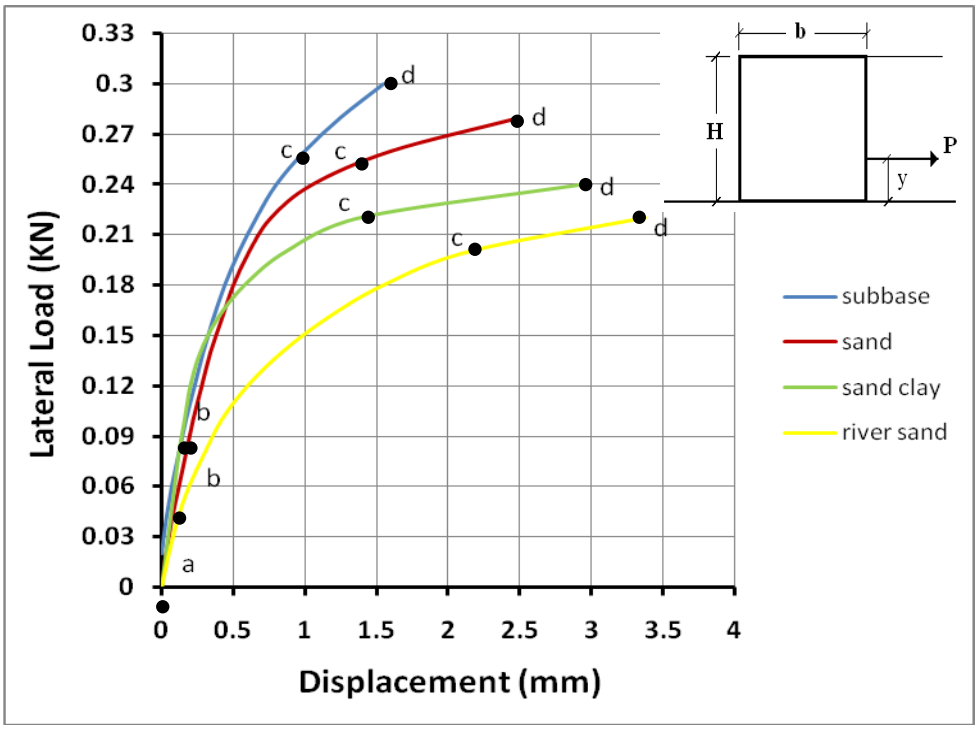

Fig. (4-2): Displacement vs. lateral load, $\frac{b}{H}$ =0.85, and y=10 cm

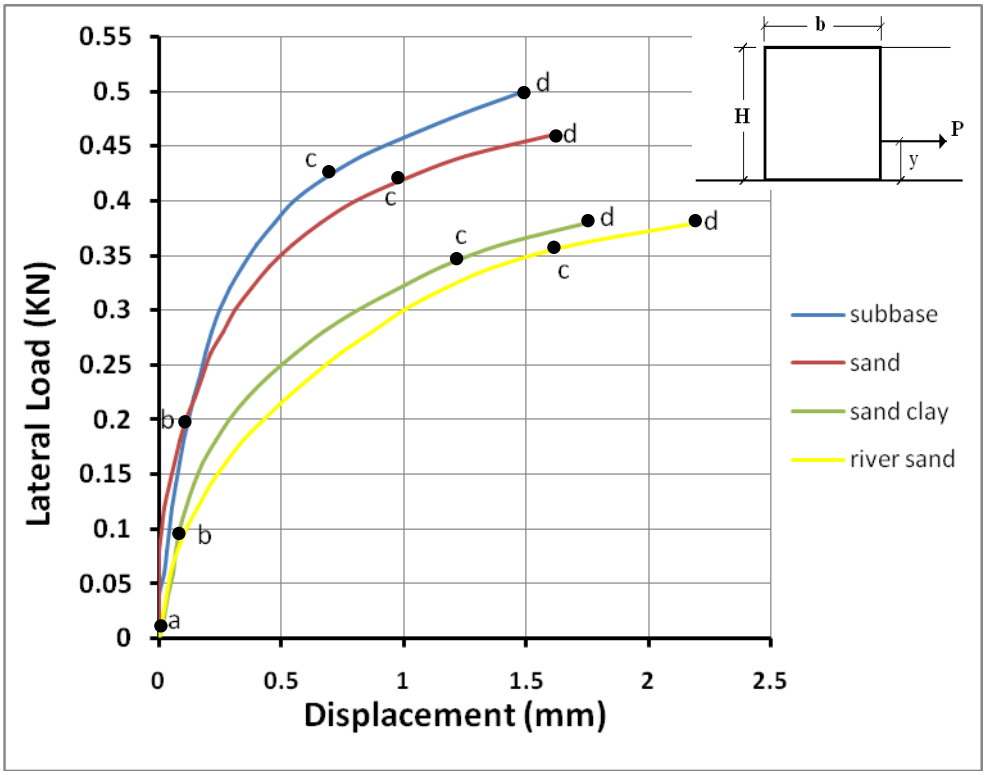

Fig (4-3): Displacement vs. lateral load, $\frac{b}{H}$ =1.0, and y=10 cm.

4.3: Mechanism of Cell Failure

As previously mentioned, all cells have been loaded until failure. It is noticed, that under any loading level below failure, the displacement of any point along the depth of cell consists of two components, translation and rotation. As far as the foundation concern; the translation results mainly from the shear distortion that takes place along the foundation level. The rotation, which results from the applied bending moment, causes a compression on the back side and tension along the front side of the cell. Thus the sheet pile of the back side tends to sink down into the ground as shown in Fig. (4-4-a) while that of front side tends to rise as shown in Fig. (4-4-b). Consequently, shear stresses along the soil/sheet pile interface surfaces are then generated. The amount and direction of these stresses depend on the magnitude and direction of

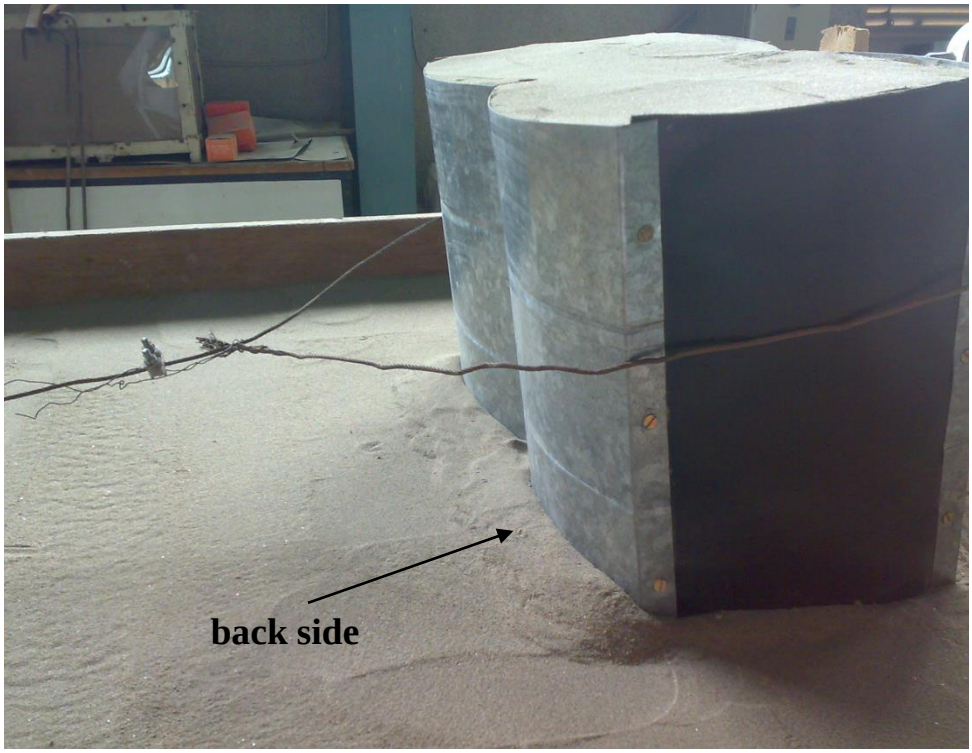

(a)Sink in the back side of the cell

(b) The front side tend to rise

Fig. (4-4): effect of bending moment on cell.

the relative displacement. The soil may therefore be slipped along the sheet pile wall or stick to that wall depending on weather the mobilize shear stress exceeds the shearing resisting shear or not. Besides, relative displacement along the sheetpile elements that caused by an even vertical shear may also occur. General shear failure in the foundation taken place when the ultimate bearing capacity is exceeded. Problems related to inadequate foundations result from the presence of a soft weak or highly compressible soil layer at or near the base of the cell, [**Swatek, (1967)]**.

Figure (4-5) indicates a possible bulkhead failure due to the presence of a weak soil beneath the cell. A general bearing capacity failure or a partial at the toe may be occurred causing the cell to sink or rotate excessively.

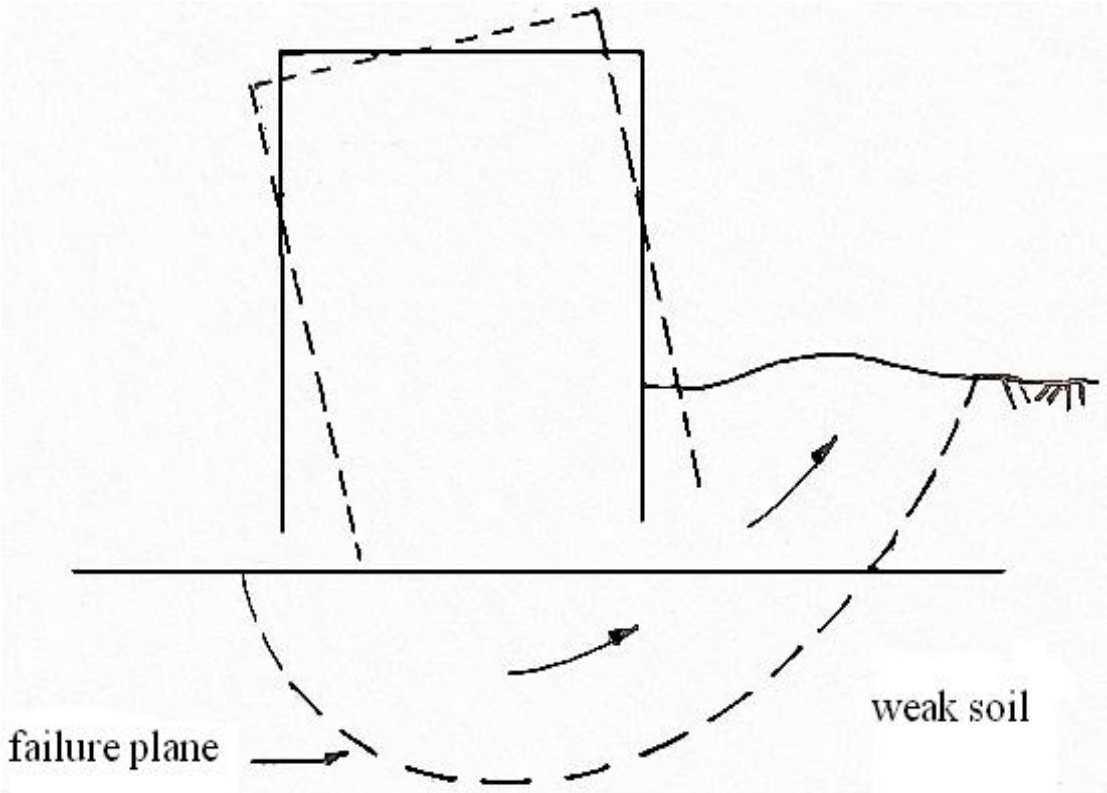

Fig. (4-5): Bearing capacity failure.

Shear failure in a relatively thin, weak zone may occur in a different manner Fig. (4-6). As the cell is filled, the soft material is squeezed out laterally in a mud. Large settlements in the middle of the cell may, therefore, result. The sheetpiles, then, subjected to a negative skin friction similar to that occurred in a pile foundation. [**Swatek, (1967)]**.

A highly compressible layer, such as soft clay or organic silt, could also result in distress to the cellular structures. Compression of this layer can cause large settlements of the cell, leading to distress of the surface topping of bulkhead. If the compressible material occurs in pockets beneath the cell, differential settlements may cause excessive tilting. [**Swatek, (1967)]**.

Experience with bulkhead construction, **[Schroeder, (1977)]**, stated that settlements in excess of nine inches can occur even if the foundation conditions are good.

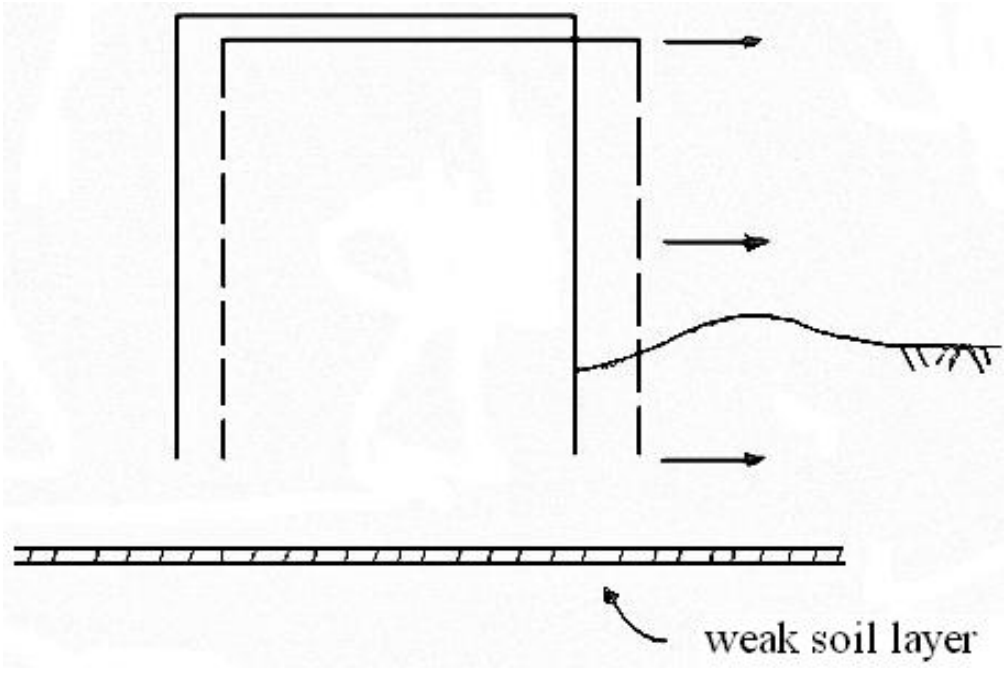

Fig. (4-6): Sliding due to zone of weakness.

Although such settlement may uniform and occur mostly during construction, it can be cause problems of alignment with appurtenant attached structures such as fender pile system.

Along the direction of loading, there are two modes of deformation that taken place; compression (passive) at the front side and expansion (active) at the back side. As stated by many authors **[Terzaghi, (1945)]**, the active failure is soon taken place while the passive failure requires much more displacement to generate. The cell resisting in this respect is mainly dependent on the soil passive resistance. Since the later passive resistance, is strongly dependent on the depth of point under consideration. Thus it may be anticipated that a progressive passive failure is taken place into the soil mass after each load increment. That is; a new location of the passive failure surface is generated after each load increment, therefore, if the sheet pile elements are well connected, and can safely withstand loading the only possible failure will be an external failure that is; sliding, overturning or shear failure in the foundation. Local failure between sheets elements under the influence of hoop tension may also be anticipated when these elements are poorly interlocked. However, the displacement of any point along the cell depth, which consists of translation and rotation, is strongly related to the applied bending moment. That is; when the load is applied at the ground surface (no bending moment) the cell will be subjected to a pure translation. The cell failure in this case will be pure shear failure. **[Schroeder, (1977)]**

4-4: Effect of Loading Height

All the cells were placed on the ground surface. It is worth mentioned that a pure translation failure has taken place for all cells if the load exerted close to the base while an overturning failure was taken place under (300 mm) height of loading. Thus, the results may indicate that the overturning resistance

of cell is generally greater than that of the sliding. The sliding resistance should be:

$$P = W * \tan\emptyset, \quad (4\text{-}1)$$

Where:

P = the lateral load.

W = the weight of the cell,

$\emptyset$ = the angle of friction of the cell fill.

on the other hand, the ultimate load that cause overturning failure may be estimated as:

$$P.y = W * \frac{b}{2}, \quad (4\text{-}2)$$

$$\text{thus, } P = W * \frac{b}{2y}, \quad (4\text{-}3)$$

where:

y = height of lateral load.

b = the cell width.

For the cases under consideration where ($\emptyset$, b and y) are known, a comparison between the values of (P) resulted from eq. (4-1) and eq. (4-3) was listed in table (4-1). This table indicate that the overturning resistance greater than the sliding resistance.

In an attempt to define the critical height above which an overturning failure is taken place, the value of (P) obtained from equation (4-1) is equated to that of equation (4-3).

$$W * \tan\emptyset = W * \frac{b}{2y}, \quad (4\text{-}4)$$

$$\therefore y_{cr} = \frac{b}{2\tan\emptyset}$$

The (y_{cr}) values for all tests are listed in Table (4.2).

Table (4.1): The anticipated values of cellular resistance.

soil type		$(\frac{b}{H} = 1.0)$	$(\frac{b}{H} = 0.85)$	$(\frac{b}{H} = 0.75)$
subbase	***Sliding resistance***	0.78*W	0.78*W	0.78*W
	Overturning resistance	1.5*W	1.275*W	1.125*W
sand passing sieve No.4	***Sliding resistance***	0.661*W	0.661*W	0.661*W
	Overturning resistance	1.5*W	1.275*W	1.125*W
River sand	***sliding resistance***	0.612*W	0.612*W	0.612*W
	Overturning resistance	1.5*W	1.275*W	1.125*W
Sandy clay	***Sliding resistance***	0.383*W	0.383*W	0.383*W
	Overturning resistance	1.5*W	1.275*W	1.125*W

Table (4-2): The y_{cr}(mm) values for all tested models.

Type of soil	Angle of friction	$\frac{b}{H} = 1.0$	$\frac{b}{H} = 0.85$	$\frac{b}{H} = 0.75$
Subbase	38	192	163	144
Sand passing sieve No.4	33.5	226.6	192.6	170
River sand	31.5	245	208	183.5
Sandy Clay	21	290	232	293

4-5: Effect of $(\frac{b}{H})$ Ratio

To understand the effect of $(\frac{b}{H})$ ratio, three diaphragm cells with different ratio (0.75, 0.85, 1.0) were tested under lateral load applied at one third of the cell height, mean while all the cells were placed at the ground surface, the effect of $(\frac{b}{H})$ ratio was illustrated in Fig. (4-7).

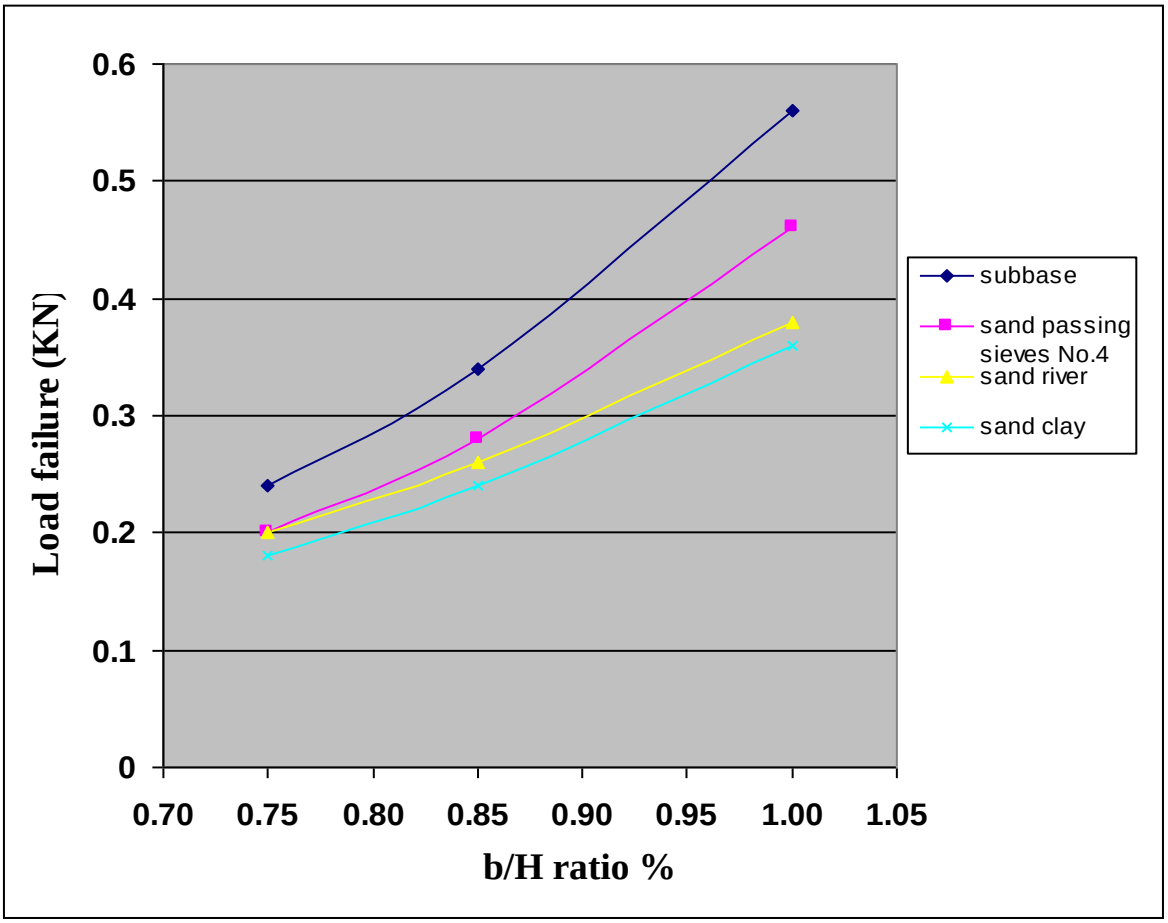

Fig. (4-7): Effect of $(\frac{b}{H})$ ratio on cell filled.

It is clear that the resistance decreases as the $(\frac{b}{H})$ ratio of the cell decreases. This is due to decreasing in the width of cell for the same height leading the weight accordingly the resistance of cell should be decreasing. The ratio of decreasing illustrated in Table (4-3).

Table (4-3): Ratio of decreasing in resistance according to the ($\frac{b}{H}$) ratio.

Type of soil	Decreasing ratio of resistance from $\frac{b}{H} = 1.0$ to 0.85	Decreasing ratio of resistance from $\frac{b}{H} = 0.85$ to 0.75	Decreasing ratio of resistance from $\frac{b}{H} = 1.0$ to 0.75
Subbase	39%	29.4%	57%
Sand passing No.4	38.6%	28.5%	56.4%
Sandy clay	33.3%	25%	50%
River sand	31.5%	23%	47%

4-6: Effect of Soil Type

To show the effect of soil type which be used in the cell fill, the failure load of diaphragm cell is drawn against type of soil, as shown in Figs. (4-8). It is clear that the cell resistance decreased as the unit weight and the angle of friction of fill decreased (river sand and sandy clay), when width to depth ratio decreased from 1 to 0.75, so that the cell resistance of the subbase greater than the other soils. So that the cell resistance of sand passing No.4 was greater than that in the river sand and sandy clay soils fill because it has a height unit weight and angle of friction. There for the best soil is the maxing between sand , clay and gravel which is represented by subbase soil.

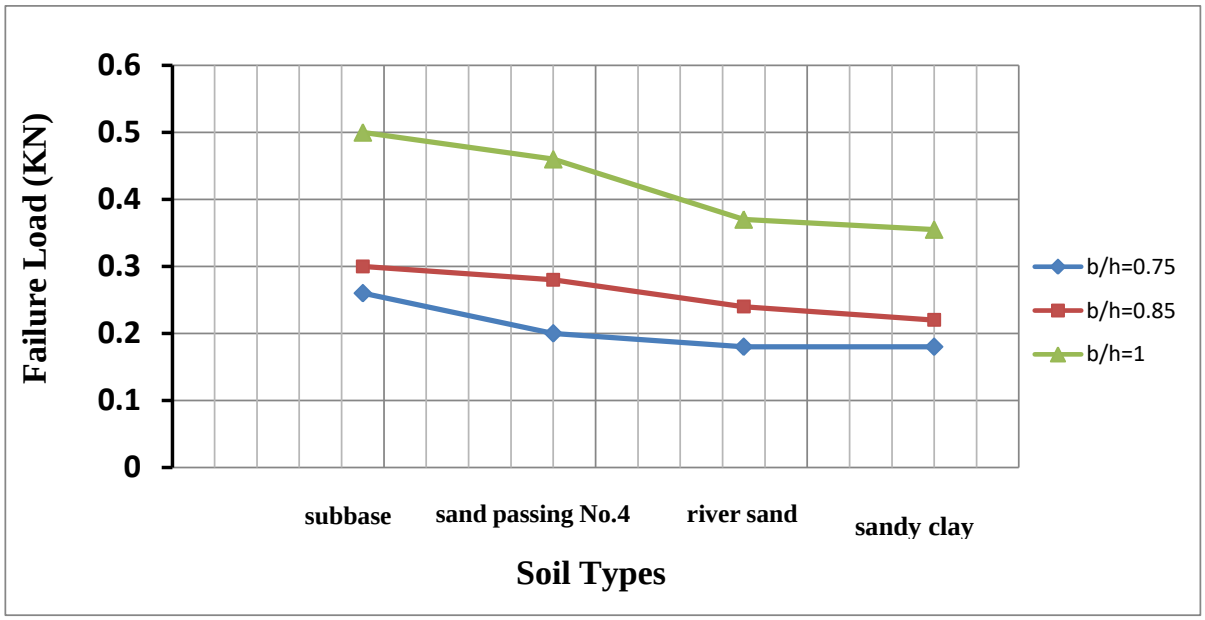

Fig. (4-8): Effect of soil type on cell resistance.

4-7: Effect of Embedment depth

To understand the effects of the embedment depth, a diaphragm cell of 450mm length, 300mm height, 225mm width and subjected to a load applied at one third of the cell height have been tested. The lower end, of the cell considered in study, was placed (0.15, 0.30, 0.45) depth (D) to height (H) ratios below the ground surface. It is worth mention that the curve form vary from cell to others according to the (D/H) ratio and type of soil used in the filling. It was found that the resistance of cell increased and the deformation decreased if compared when the cell was placed on the ground surface. Thus, an embedment of 15% has increase the cell resistance by approximately as much as 8.5%, when used embedment of 30% has increase the cell resistance 25% and the embedment of 45% the cell resistance increased to 32%. The figures from (4-9) to (4-20) is showed the effects of embedment depth on resistance and deformation of the cofferdam. And the tables in the appendix illustrated the effects embedment depth.

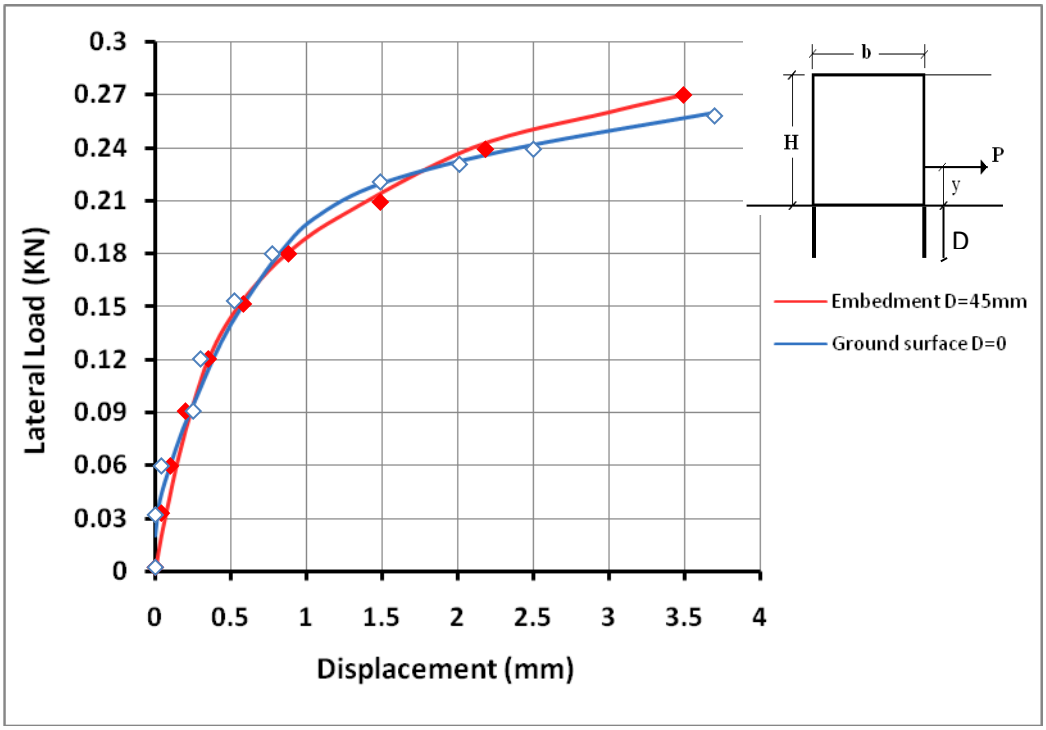

Fig. (4.9): Displacement vs. lateral load for cell filled with subbase, embedment depth D/H=0.15 and y=10 cm.

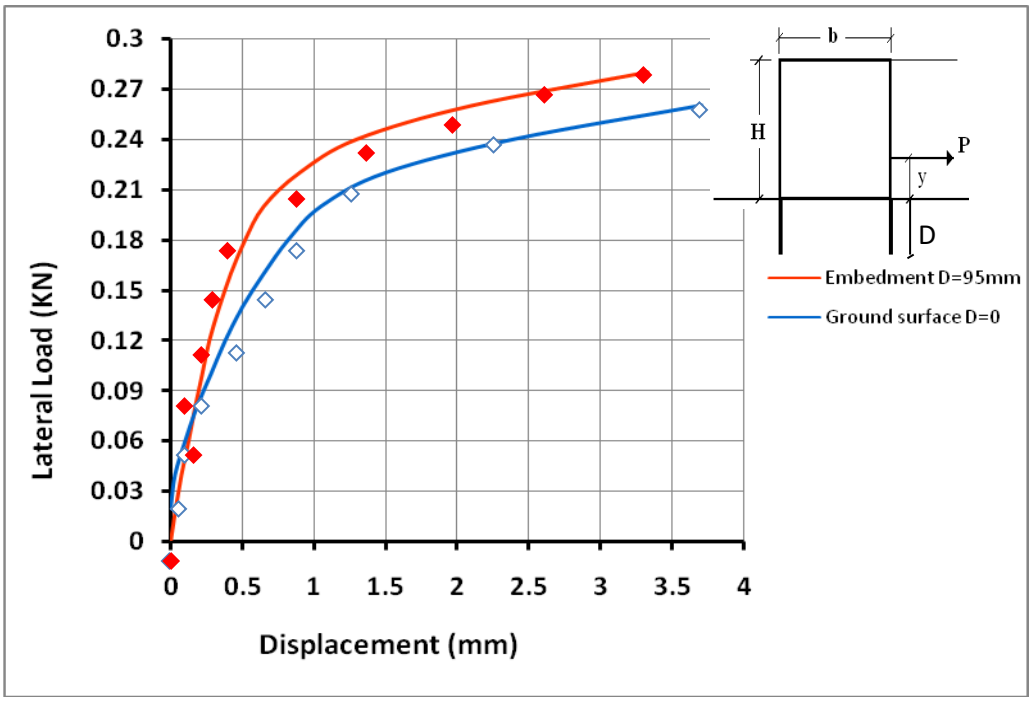

Fig. (4.10): Displacement vs. lateral load for cell filled with subbase, embedment depth D/H=0.3 and y=10 cm .

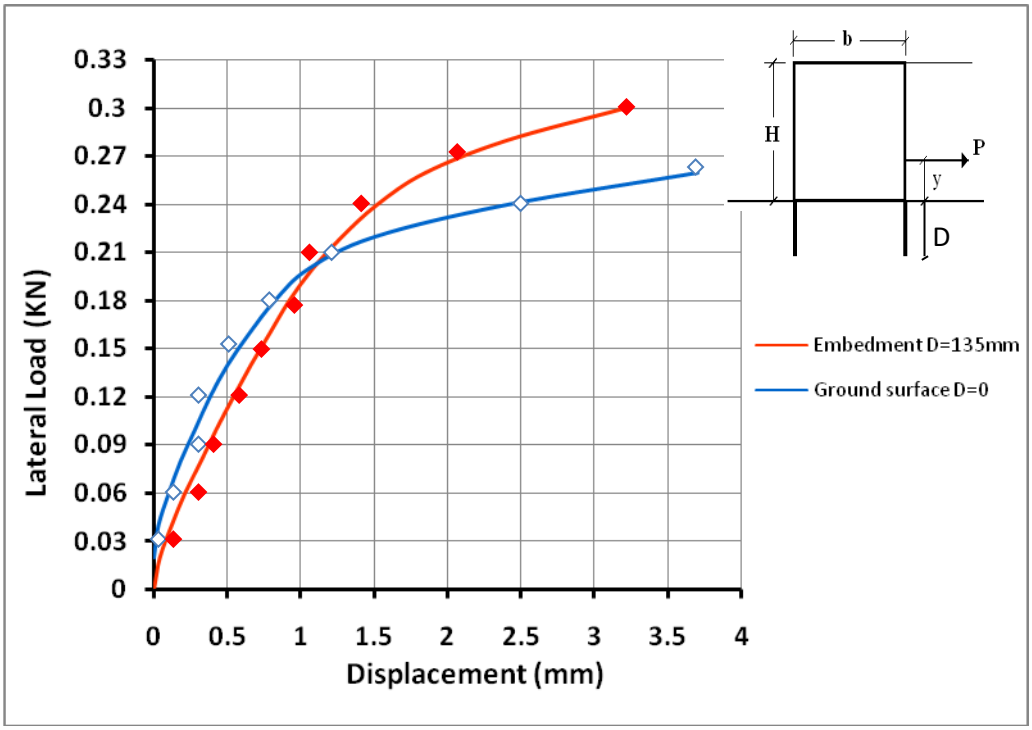

Fig. (4.11): Displacement vs. lateral load for cell filled with subbase, embedment depth D/H=0.45 and y=10 cm

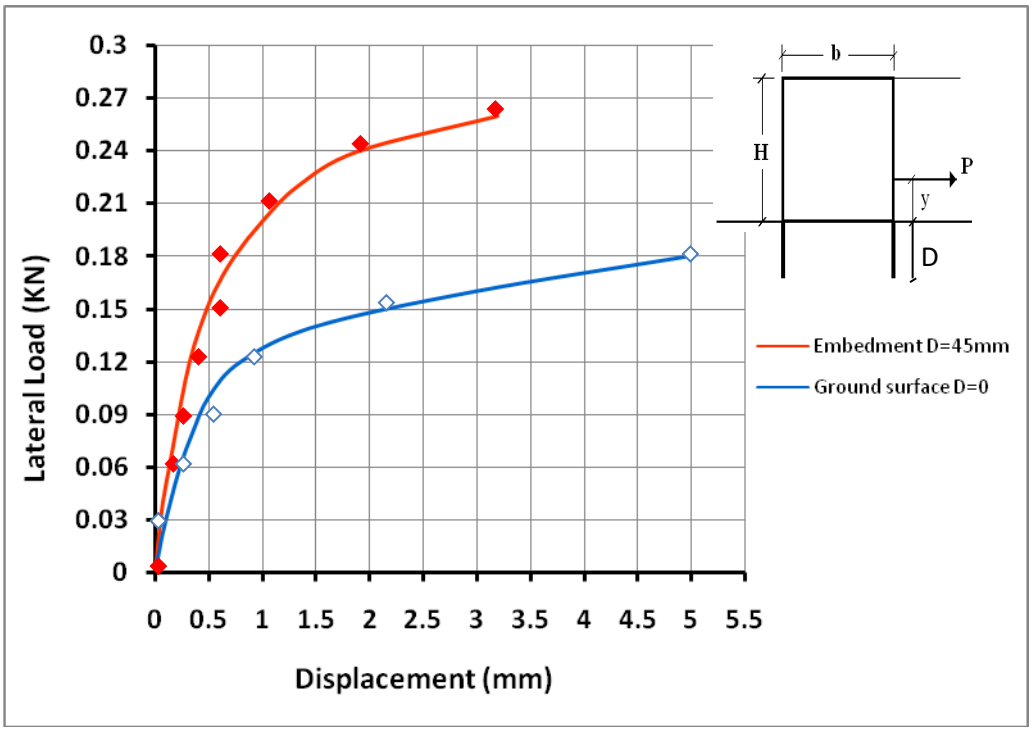

Fig(4-12):Displacement vs. lateral load for cell filled with sand passing sieve No.4, embedment depth D/H=0.15 and y=10 cm .

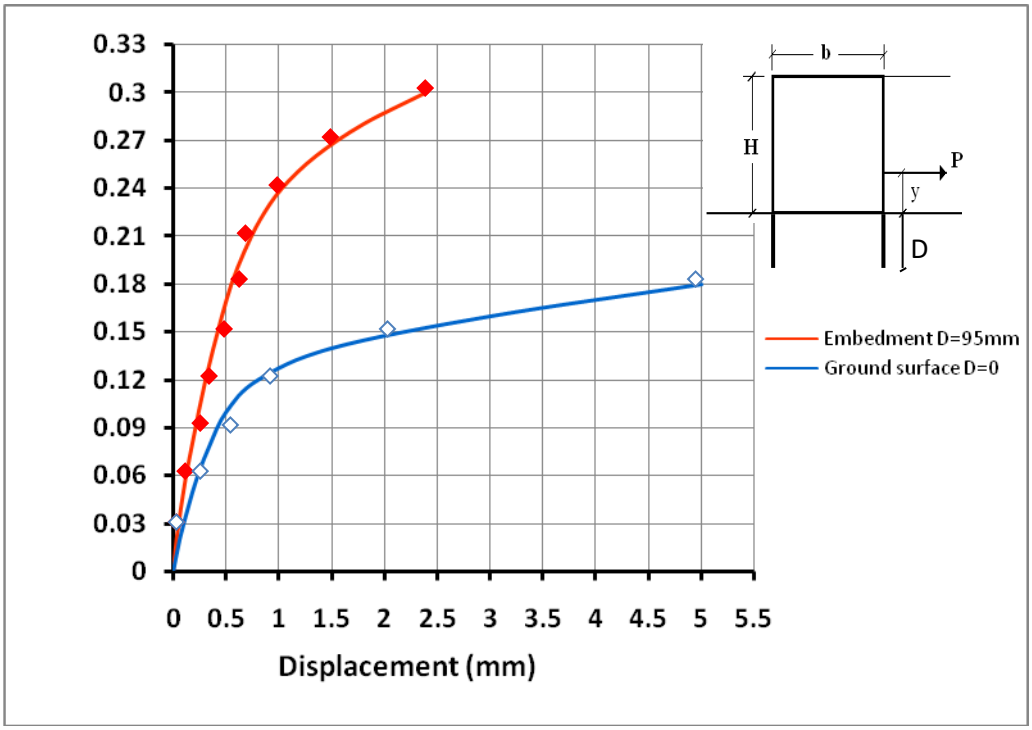

Fig(4-13):Displacement vs. lateral load for cell filled with sand passing sieve No.4, Embedment depth D/H=0.3 and y=10 cm .

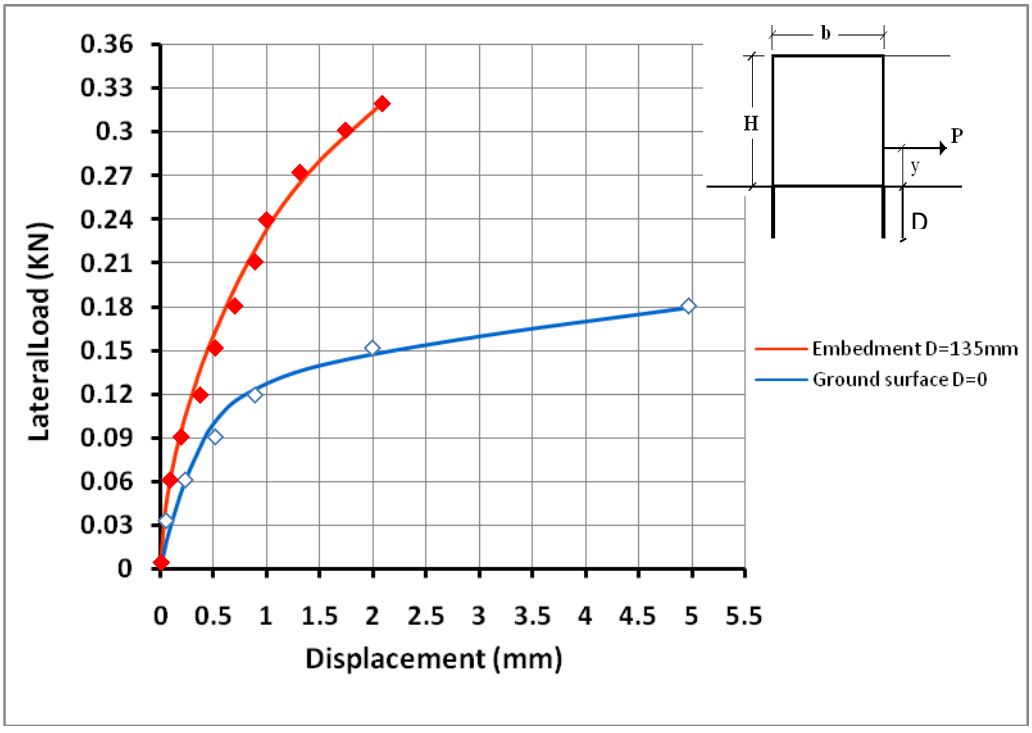

Fig(4-14):Displacement vs. lateral load for cell filled with sand passing sieve No.4, Embedment depth D/H=0.45 and y=10 cm .

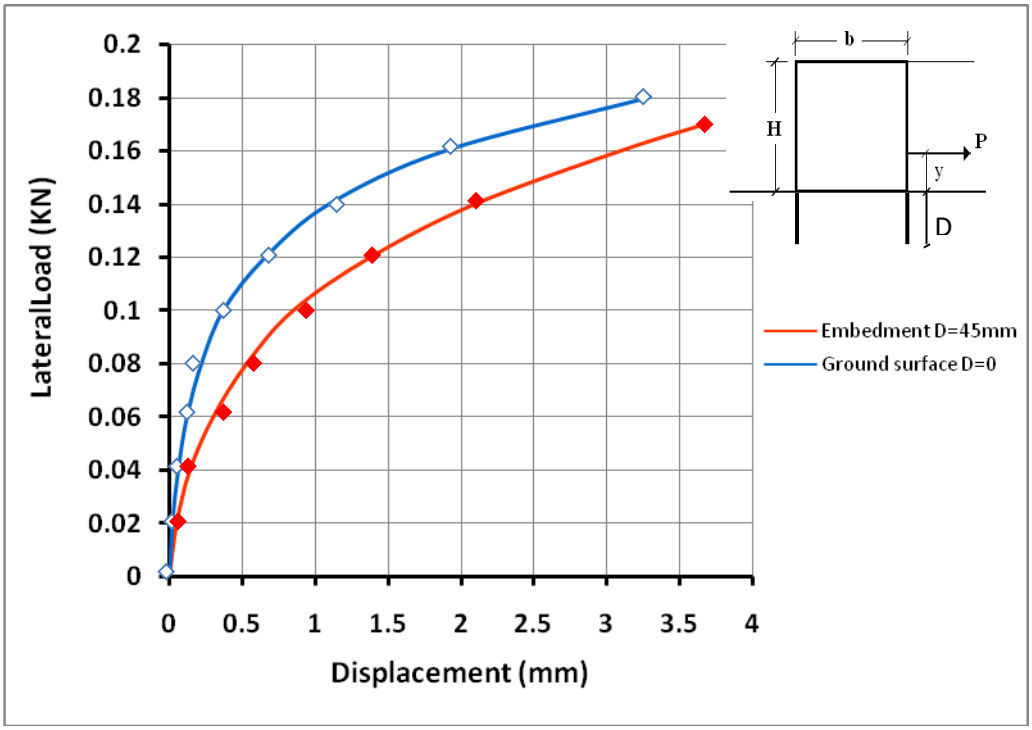

Fig(4-15):Displacement vs. lateral load for cell filled with river sand, Embedment depth D/H=0.15 and y=10 cm .

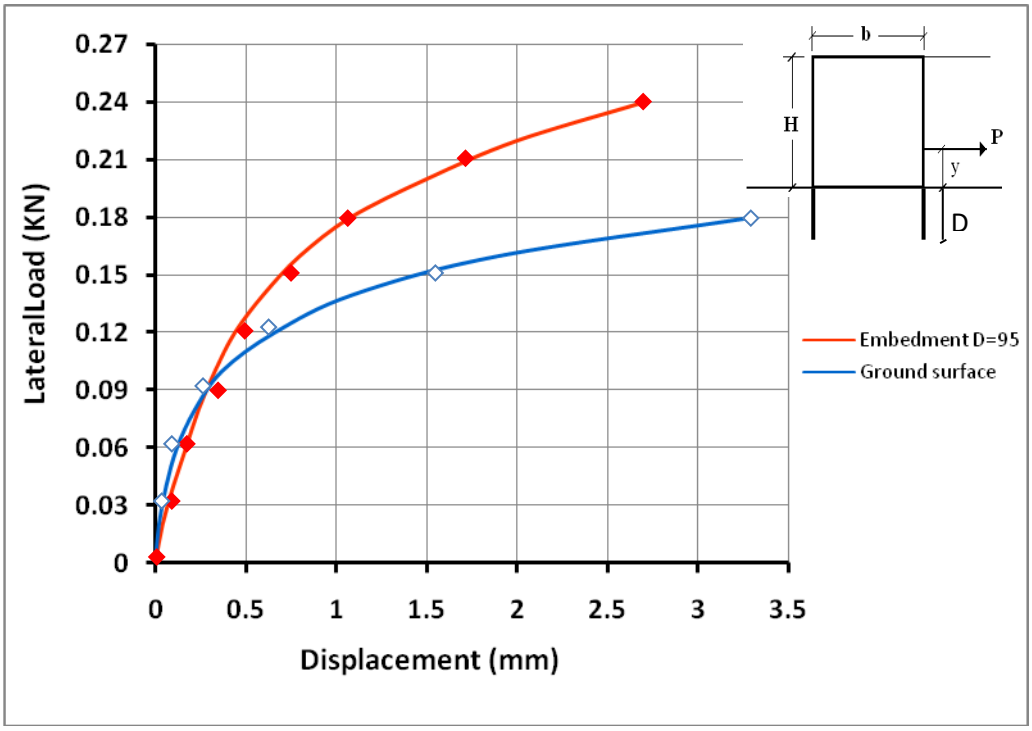

Fig(4-16):Displacement vs. lateral load for cell filled with river sand, Embedment depth D/H=0.3 and y=10 cm .

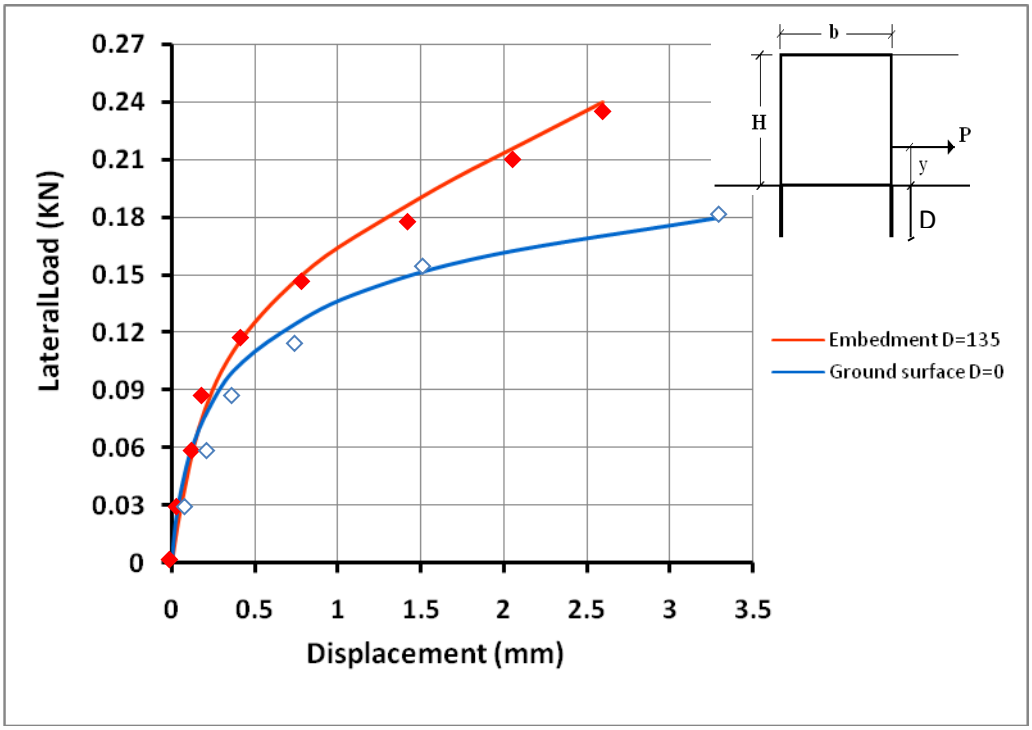

Fig(4-17):Displacement vs. lateral load for cell filled with river sand, Embedment depth D/H=0.45 and y=10 cm .

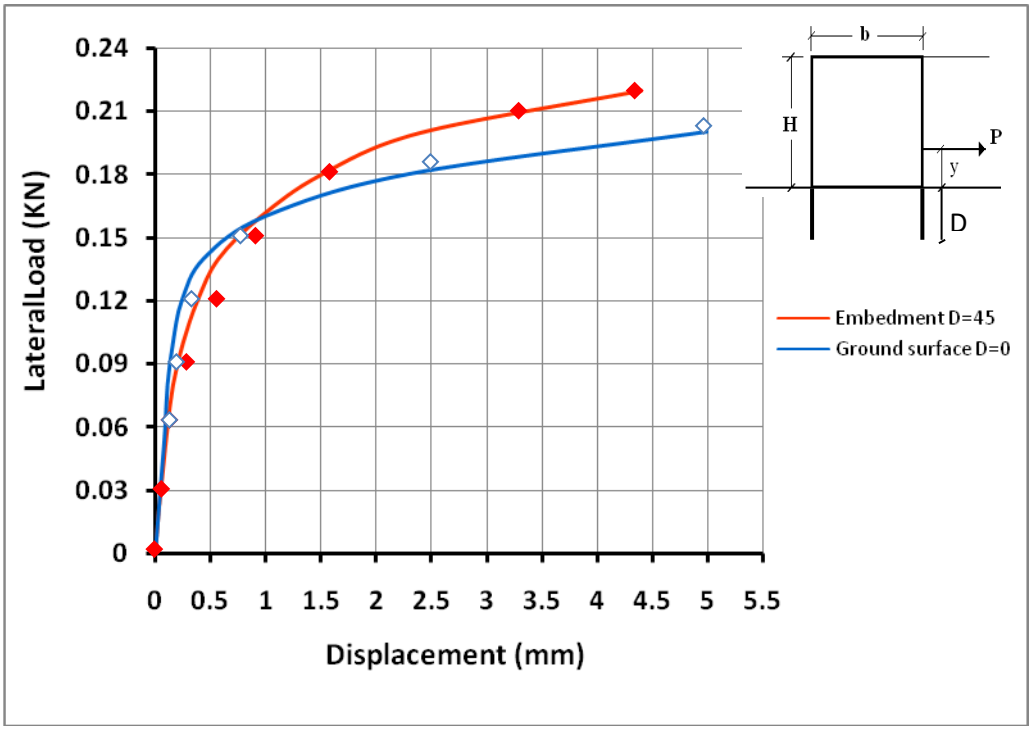

Fig(4-18):Displacement vs. lateral load for cell filled with sandy clay, Embedment depth D/H=0.15 and y=10 cm .

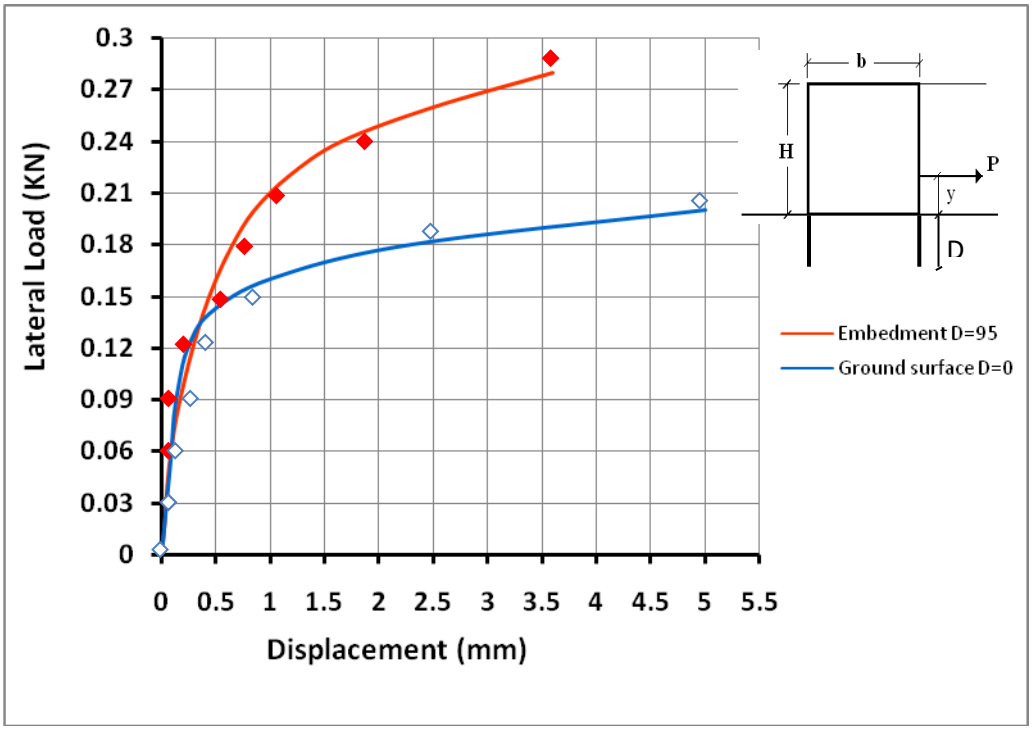

Fig(4-19):Displacement vs. lateral load for cell filled with sandy clay, Embedment depth D/H=0.3 and y=10 cm .

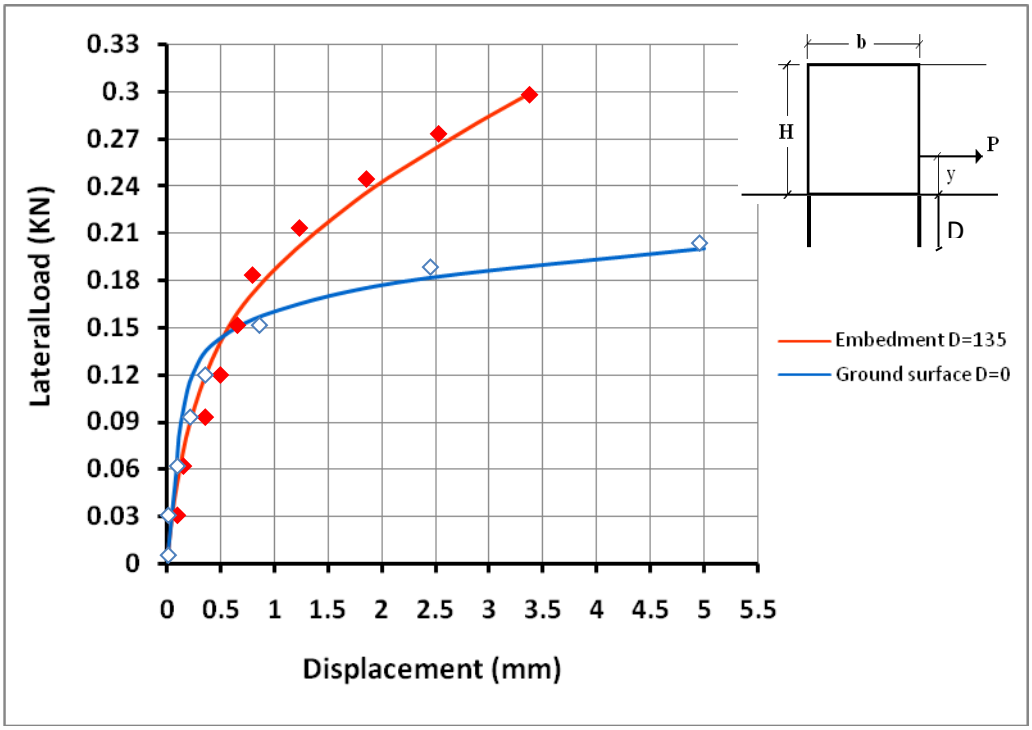

Fig(4-20):Displacement vs. lateral load for cell filled with sandy clay, Embedment depth D/H=0.45 and y=10 cm .

4-8: Brinch Hansen's Equilibrium Method

Where the driving depth of such a cofferdam is shallow (D/H=0.15), the entire dam, at failure, will rotate as one rigid body about a point located below the cofferdam, which getting line rupture, a so-called X-rupture, between the walls, as shown in Figs.(4-21).**[Hansen's, (1953)]**.

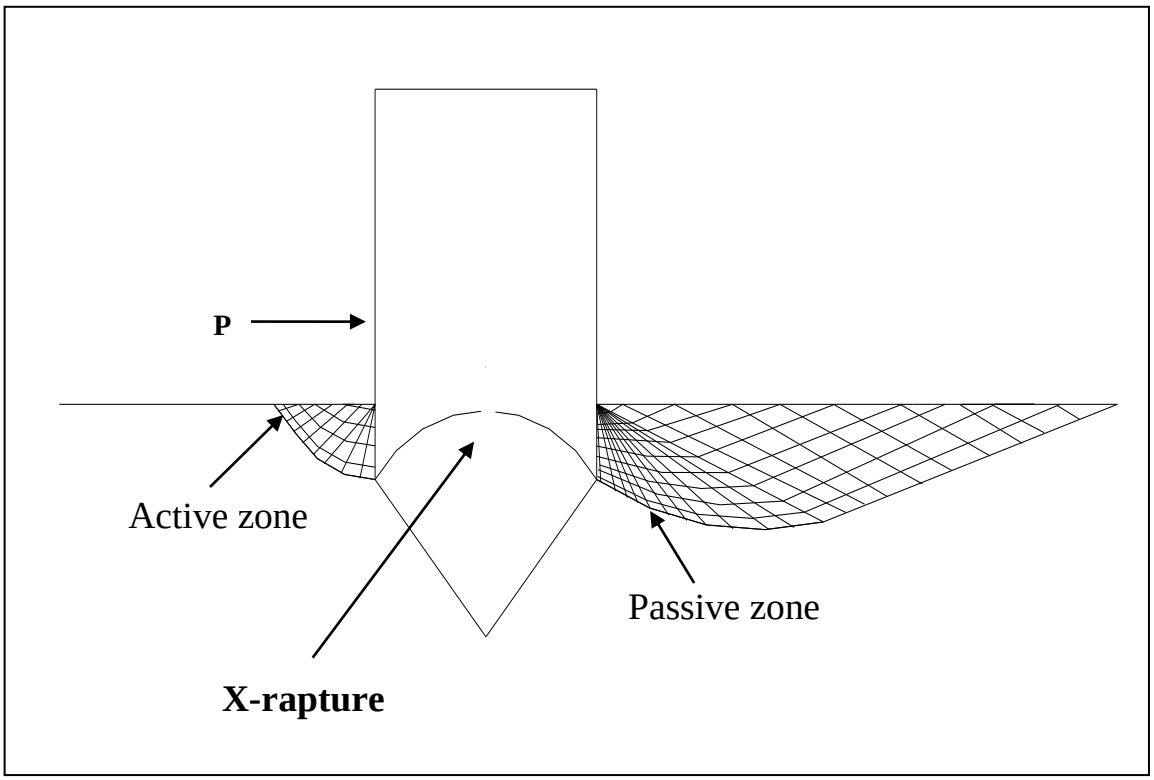

Fig. (4-21): Pattern of rupture for cellular cofferdam on a soil stratum (shallow depth)

Notice that the active zone rupture on the left of the cofferdam's outside and either a passive or composite rupture on the right of the cofferdams outside.

With greater driving depth the cofferdam, when in a state of failure, will rotate about a point located above the foot of the cofferdam, as shown in Fig.(4-22). Between the walls a concave line-rapture, a so-called A-rapture. A composite rupture will appear on the outside of either wall. **[Hansen's, (1953)]**.

.

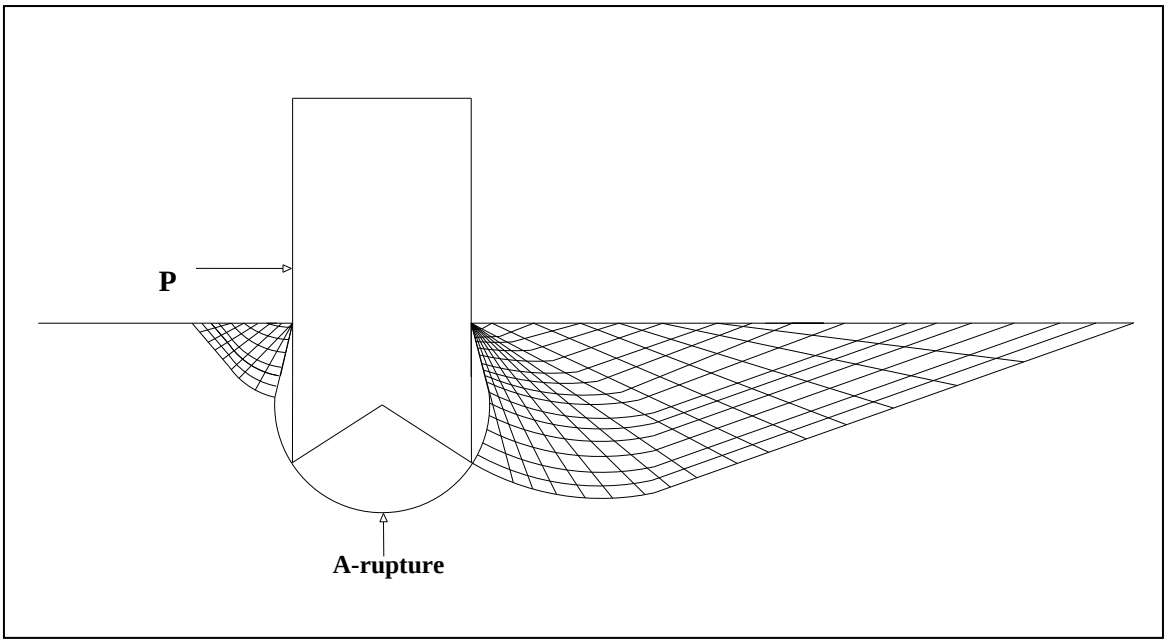

Fig. (4-22): Figure of rupture for cellular cofferdam on a soil stratum

It is noted be that these increase related to passive resistance of soil behind the soil, Fig.(4-23) is shown a resistance forces on cellular cofferdam, the embedment has shallow depth. By projection on the horizontal and vertical, and taking moments about the chord's mid-point the following three equations of equilibrium may be derived:

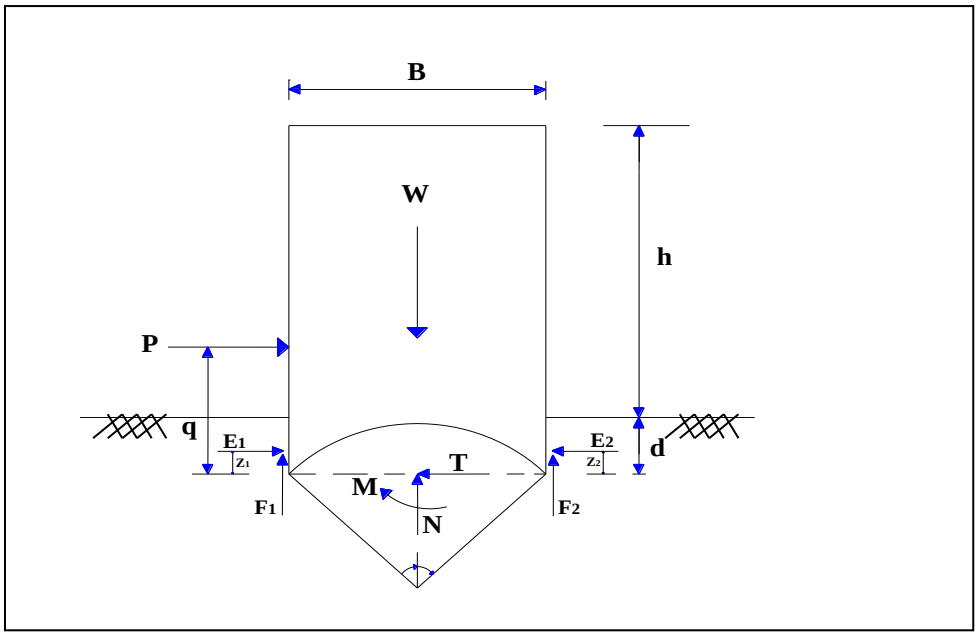

Fig. (4-23): Forces affecting on cellular cofferdam (shallow depth)

$\Sigma F_X=0$

$T=P+E1-E2,$ (4-5)

$\Sigma FY=0$

$N = W – F1 –F2,$ (4-6)

$\Sigma FM=0$

$M = P*q + F1*B/2 + E1*z1 – F2*B/2 – E2*z2,$ (4-7)

In case of very great driving depths (0.45) depth to height ratio as shown in Fig.(4-24). The figure is shows that the affects forcing same forces in previous state, but the difference is the distances from these forces which more stability of cofferdam.

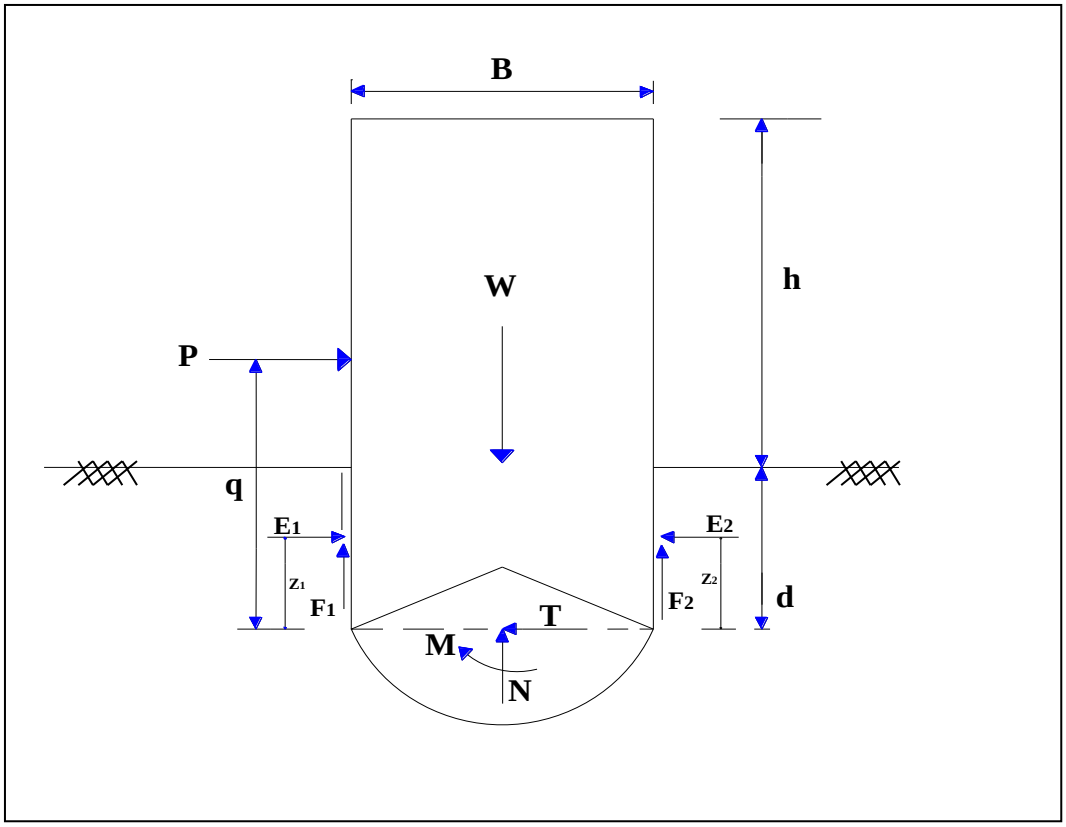

Fig. (4-24): Forces affecting on cellular cofferdam (great depth)

4.9: Evaluation of The Current Design Method

Tables (4-4), (4-5), and (4-6), show comparison between the observed and calculated resistance of different diaphragm cofferdams. The method of calculation has been considered for this purpose, the horizontal shear (Cummings) method. It is clear from the tables, that the Cummings method is overestimating the capacity. The horizontal shear method gives a load capacity which in not good agreement with the observed. And all of tables included the factor of safety (F.S) for each case, a factor of safety for all cases is more than the limited 1.10 to 1.25 that recommended (Bowles 1977) but the factor of safety for the model have been width (b) to height (H) ratios equal to 0.75 is near to limited that show in table (4-4), therefore, the case that the cofferdam have embedment depth based on 0.75 as ratio width (b) to height (H).

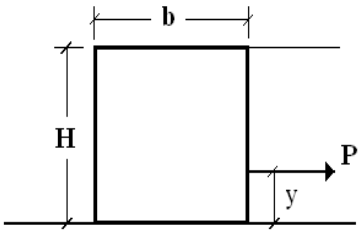

Table (4-4): Comparison of the resistance observed and those calculated by horizontal shear method for cell with (b/H) =0.75

Soil type	H mm	b mm	Resistance KN/m		Difference %	Factor of safety	Remark
			bserved	calculated			
Subbase	300	225	0.57	0.76	-25%	1.21	in all cases, the load applied at one third of the cell height.
Sand passing No.4	300	225	0.45	0.75	-40%	1.23	
River sand	300	225	0.40	0.56	-28%	1.28	
Sandy clay	300	225	0.40	0.37	8%	1.31	

Table (4-5): Comparison of the resistance observed and those calculated by horizontal shear method for cell with (b/H)=0.85

soil type	H mm	b mm	resistance KN/m		difference %	Factor 0f safety	remark
			observed	calculated			
subbase	300	255	0.68	0.93	-27%	1.55	in all cases, the load applied at one third of the cell height.
sand passing No.4	300	255	0.55	0.90	-38.8%	1.63	
River sand	300	255	0.43	0.69	-36%	1.71	
Sandy clay	300	255	0.47	0.44	+7%	1.67	

Table (4-6): Comparison of the resistance observed and those calculated by horizontal shear method for cell with (b/H)=1.0

soil type	H mm	b mm	resistance KN/m		difference %	Factor 0f safety	remark
			observed	calculated			
subbase	300	300	0.83	1.08	-23%	1.88	in all cases, the load applied at one third of the cell height.
sand passing No.4	300	300	0.76	1.04	-24%	1.81	
River sand	300	300	0.61	0.81	-24%	1.97	
Sandy clay	300	300	0.60	0.52	16%	2.11	

Table (4-7): Comparison of the resistance observed and those calculated by horizontal shear method for cell with (D/H) =0.15

soil type	H mm	b mm	resistance KN/m		difference %	Factor 0f safety	remark
			observed	calculated			
subbase	300	225	0.64	0.86	-25%	1.2	in all cases, the load applied at one third of the cell height.
sand passing No.4	300	225	0.63	0.81	-22%	1.23	
River sand	300	225	0.42	0.62	-32%	1.36	
Sandy clay	300	225	0.5	0.4	25%	1	

Table (4-8): Comparison of the resistance observed and those calculated by horizontal shear method for cell with (D/H) =0.3

soil type	H mm	b mm	resistance KN/m		difference %	Factor 0f safety	remark
			observed	calculated			
subbase	300	225	0.68	0.90	-24.5%	1.3	in all cases, the load applied at one third of the cell height.
sand passing No.4	300	225	0.71	0.92	-23%	1.25	
River sand	300	225	0.57	0.69	-17.3%	1.22	
Sandy clay	300	225	0.64	0.455	40.6%	0.95	

Table (4-9): Comparison of the resistance observed and those calculated by horizontal shear method for cell with (D/H) =0.45

soil type	H mm	b mm	resistance KN/m		difference %	Factor 0f safety	remark
			observed	calculated			
subbase	300	225	0.715	0.99	-27.7%	1.6	in all cases, the load applied at one third of the cell height.
sand passing No.4	300	225	0.79	1	-21%	1.3	
River sand	300	225	0.607	0.75	-19%	1.23	
Sandy clay	300	225	0.67	0.49	37%	0.99	

4.10: Reliability of Results by Statistical Analysis

The results that obtained from experimental tests represent the relation between the deformations that occurred after applied load and the embedment depth, beginning from D/H = 0, 0.15, 0.30 and 0.45 the depth is measured from the ground surface. The tables (4-10), (4-11), (4-12) and (4-13) shows the relation between these variables.

Table (4-10): Effect of embedment depth on deformation for cell filled with subbase

D/H (%)	Load Failure (KN)	Deformation (mm)
0	0.261	3.411
015	0.27	3.282
030	0.285	3.21
045	0.3103	3.852

Table (4-11): Effect of embedment depth on deformation for cell filled with sand passing sieve No.4

D/H (%)	Load Failure (KN)	Deformation (mm)
0	0.201	5.11
15	0.261	3.299
30	0.304	2.706
45	0.3304	2.42

Table (4-12): Effect of embedment depth on deformation for cell filled with river sand

D/H (%)	Load Failure (KN)	Deformation (mm)
0	0.176	3.71
15	0.181	3.521
30	0.241	2.923
45	0.255	2.71

Table (4-13): Effect of embedment depth on deformation for cell filled with sandy clay soil

D/H (%)	Load Failure (KN)	Deformation (mm)
0	0.191	5.106
15	0.213	4.512
30	0.271	3.626
45	0.312	3.426

Then, the results in table (4-10) above using in statistica nonlinear estimation by using Statistica software to create equation deal with three variables are (D) , (F) and (δ), embedment depth , load failure and deformation respectively. At the first, the regression models have the following form as follows:

dependent variable = expression including independent variables

$$\triangle = C_1F - C_2D + C_3 \qquad (4\text{-}8)$$

the equation (4-8) represents the first specify a regression models and loss function, on the left side of the equation specify the dependent variable, represents by the deformation (△), on the right side specify the expression including independent variables; embedment depth (D) and load failure (F), and parameter (C_1 (unitless), C_2 (unitlss), C_3 (mm/KN)) to be estimated. The maximum number of iteration is used equal to (1000) and convergence criterion equal to(0.000001). The table (4-14) shows the functions and parameters that obtained from statistica nonlinear estimation, in addition, squared regression (R^2) and variance explained (V). Table (4-15) gives comparison between the observed and predicted values of deformation.

Table (4-14): Estimation of functions and parameters for subbase soil

Equations	Parameters			variance explained (V) %	square regression (R^2) %
	C_1	C_2	C_3		
△=C_1F-D^2	12.498	0	0	48.95	69.96
△ =C_1F-C_2SIN(D)+C_3	9.612	0.341	0.838	52.41	72.34
△ =C_1SIN(F)^2+C_2COS(D)^2	28.142	1.358	0	53.69	73.27
△ =C_1F-C_2SIN(D)	12.634	0.592	0	61.32	78.35
△ = C_2D^2- C_1SIN(F)^2 +C_3	134.92	19.70	12.34	68.04	82.48
△ = C_3- C_1SIN(F)-C_2COS(D)	82.189	42.79	67.41	75.68	86.99
△ =C_2√D-C_1F+C_3	21.843	0.817	8.993	87.086	93.33
△ =-C_1COS√F-C_2√D+C_3	164.64	1.174	165.2	88.61	94.13
△ =C_1TAN(F) ^{2}-C_2D/2	47.502	4.941	0	90.76	95.27
△ =C_1SIN(F)^2-C_2D-C_3	82.70	4.009	2.068	96.48	98.22
△ =C_1[TAN(4F)]^3-C_1D-C_3	0.059	1.693	-3.118	99.57	99.78
△ =C_1 [TAN(4*F)]^4-C_2D+C_3	0.016	1.42	3.273	99.80	99.90
△ =C_1[4LOG(4F)]^4-C_2D+C_3	1.646	1.073	3.415	99.89	99.95

Table (4-15): Comparison between the observed and predicted values of deformation for subbase soil.

N0.	Observed values (mm)	Predicted values, D (mm)						
		δ for Equ.1	δ for Equ.2	δ for Equ.3	δ for Equ.4	δ for Equ.5	δ for Equ.6	δ for Equ.7
1	3.411	3.261	3.231	3.232	3.316	3.359	3.400	3.296
2	3.282	3.352	3.326	3.330	3.336	3.188	3.167	3.416
3	3.210	3.472	3.471	3.464	3.439	3.451	3.412	3.219
4	3.852	3.675	3.7I6	3.725	3.677	3.754	3.773	3.822

Predicted values, D (mm)					
δ for Equ.8	δ for Equ.9	δ for Equ.10	δ for Equ.11	δ for Equ.12	δ for Equ.13
3.433	3.388	3.438	3.422	3.419	3.416
3.176	3.267	3.213	3.256	3.264	3.269
3.332	3.336	3.265	3.226	3.220	3.217
3.812	3.772	3.837	3.849	3.850	3.851

then, It is clear from the table (4-14) the best function is in the thirteen raw, where the raw is shaded in red colour. and this function has a good squared regression (R^2) equal to 99.95 % and variance explained (V) equal to 99.89 % if comparison with other function is done, so the table (4-15) gives a good predicted values of deformation; therefore, these functions will be depending it in the design of cellular cofferdam and soil material for cell filled is subbase. And so on the function in the final form is:

△=1.64[4LOG (4F)] ^4-1.07D+3.41 (4-9)

The whole previous works as well as the data that used in statistica nonlinear estimation and the final equation were be found for the cells filled with subbase, to return to table (4-11) to treatment these data and create function dependent on embedment depth and soil material; soil in this case is sand passing sieve No.4.

At the first checking the function (4-9), however, use this equation by means of the data in table (4-11), the results can be summarized in the table (4-16)

Table (4-16): Estimation of functions and parameters for sand passing sieve No.4 soil

Equations	**Parameters**			variance explained (V) %	square regression (R^2) %
	C1	**C2**	**C3**		
△=C_1[4LOG(4F)]^4-C_2D+C_3	0.019	3.024	3.703	99.67	99.83
△ =C_1[2LOG(2F))^2-C_2D+C_3	0.237	2.118	3.175	99.827	99.913
△ =C_1 [LOG(2F)]^2-C_2D+C_3	0.951	2.118	3.175	99.827	99.913
△ =C_1[TAN(2F)]^2+C_2*D+C_3	-10.14	6.31	5.717	99.995	99.997
△ =C_1[SIN(2F)]^2+C_2D+C_3	-10.74	1.66	5.718	99.999	99.999

It can be seen from the table (4-16) the function that used with subbase soil, equation (4-9) is a good function with sand passing sieve No.4 soil but if this

equation is modified it will be obtained more confidence function and it represents in the raw has red color in table (4-16), and the function has a good squared regression (R^2) which is equal to 99.999 % and variance explained (V) equal to 99.999 %. The formulation of this function is:

$$\triangle = C_1[SIN(2F)]\ ^2 + C_2D + C_3 \qquad (4\text{-}10)$$

then, substitute the parameters that getting from table (4-16) in equation (4-11) to obtain final form for sand soil:

$$\triangle = -10.74[SIN(2F)]\ ^2 + 1.66D + 5.71 \qquad (4\text{-}11)$$

the table (4-17) shows the predicted values of (△) for the data that concerning with sand soil, the column has red color represents the predicted values is very close if it is compared with the column has green color which it represents the observed values.

Table (4-17): Comparison between the observed and predicted values for deformation for sand passing sieve No.4 soil.

N0.	Observed values (mm)	Predicted values, D (mm)				
		δ for Equ.1	δ for Equ.2	δ for Equ.3	δ for Equ.4	δ for Equ.5
1	5.110	5.110	5.112	5.112	5.108	5.110
2	3.299	3.249	3.260	3.260	3.306	3.296
3	2.706	2.803	2.776	2.776	2.695	2.710
4	2.420	2.371	2.386	2.386	2.424	2.418

After formulation of subbase and sand by functions, these functions is taked and checked with sand river which is using the equation (4-9) for the first case and using the equation (4-11) for the two case for the data in table (4-11), and the results of nonlinear estimation in this case represented by equations

which is shown in table (4-17). Therefore, the best square regression (R^2) equal to 99.999 % and the variance explained (V) equal to 99.999 %.

Table (4-18): Estimation of functions and parameters for river sand soil

Equations	Parameters			variance explained (V) %	square regression (R^2) %
	C_1	C_2	C_3		
△ =C_1 [4LOG(4F)]^4-C_2D+C_3	5.624	2.987	0	76.442	87.431
△ =C_1[4*LOG(4F)]^4-C_2D+C_3	-9.113	3.925	0	94.733	97.331
△ =C_1SIN(F)-C_2COS(D)	-6.768	-4.83	0	97.663	98.824
△ =C_1[4LOG(4F)]^4-C_2D+C_3	0.131	1.134	3.252	98.640	99.318
△=C]SIN(2F)^2+C_2COS(2D)^2+ C_3	-6.237	0.348	4.044	98.884	99.440
△=C_1[TAN(2F)])^2+C_2D+C_3	-3.452	0.870	4.158	99.726	99.863
△ =C_1[LOG(2F)]^2-C_2]D+C_3	0.920	0.918	2.707	99.999	99.999

The seven raw in the table (4-18) shows good function for the river sand; this function is as follows:

△ =C1[LOG (2F)] ^2-C2D+C3 (4-12)

If the parameters (C_1, C_2, C_3) are substituted, the final function will be obtained the following form:

△ =0.92[LOG (2F)] ^2-0.91D+2.7 (4-13)

Table (4-19) shows predicted values of (△) for the data that concerning with river sand.

Table (4-19): Comparisons between the observed and predicted values for deformation for river sand.

N0.	Observed values (mm)	Predicted values, D (mm)							
		δ for Equ.1	δ for Equ.2	δ for Equ.3	δ for Equ.4	δ for Equ.5	δ for Equ.6	δ for Equ.7	δ for Equ.8
1	3.71	3.656	3.646	3.649	3.762	3.650	3.692	3.696	3.710
2	3.521	3.431	3.542	3.562	3.447	3.579	3.532	3.531	3.521
3	2.923	3.243	3.063	3.003	2.911	2.941	2.952	2.943	2.923
4	2.71	2.494	2.603	2.646	2.741	2.692	2.686	2.692	2.71

After obtaining the final function for subbase at function (4-9), sand passing sieve No.4 at function (4-11) and river sand soil at function (4-13), using these functions for checking the deformation that concerning with model has fill sandy clay soil as shown in table (4-20).

Table (4-20): Estimation of functions and parameters for sandy clay soil

Equations	Parameters			variance explained (V) %	square regression (R^2) %
	C_1	C_2	C_3		
$\triangle = C_1 [SIN (2F)] \hat{}2 - C_2 D + C_3$	0.238	4.062	5.026	95.301	97.622
$\triangle = C_1 [4LOG(4F)] \hat{}4 - C_2 D + C_3$	0.204	3.631	4.875	97.108	98.543
$\triangle = C_1 [4LOG(4F)] \hat{}4 - C_2 D + C_3$	3.198	1.303	2.073	99.088	99.543
$\triangle = C_1 [LOG(2F)] \hat{}2 - C_2 \sqrt{D} + C_3$	1.976	0.518	3.263	99.225	99.612
$\triangle = C_1 [LOG(2F)] \hat{}4 - C_2 \sqrt{D} + C_3$	2.541	0.773	2.933	99.952	99.976

Then, from table (4-20) noted the best function has more proportion of variance, which square regression (R^2) equal to 99.976 % and variance explained (V) equal to 99.952 % and has a good parameters values (C1, C2, C3); therefore, choice the function in the five raw that shaded by light red color takes the following form:

$$\triangle = C_1 [LOG (2F)] \hat{}4 - C_2 \sqrt{D} + C_3 \quad \textbf{(4-14)}$$

After substitute the parameters in the equation above are:

$$\triangle = 2.541 [LOG (2F)] \hat{}4 - 0.773 \sqrt{D} + 2.933 \quad \textbf{(4-15)}$$

The table (4-21) represents the comparison between observed and predicted deformation values. Then, the five column in this table has an approximated magnitude which is equal to observed value.

Table (4-21): comparison between the observed and predicted values for deformation for sandy clay soil.

N0.	Observed values (mm)	Predicted values, D (mm)				
		δ for Equ.1	δ for Equ.2	δ for Equ.3	δ for Equ.4	δ for Equ.5
1	5.106	5.059	5.150	5.035	5.093	5.112
2	4.512	4.458	4.364	4.598	4.501	4.504
3	3.626	3.871	3.787	3.664	3.720	3.606
4	3.426	3.280	3.367	3.371	3.354	3.446

Chapter Five

Analysis of Cellular Cofferdam by PLAXIS

5.1: Introduction

PLAXIS is a finite element code specially developed for the analysis of deformation and stability of geotechnical structures. The name PLAXIS is an acronym for plasticity AXISSymetric but the computer code may also be used to solve plane strain problems. The initial brief was to develop an easy-to-use finite element code for the analyses of river embankment on the soft soils of the lowlands of Holland. In subsequent years, PLAXIS was extended to cover most areas of geotechnical engineering. PLAXIS intends to provide a practical analysis tool for use by geotechnical engineering who is not necessarily numerical specialists. Geotechnical application requires advanced constitutive models for simulation of the non-linear and time-dependent behavior of soils.

In order to carry out a finite element analysis using PLAXIS, one needs to model and specify the material properties and boundary conditions. This is done by an input program. To set up a finite element model, the user must create a tow-dimensional geometry model composed of points, lines and other components. The generation of an appropriate finite element mesh and generation of properties and boundary conditions on an element level are automatically preformed by PLAXIS based on the input of geometry model. The final part of the input comprises the generation of water pressures and initial effective stresses to set the initial state. After the geometry has been completed, the data set of material parameters should be composed and assigned to the corresponding geometry components have their properties, the geometry model complete and the mesh can be generated. In order to perform finite element calculations, the geometry has to be divided into elements. A composition of finite elements is called a finite element mesh. The basic elements are 6-node triangular element and the 15-node triangular element. After the generation of a

finite element model, the actual finite element calculation can be executed. The main output quantities of a finite element calculation are the displacements at the nodes and the stresses at the stress points. In addition, when a finite model involves structural elements, structural forces are calculated in these elements. The curve program can be used to draw load- displacement curves, and stress or strain paths of preselected points in geometry. These curves visualize the development of certain quantities during the various calculation phases, which gives an insight into the global and local behavior of the soil (**Brinkgreve**, **2008**). The program will be analyzed the construction by finite element method to obtain the deformation that occurred into cells and calculated the effective stress, sheer stress and horizontal displacements. The study include two case, in the first case the structure of width to depth ratio (b/H) is 0.75 and it is placed on the ground surface; and the second case the structure have been driven into soil with height to embedment depth ratio (D/H) are (0.15,0.3,0.45). In each case the four types of soils have been used (subbase, sand passing save No.4, river sand and sandy clay).

5.2: Creating Geometry Model

In order to carry out a finite element analysis, a geometry model of soil layer is required. For drawing the full geometry contour it is preferred to form a table including the x and y coordinates of each point as the accuracy is higher than that drawing by mouse directly. Consequently lines and clusters are generated geometry contour is completed for each stage. The geometry models created for the structure placed on the ground surface with width to depth ratio (b/H) is 0.75 and the body of structure has driven into soil with height to embedment depth ratio(D/H = 0.45), they are presented in figures (5-1) and (5-2).

5.3: Loads and Boundary Condition

To set up the boundary condition, the standard fixities option is used. As a result a full fixity at the base and free condition at the horizontal side of

geometry are generated. It is worth mentioned that the point loads were take in state failure of cellular cofferdam in the laboratory tests, the point loads for two case in the figures (5-1) and (5-2) are 0.57 KN/m and 0.71KN/m are applied on structure.

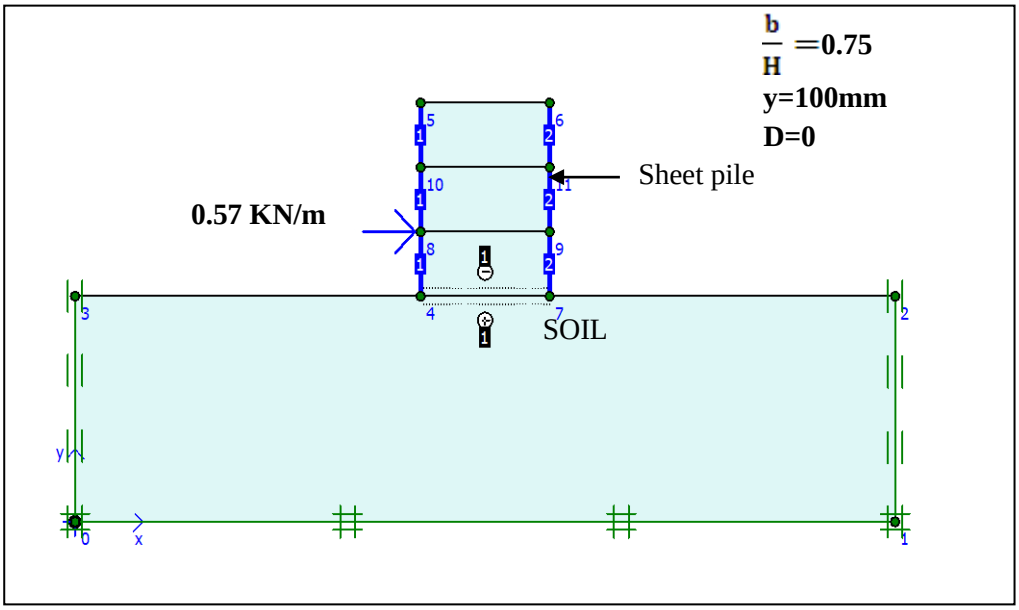

Fig (5-1): Geometry of model for cell filled with subbase

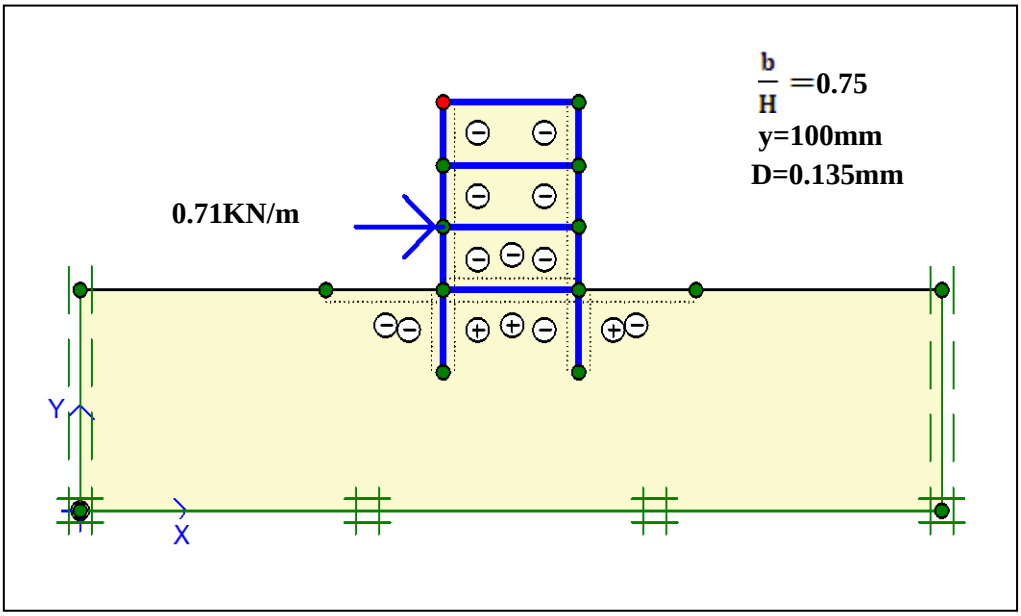

Fig (5-2) Geometry of model for cell filled with subbase

5.4: Setting Material Data Base

Soil properties are stored in material data base. For fill, subbase, sand passing sieve No.4, sandy clay and river sand unit's different material data sets have been created and the material properties are given in Table (5-1).

In order to modeling the PLAXIS requires the soil parameters are obtained from laboratorial tests. In the analysis elastic-plastic Mohr-Coulomb model is used as material model. It involves four parameters namely, Young's Modulus (E) and poison's ratio (ν) effect on soil elasticity, friction angle (ϕ) and cohesion (c) effect on soil plasticity.

5.5: Mesh Generation and Calculation

After assigning the material properties to the related layer, the geometry model required to carry out a finite element analysis has been completed. The second step for the performance of finite element calculations is the division of the geometry into elements. Finite element mesh, which is a composition of the finite elements, is generated fully automatic in PLAXIS. The mesh generated for two cases to the cellular cofferdam as shown in figures (5-3) and (5-4).

Once the mesh has been generated, the finite element model is complete. Before starting the calculations, however, the initial conditions must be generated. In general, the initial conditions comprise the initial groundwater conditions, the initial geometry configuration and the initial effective stress state. The soil layer in the cellular cofferdam project is dry, so there is no need to enter groundwater conditions as shown in figures (5-5) and (5-6).

Table (5-1): Material properties.

Parameter	Name	Subbase	Sand Passing Sieve No.4	River Sand	Sandy Clay	Unit
Material model	Model	Mohr-Coulomb	Mohr-Coulomb	Mohr-Coulomb	Mohr-Coulomb	-
Material of behavior	Drained	Drained	Drained	Drained	Drained	-
Soil unit weight	**γdry**	17.5	16.5	15.3	14.5	KN/m³
Soil unit weight	**γs**	18.4	17.2	16.5	15.7	KN/m³
Young's modules	**E**	10000	7000	7000	4000	KN/m²
Poison's ratio	**ν**	0.15	0.15	0.15	0.15	◦
Cohesion	**c**	1	3	3	7	KN/m²
Angle of friction	**ϕ**	38	34	32	22	◦

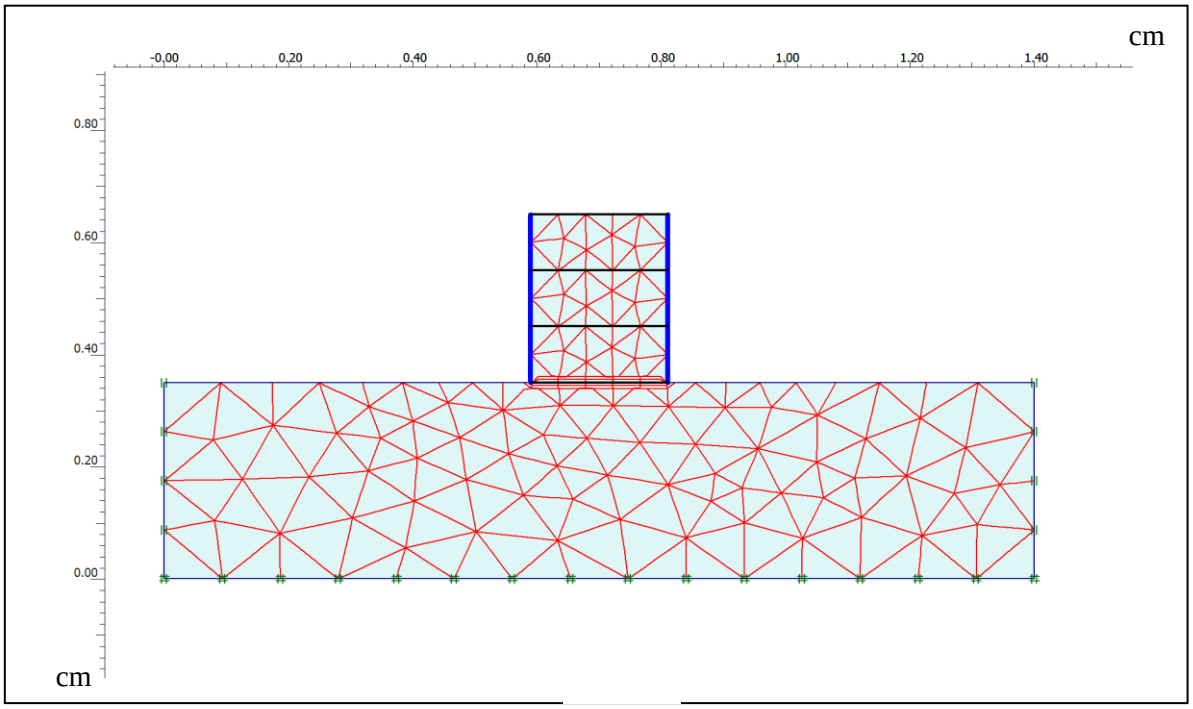

Fig.(5- 3): Generated finite element mesh for cofferdam place on ground surface

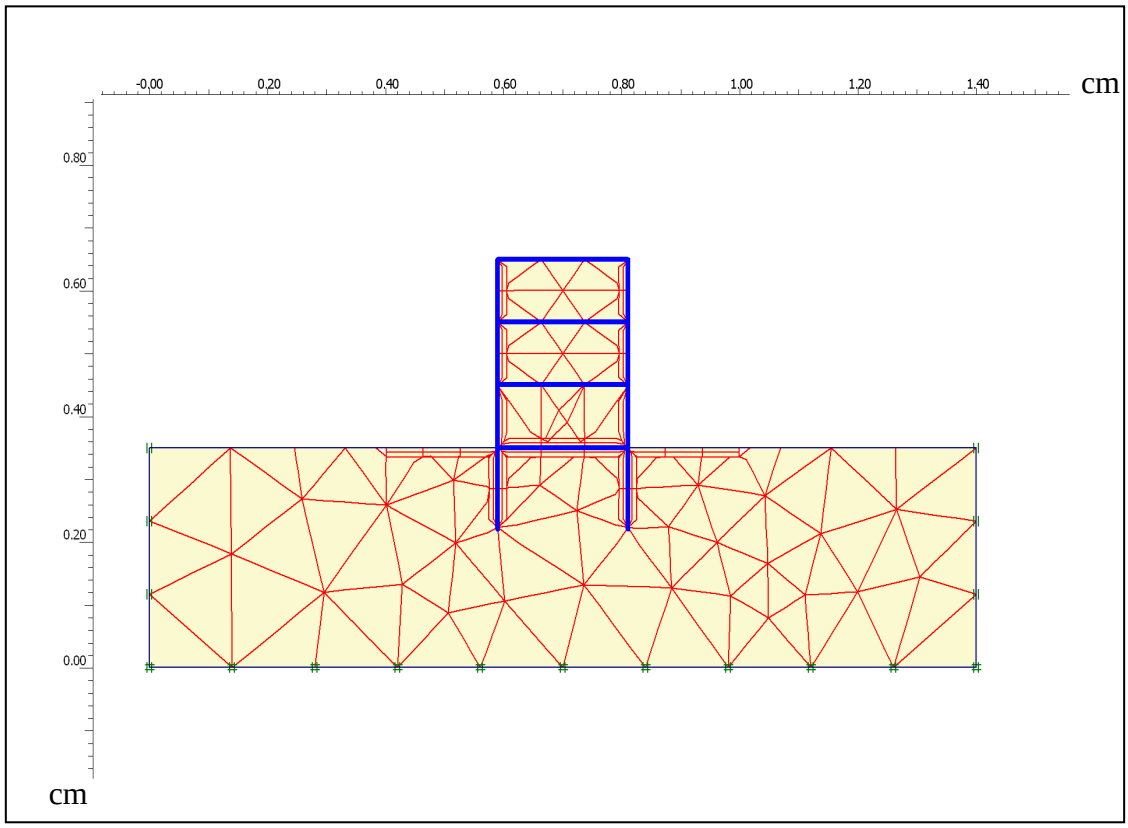

Fig (5-4): Generated finite element mesh for cofferdam with embedment depth

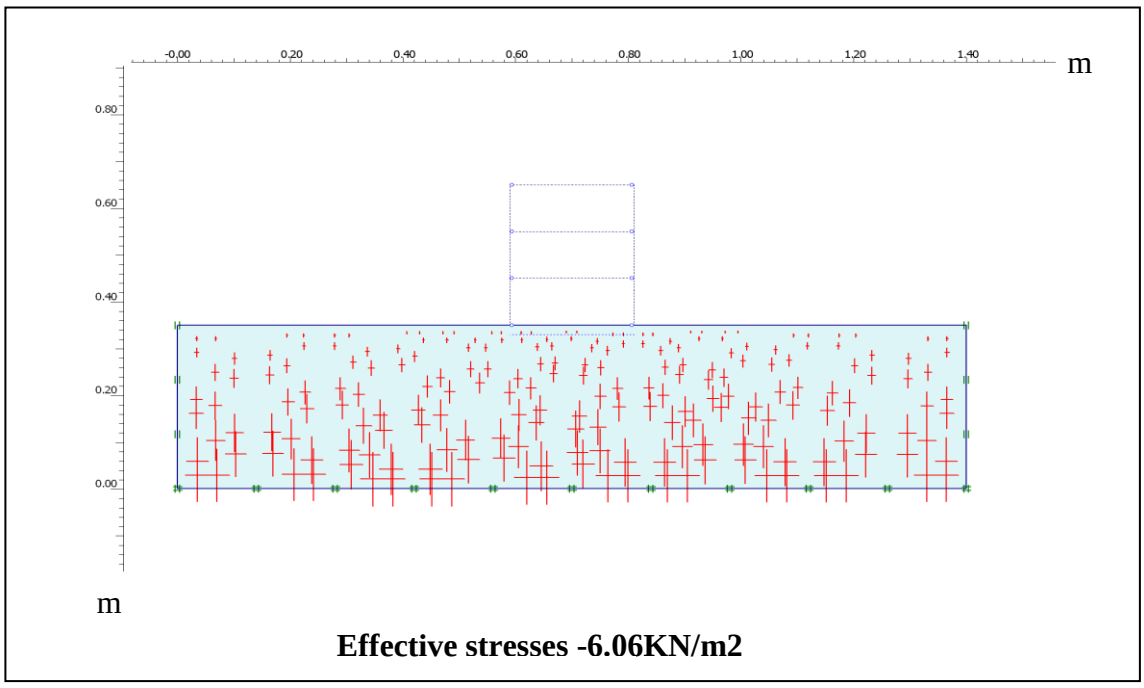

Fig (5-5): Initial Stress Field in the Geometry for cofferdam place on ground surface

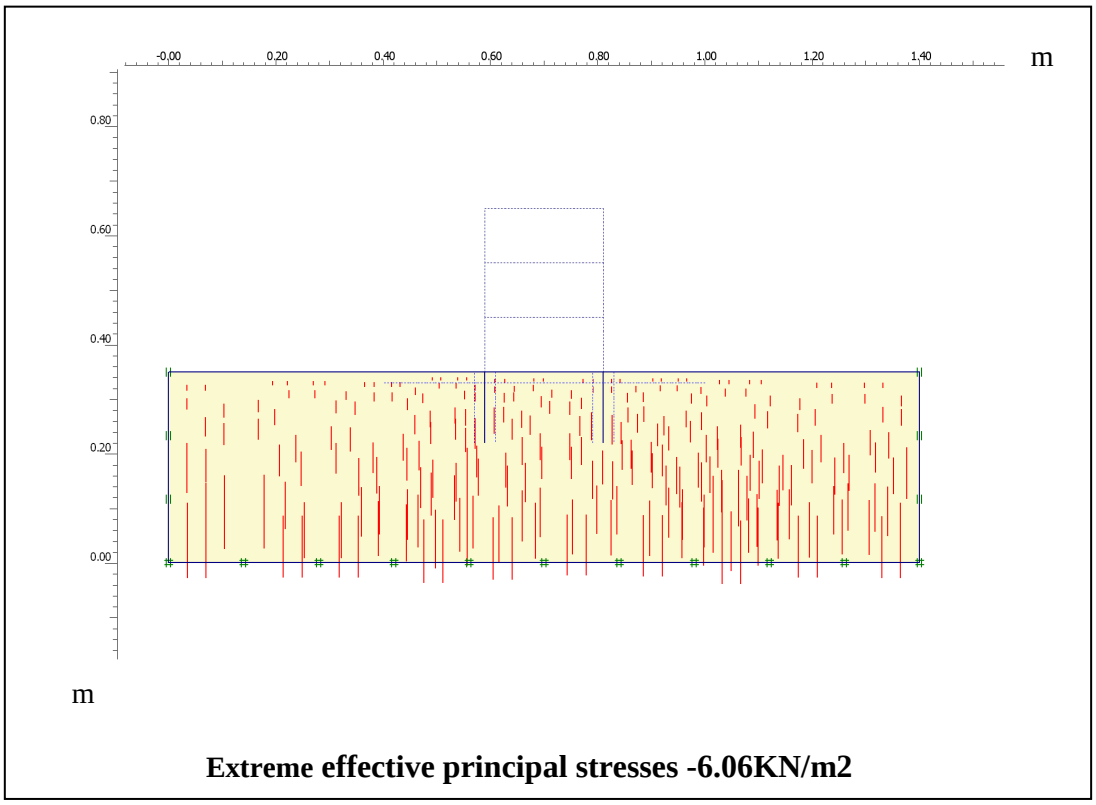

Fig (5-6): Initial Stress Field in the Geometry for cofferdam with Embedment Depth

5.6: Results of Analysis

The calculations were based on values taken from laboratorial tests for each soil. The results obtained are discussed in the following paragraphs.

(i) Deformation Mesh

Fig. (5-7) shows the deformation mesh and the extreme total displacement for cofferdam that placed on ground surface is equals to 3.73 mm. The position of this displacement in the top point of cofferdam, and the Fig. (5-8) illustrates the deformation mash that occurred in structure embedded into soil and the results shows that magnitude of this displacement equal to 2.63 mm; the deformation of embedment structure (D/H= 0.45) is less than this which resulted in case of the structure placed on ground surface.

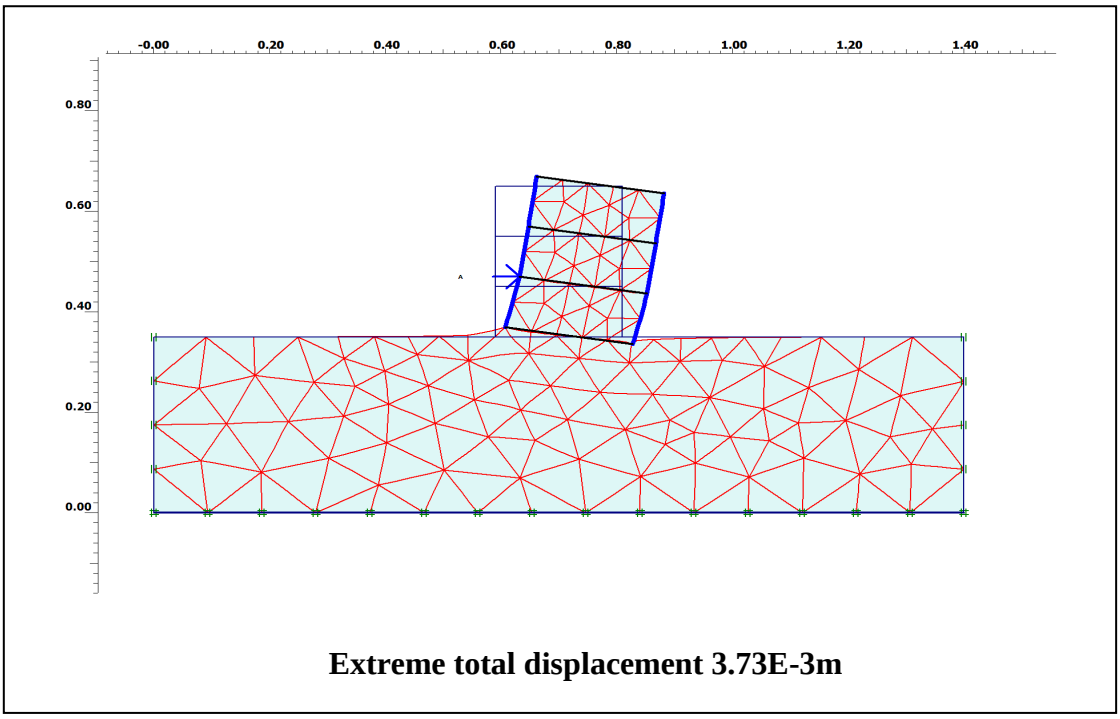

Fig (7): Deformed mesh in the retaining structure and body soil

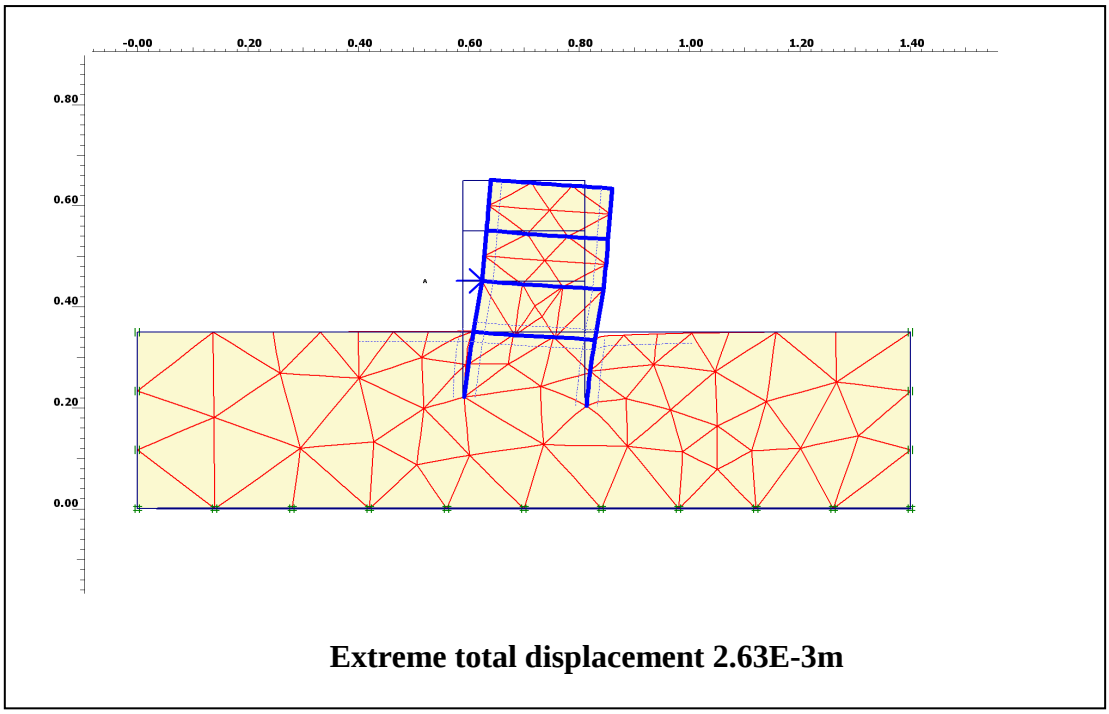

Fig (5-8): Deformed mesh in the cofferdam and body soil in the embedment state

(ii) Effective Stresses on Cofferdam

Figures. (5-9) and (5-10) shows the magnitude and the direction of the principal effective stresses, the menus sing represent the opposite direction of the applied load. The effective stresses are defined as the stress perpendicular to the cross-section. The orientation of the principle stresses indicates large passive zone in beneath part of the load of the cofferdam and continues to the foundation, which the soil under right zone for the cofferdam. It can be seen that the effective stresses at the top of the cofferdam and the right hand side of the foundation are nearly equal to zero. Fig (5-10) shows the stresses by shaded areas which are colored with red color represent the zone large stresses and these zones concerning in toe of the structure.

(iii) Shear Stresses on Cofferdam

From Fig (5-11) the shadings for the shear stresses of the cofferdam placed on ground surface are noted, the shear stress is defined as the shear stress along the cross-section line, it can also be seen that there is maximum shear stress concentration under the right side of the sheet pile (toe zone) which equal to (6.27 KN/m2). And the Fig (5-12) shows the maximum shear stress for cofferdam with embedment depth, all so in toe zone but behind the right side of the sheet pile which equal to (10.22 KN/m2). The shear stress in case the cofferdam have been embedment more than in case the cofferdam place on ground surface is noted. And tables (5-2) and (5-3) illustrated the stresses and strain in body of cofferdams. The stresses and strain for all of cases in appendix A.

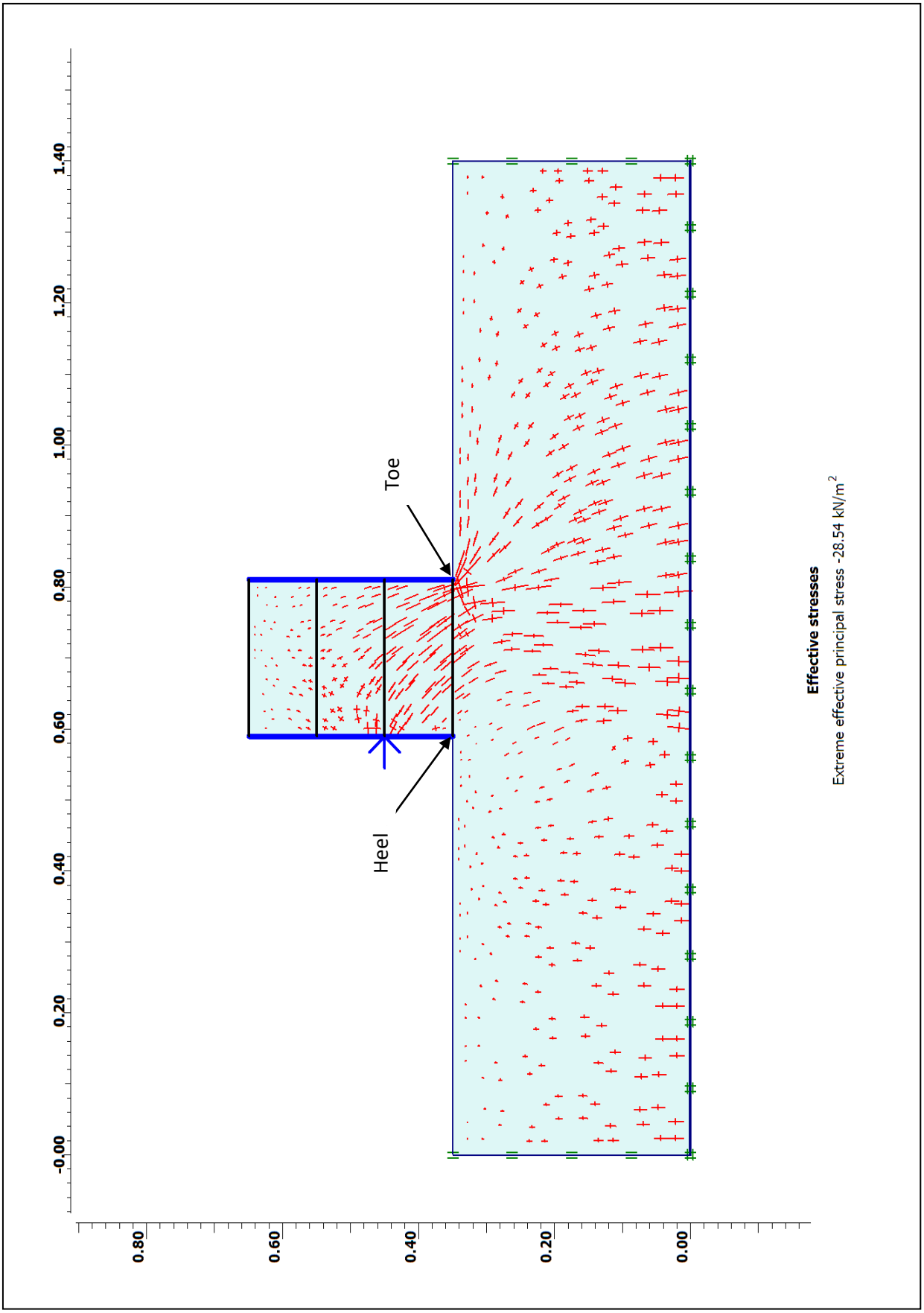

Fig. (5-9) Effective principal stress of cellular cofferdam on ground

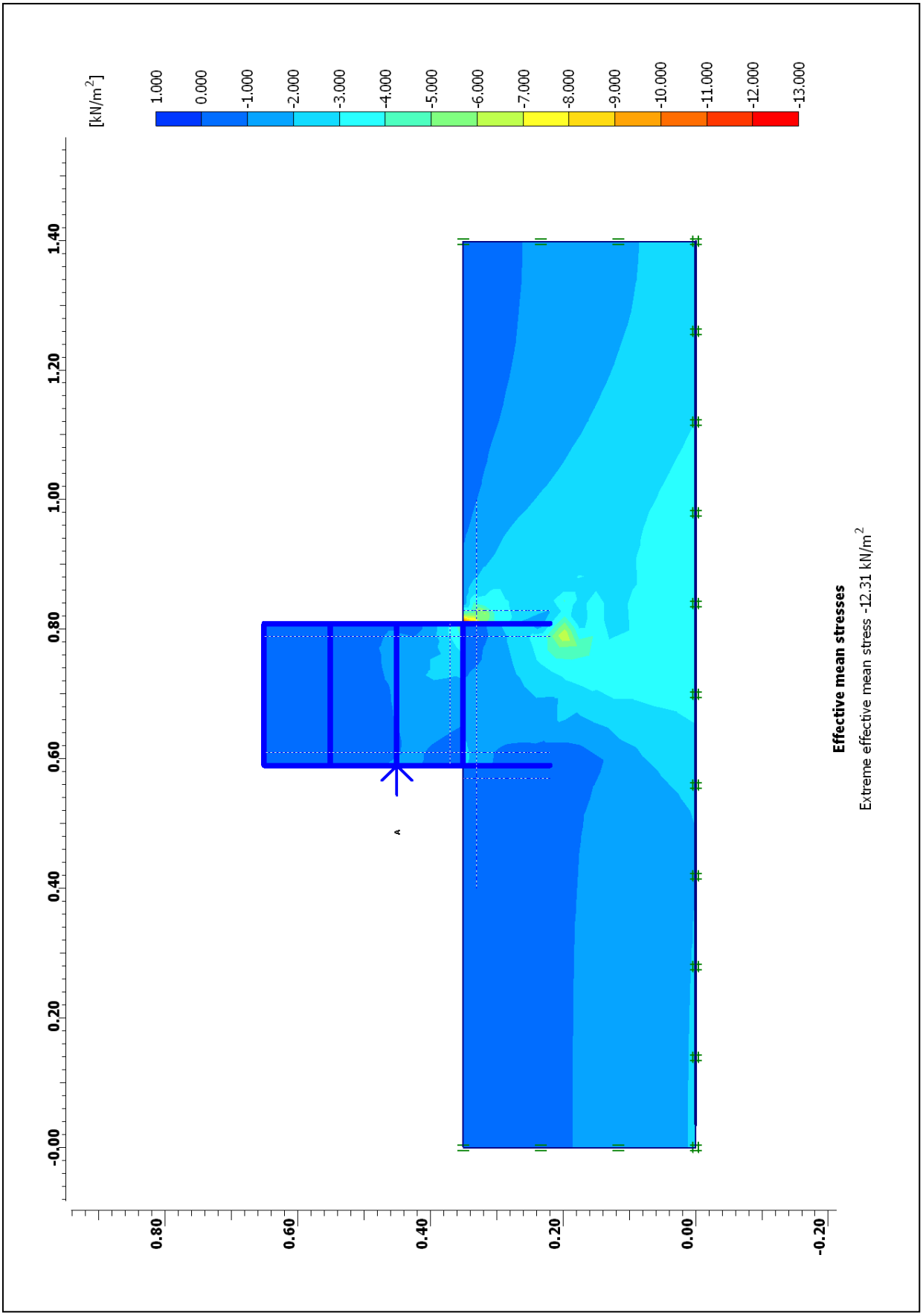

Fig (5-9): Effective stresses of cofferdam driven into soil

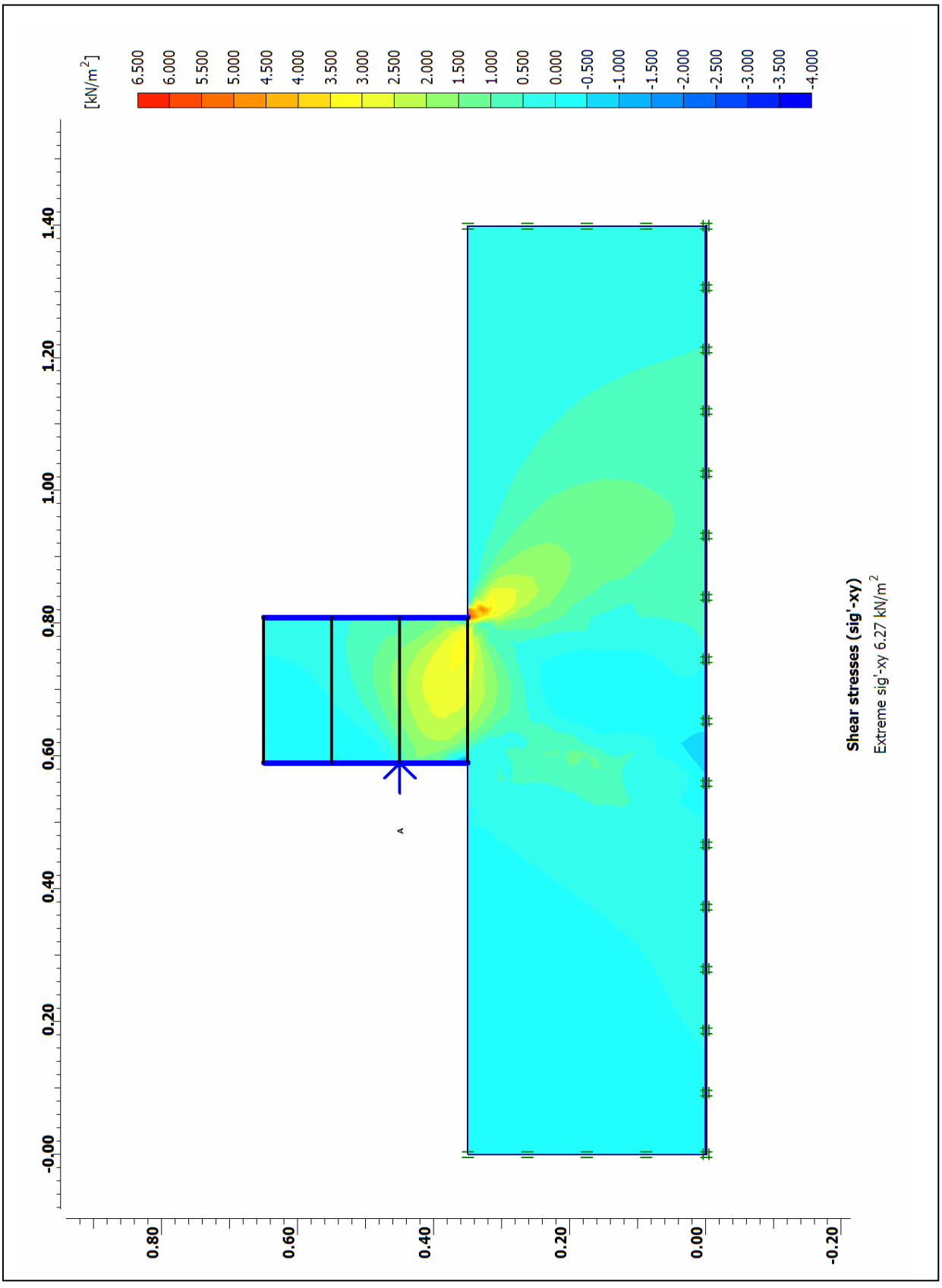

Fig (5-11): Shear stress in the cofferdam (xy)

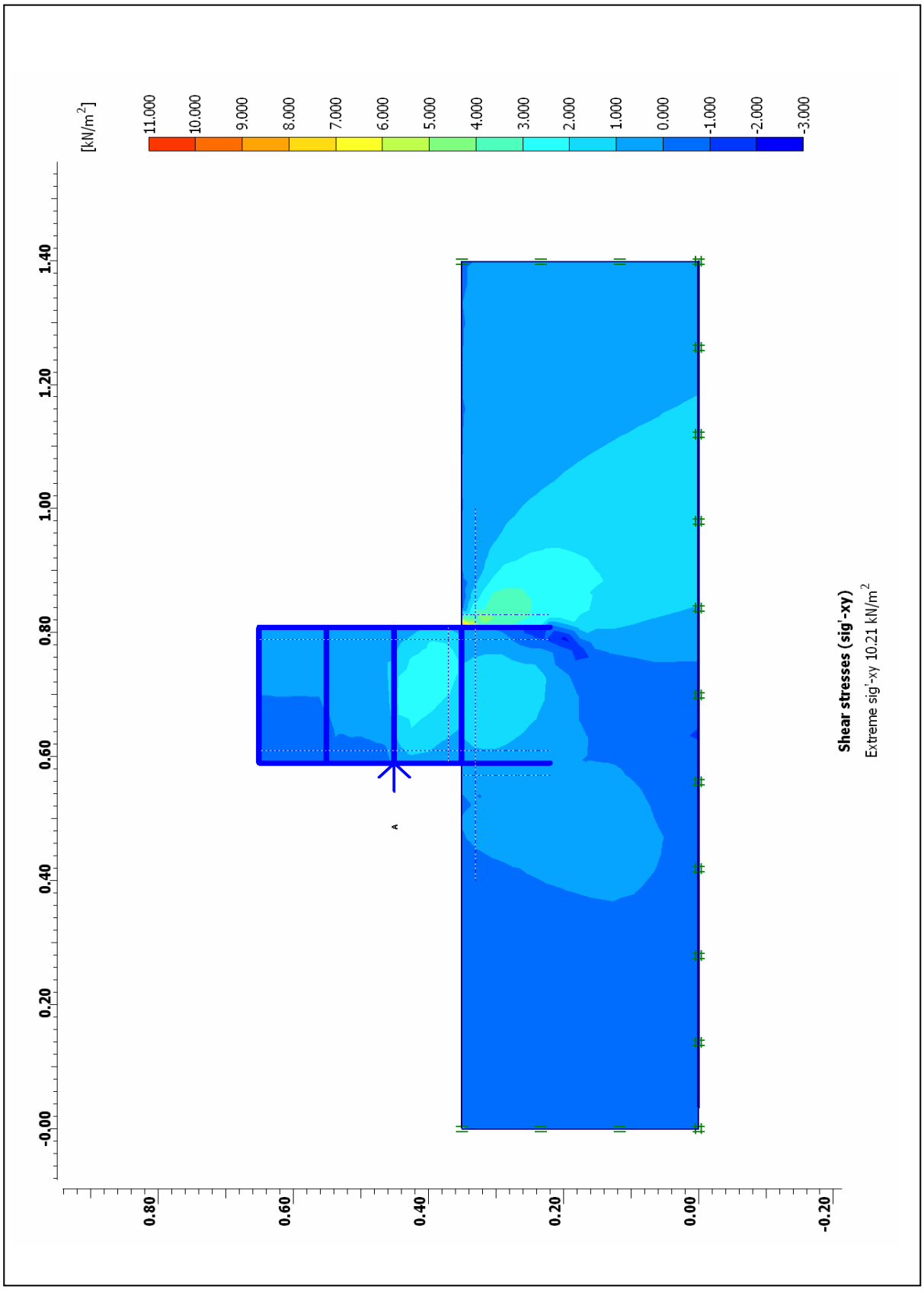

Fig (5-12): Shear Stress in the Cofferdam (xy)

Table (5-2): The stresses and strain in body of cofferdams, with (b/H) =0.75

Soil Type	Applied Load KN/m	Effective Stresses KN/m²	Shear Stress KN/m²	Horizontal Stress KN/m²	Shear Strain %
Subbase	0.57	-19.02	5.36	-11	2.69
Sand passing No.4	0.47	-16.5	5.1	-12.8	1.3
River sand	0.42	-15.27	4.53	-11	1.28
Sandy clay	0.47	-15.36	4.76	-11.4	2.2

Table (5-3): The stresses and strain in body of cofferdams, with D/H =0.45

Soil Type	Applied Load KN/m	Effective Stresses KN/m²	Shear Stress KN/m²	Horizontal Stress KN/m²	Shear Strain %
Subbase	0.76	-20.51	10.21	-18.35	3.15
Sand passing No.4	0.71	-18.2	8.6	-15.22	2.42
River sand	0.57	-16.5	7	-13.1	1.92
Sandy clay	0.66	-17.9	6.8	-11.9	3.41

5.7: Generating a Load-Displacement Curve

In addition to the results of the final calculation step, it is often useful to view a load-displacement curve for purpose of comparison. Therefore, the PLAXIS package is used. In order to generate the load displacement curve as given in figure (5-13). The X-axis is represent the displacement and the Y-axis is represented Sum-Mstage. Hence, the quantity to be plotted on the y-axis is the amount of the specified changes that has been applied. Hence the curve will range from 0 to 1, which means that 100% of the prescribed load (0. 26KN) has been applied and the prescribed ultimate state has been fully reached, and the figures (5-13) and (5-14) are represented load-displacement behavior for the cofferdam place on ground surface and the cofferdam with embedment depth respectively and the figures (5-15) and (5-16) are represented the comparison of displacement between software PLAXIS and experimental test.

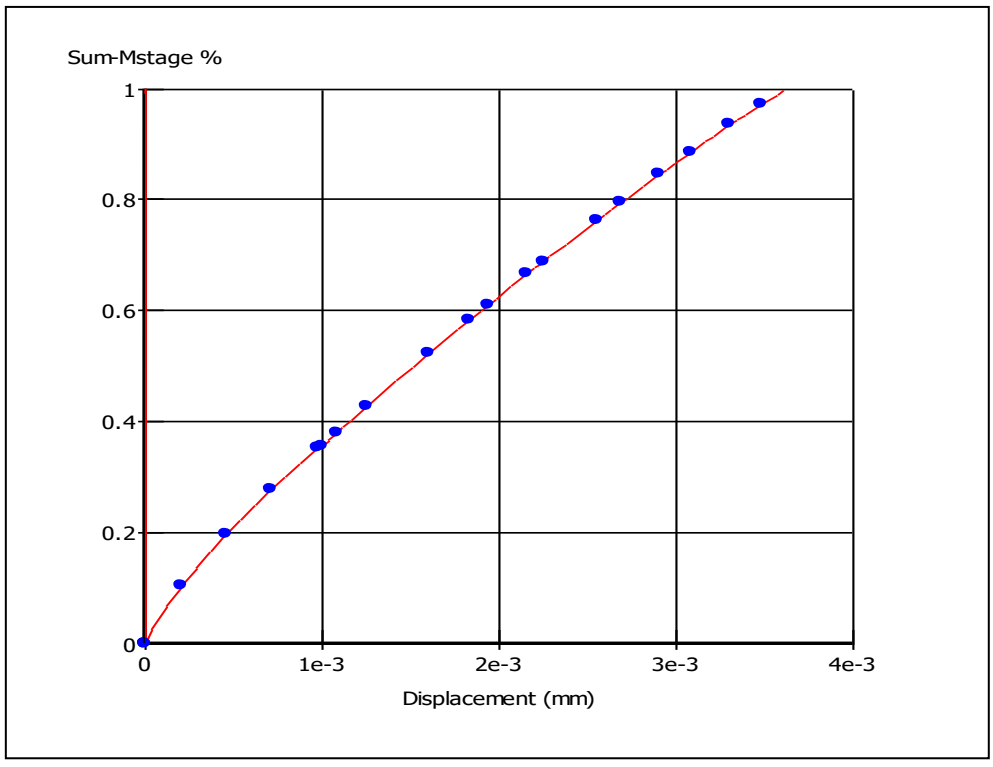

Fig (5-13): Load- Displacement curve for the cofferdam place on ground surface

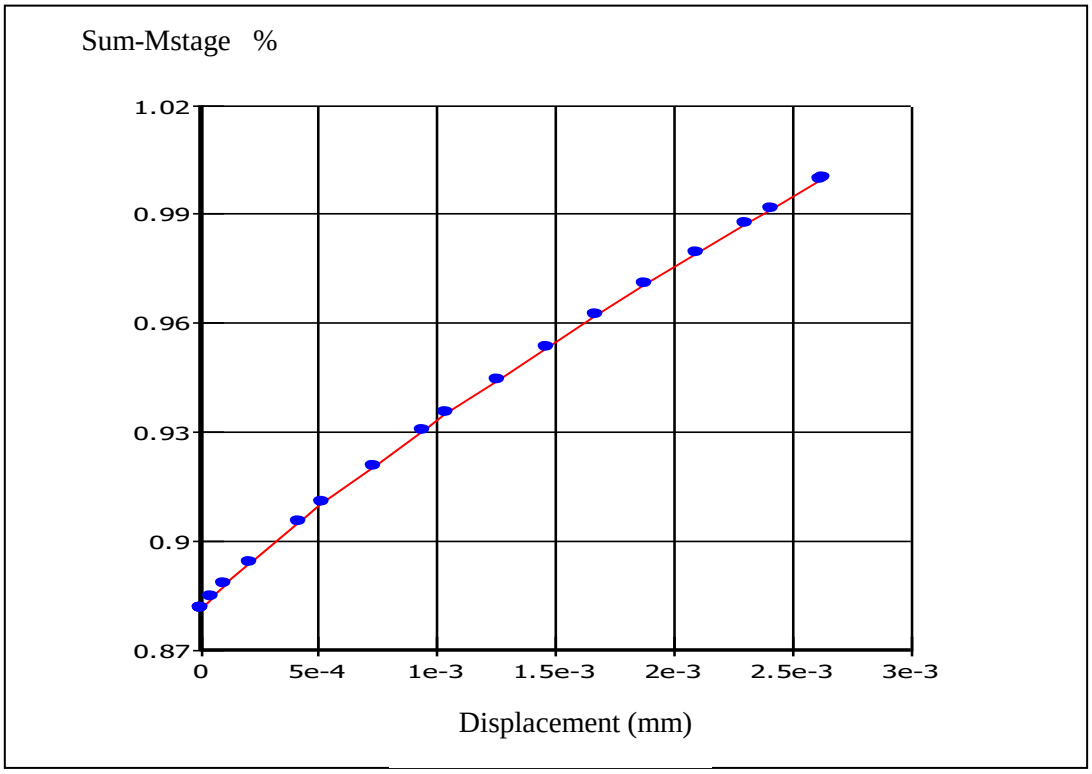

Fig (5-14): Load- Displacement curve for the cofferdam with embedment depth

5.8: Comparison Between Laboratory Tests and Software PLAXIS

The results of the PLAXIS analysis compared with experimental tests were presented in Figures (5-15) and (5-16). It can be seen that the displacement for the cellular cofferdam place on ground surface in the laboratory test equal to 3.72mm and the displacement that obtain from PLAXIS equal to 3.22mm, and the displacement for cofferdam with embedment depth in laboratory test equal to 3.21mm and the displacement from software PLAXIS equal to 2.61mm. Therefore, the different between two methods is very small but the different between the cellular cofferdam place on ground surface and the cofferdam with embedment depth equal 0.45 depth to height ratio is 23.3%. The PLAXIS software prediction of lateral displacement for cellular cofferdam is agrees with laboratory test. And the curves in PLAXIS are nearly line if comparison with the curves that obtained from experimental test.

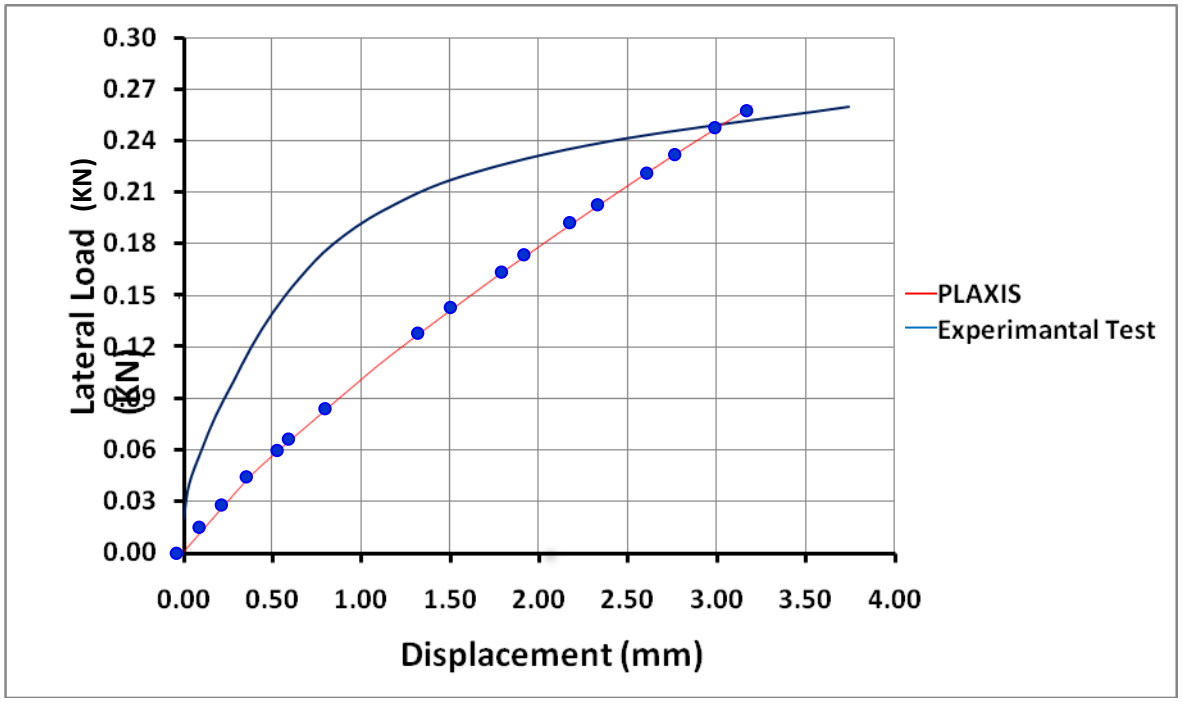

Fig (5-15): Load- Displacement curves comparison for the cofferdam place on ground surface

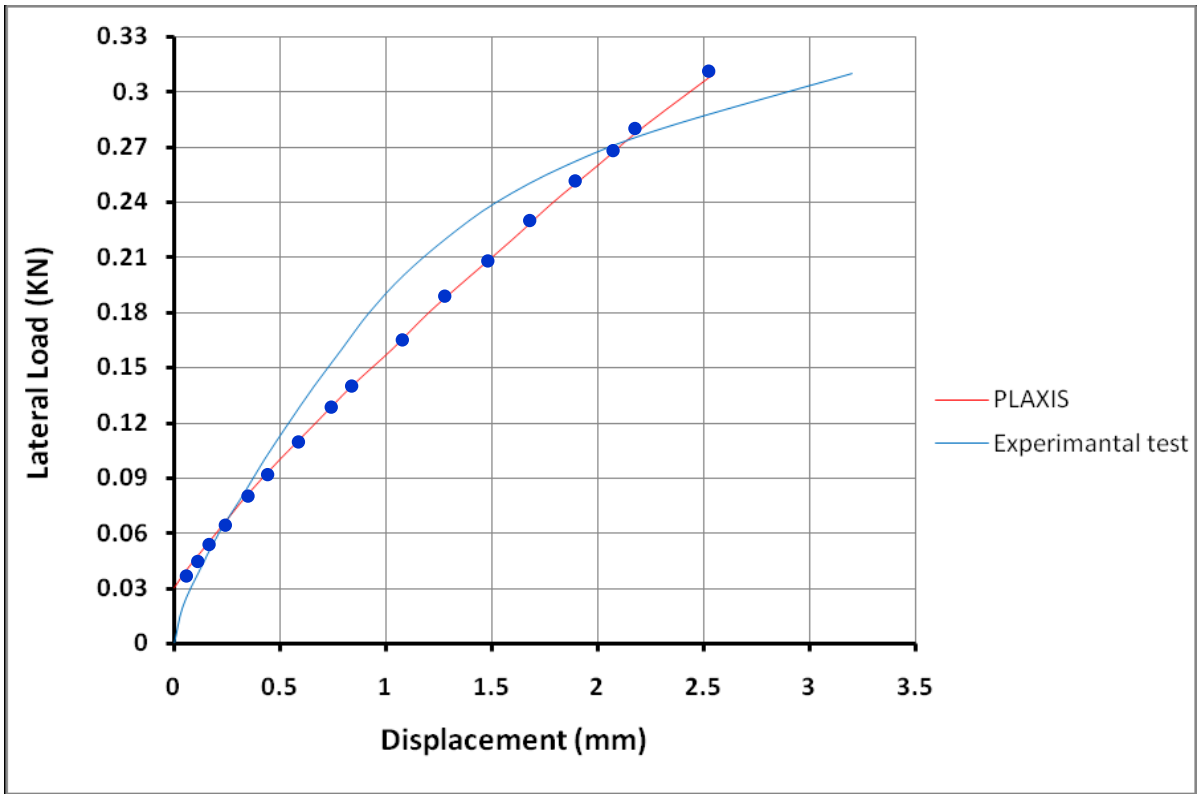

Fig (5-16): Load- Displacement curve comparison for the cofferdam with embedment depth

Then, tables (5-2), (5-3) and (5-4) show comparison of the deformation that obtained from experimental and the results obtained from PLAXIS software for the cofferdam placed on ground surface, and the different ratio height to depth of embedment (D/H) are (0.15, 0.3, 0.45) presented in tables (5-5), (5-6) and (5-7) with different soil material.

Table (5-2): Comparison of the deformation observed and PLAXIS software, with (b/H) =0.75, D/H=0

Soil Type	Applied Load KN/m	Deformation in Experimental (m)	Deformation Mash in PLAXIS (m)	Difference %
Subbase	0.57	3.75E-3	3.1E-3	20
Sand passing No.4	0.45	3.6E-3	1.9E-3	89
River sand	0.40	2.8E-3	1.65E-3	69
Sandy clay	0.40	4E-3	1.8	99

Table (5-3): Comparison of the deformation observed and PLAXIS software, with (b/H)=0.85, D/H=0

Soil Type	Applied Load KN/m	Deformation (m) in Experimental	Deformation Mash (m) in PLAXIS	Difference %
Subbase	0.68	2.3E-3	2.7E-3	-14
Sand passing No.4	0.55	2.12E-3	1.7E-3	24
River sand	0.43	3.2E-3	1.33E-3	140
Sandy clay	047	2.9E-3	1.2E-3	141

Table (5-3): Comparison of the deformation observed and PLAXIS software, with (b/H)=1, D/H=0

Soil Type	Applied Load KN/m	Deformation in Experimental (m)	Deformation Mash in PLAXIS (m)	Difference %
Subbase	0.83	2.7E-3	3.8E-3	28
Sand passing No.4	0.76	1.8E-3	1.96E-3	6
River sand	0.61	2.1E-3	1.6E-3	31
Sandy clay	0.6	1.55E-3	1.2E-3	29

Table (5-3): Comparison of the deformation observed and PLAXIS software, with (b/H)=0.75, D/H=0.15

Soil Type	Applied Load KN/m	Deformation in Experimental (m)	Deformation Mash in PLAXIS (m)	Difference %
Subbase	0.64	3.2E-3	2.7E-3	18
Sand passing No.4	0.63	3E-3	2.6E-3	15
River sand	0.42	4.45E-3	1.9E-3	134
Sandy clay	0.5	4.1E-3	3E-3	36

Table (5-3): Comparison of the deformation observed and PLAXIS software, with (b/H)=0.75, D/H=0.3

Soil Type	Applied Load KN/m	Deformation in Experimental (m)	Deformation Mash in PLAXIS(m)	Difference %
Subbase	0.68	3.2E-3	2.9E-3	10
Sand passing No.4	0.71	2.55E-3	2.78E-3	-8
River sand	0.57	2.7E-3	2.4E-3	12
Sandy clay	0.64	3.4E-3	3.26E-3	4

Table (5-3): Comparison of the deformation observed and PLAXIS software, with (b/H)=0.75, D/H=0.45

Soil Type	Applied Load KN/m	Deformation in Experimental (m)	Deformation Mash in PLAXIS (m)	Difference %
Subbase	0.71	3.1E-3	2.63E-3	17
Sand passing No.4	0.79	1.9E-3	2.24E-3	-15
River sand	0.6	3E-3	2.04E-3	47
Sandy clay	0.67	2.8E-3	2.9E-3	-3

Chapter Six

Conclusions and Recommendations

6.1: Conclusions

From this study the following conclusions are obtained:

1. There are two types of failures, these failure are sliding (translation) failure and overturning (rotation) failures. The failure is either sliding or overturning depending on the dimensions of cellular cofferdams. The overturning resistance of cell is greater than that of the sliding load resistance.
2. Cumming's analysis by horizontal shear overestimates the resistance to overturning of embedded cells by about 20%.
3. Increasing the width to depth ratio leads to increase resistance of structure but causes increase in construction cost.
4. The properties of soil are effect on stability of cell, where increase of angle of internal friction of soil (Ø) and cohesion (c) lead to increase resistance of cell.
5. The embedment depth increases the resistance force of cell and decreases the deformation.
6. The formulas (4-9, 4-11, 4-13 and 4-15) are created to a known the magnitude of the deformations after available lateral loads and embedment depths
7. The displacement of cellular cofferdam places on ground surface in the laboratory test equal to 3.72mm and the displacement that obtain from PLAXIS equals to 3.22mm, while the displacement for cofferdam with embedment depth in laboratory test equal to 3.21mm and the displacement from software PLAXIS equal to 2.61mm. Therefore, the difference between two methods is very small and PLAXIS software prediction of lateral displacement for cellular cofferdam is agrees with laboratory test.

6.2: Recommendations

Several recommendations for future studies are listed below:

1. Seepage analysis of cellular cofferdams by finite elements.
2. Analysis the change of water level in upstream of cellular cofferdam by software
3. The method of applied failure loads should be improved over the cable technique (possibly with air or hydraulic pressure) to ensure a more realistic distribution of lateral force.

Chapter Four
Results and Discussion

4.1: Introduction

This chapter presents the results obtained experimentally according to the testing program. The tests results reported in this chapter concern of two cases, at the first case diaphragm cells placed on ground surface with width to height ratios (b/H= 0.75, 0.85, 1.0) and the second case the diaphragm cells embedded to different depths which resulting depth to height ratios, D/H = 0.15, 0.3, 0.45. It is worth mentioned that the displacement term in this study indicates both translation and rotation of the top point of cell unless otherwise is stated.

4.2: Load-Displacement Behavior

A quick survey on the load-displacement behavior of all cells that placed on ground surface have been shown that they are similar and characterized by three distinguish stages, as shown in Figs. (4-1) to (4-3). The first stage (a-b), the displacement is linearly proportional to load. After that curved relationship (b-c) was obtained, which represent the second stage, the load-displacement relationship become, again, linear (c-d) until failure but with much flatter slope compared with that of the first stage. The curve form varies from cell to others according to the (b/H) ratio and type of soil used in the filling. It is worth mention that the cell loading is incrementally increased until an overall failure is taken place. The mode of failure was found to be either translation of displacement or overturning failure as that described later in the mechanism of failure. Thus the failure loading or cell resistance may be defined as the critical loading above which a general failure in the cell is taken place.

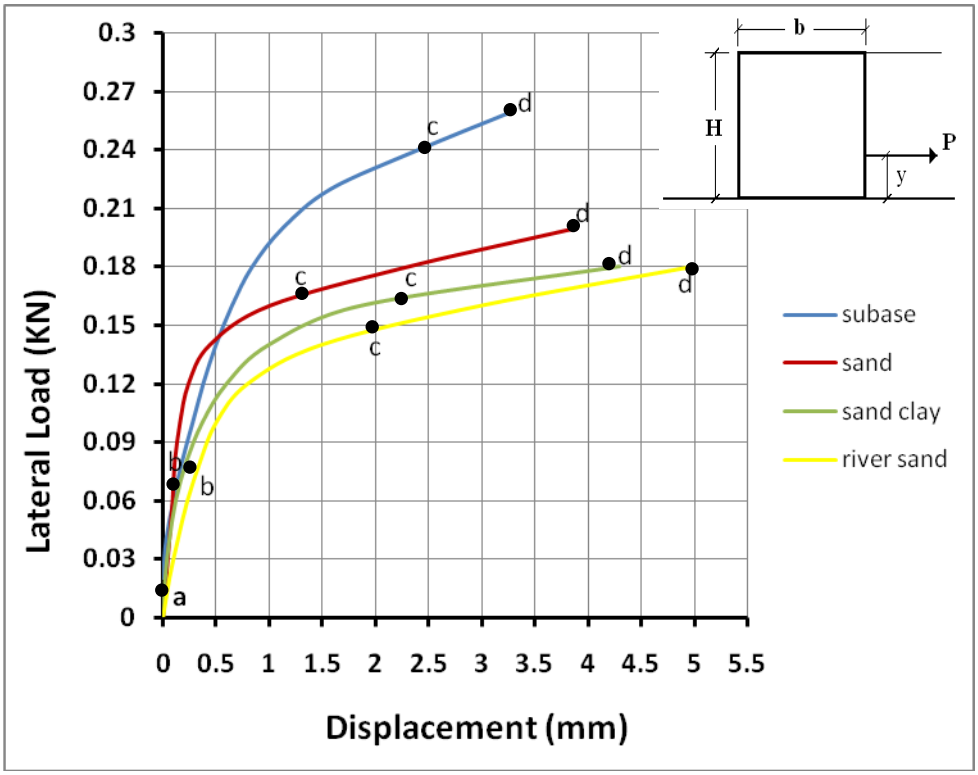

Fig. (4-1): Displacement vs. lateral load, $\frac{b}{H}$ =0.75, and y=10 cm

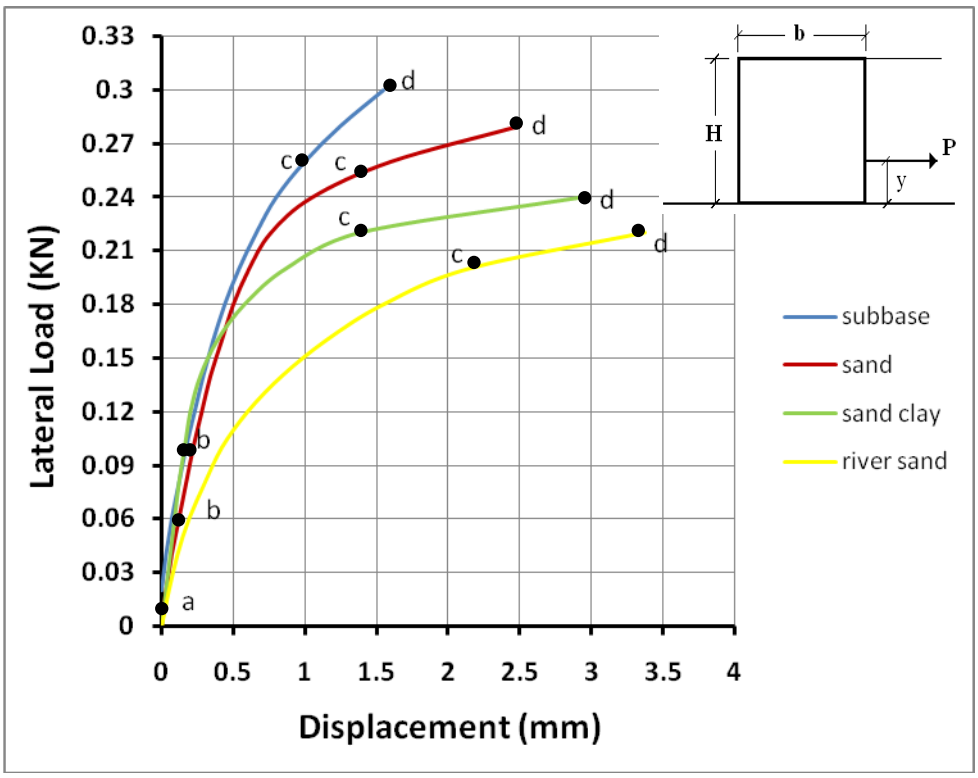

Fig. (4-2): Displacement vs. lateral load, $\frac{b}{H}$ =0.85, and y=10 cm

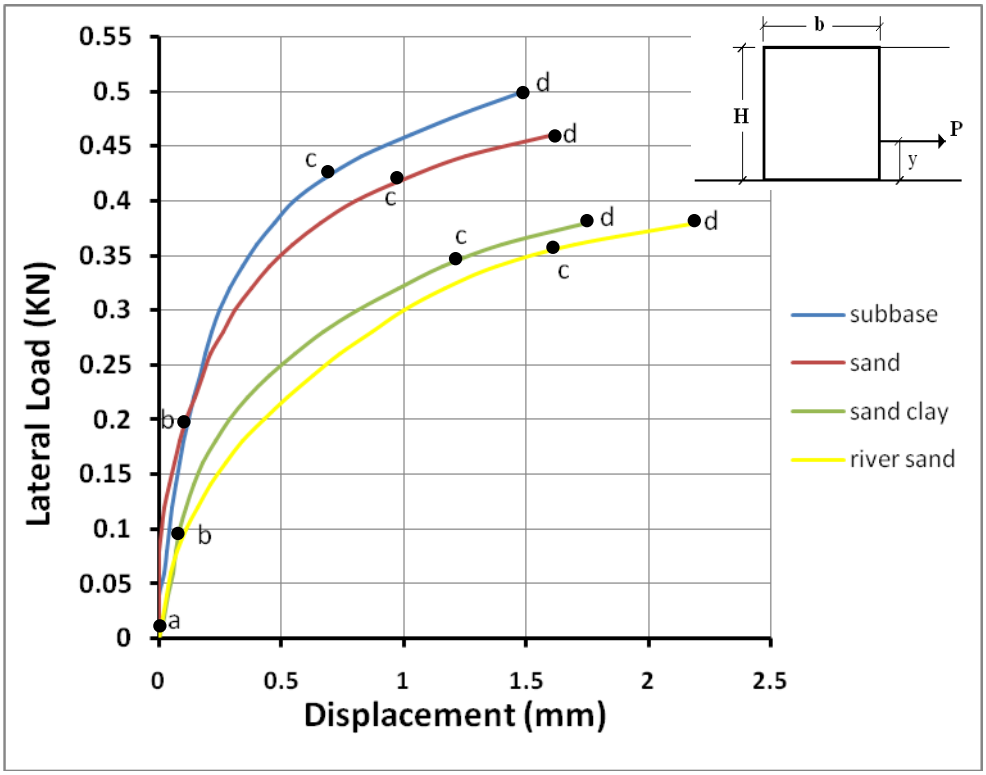

Fig (4-3): Displacement vs. lateral load, $\frac{b}{H}$ =1.0, and y=10 cm.

4.3: Mechanism of Cell Failure

As previously mentioned, all cells have been loaded until failure. It is noticed, that under any loading level below failure, the displacement of any point along the depth of cell consists of two components, translation and rotation. As far as the foundation concern; the translation results mainly from the shear distortion that takes place along the foundation level. The rotation, which results from the applied bending moment, causes a compression on the back side and tension along the front side of the cell. Thus the sheet pile of the back side tends to sink down into the ground as shown in Fig. (4-4-a) while that of front side tends to rise as shown in Fig. (4-4-b). Consequently, shear stresses along the soil/sheet pile interface surfaces are then generated. The amount and direction of these stresses depend on the magnitude and direction of

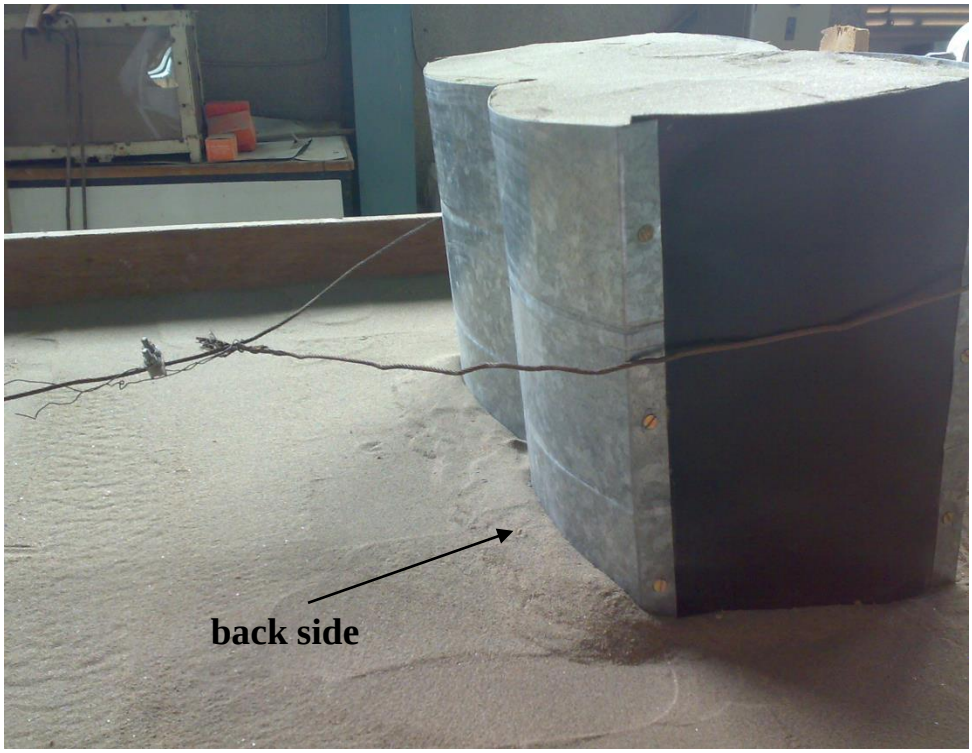

(a)Sink in the back side of the cell

(b) The front side tend to rise

Fig. (4-4): effect of bending moment on cell.

the relative displacement. The soil may therefore be slipped along the sheet pile wall or stick to that wall depending on weather the mobilize shear stress exceeds the shearing resisting shear or not. Besides, relative displacement along the sheetpile elements that caused by an even vertical shear may also occur. General shear failure in the foundation taken place when the ultimate bearing capacity is exceeded. Problems related to inadequate foundations result from the presence of a soft weak or highly compressible soil layer at or near the base of the cell, [**Swatek, (1967)]**.

Figure (4-5) indicates a possible bulkhead failure due to the presence of a weak soil beneath the cell. A general bearing capacity failure or a partial at the toe may be occurred causing the cell to sink or rotate excessively.

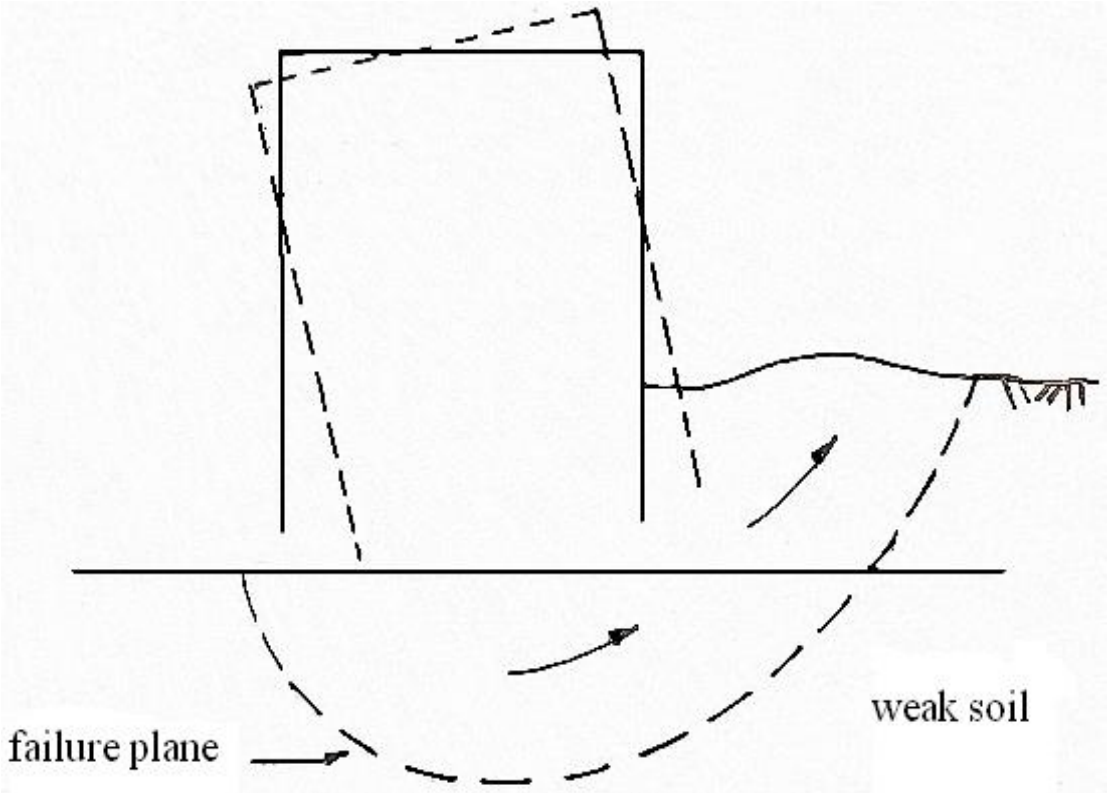

Fig. (4-5): Bearing capacity failure.

Shear failure in a relatively thin, weak zone may occur in a different manner Fig. (4-6). As the cell is filled, the soft material is squeezed out laterally in a mud. Large settlements in the middle of the cell may, therefore, result. The sheetpiles, then, subjected to a negative skin friction similar to that occurred in a pile foundation. [**Swatek, (1967)]**.

A highly compressible layer, such as soft clay or organic silt, could also result in distress to the cellular structures. Compression of this layer can cause large settlements of the cell, leading to distress of the surface topping of bulkhead. If the compressible material occurs in pockets beneath the cell, differential settlements may cause excessive tilting. [**Swatek, (1967)]**.

Experience with bulkhead construction, **[Schroeder, (1977)]**, stated that settlements in excess of nine inches can occur even if the foundation conditions are good.

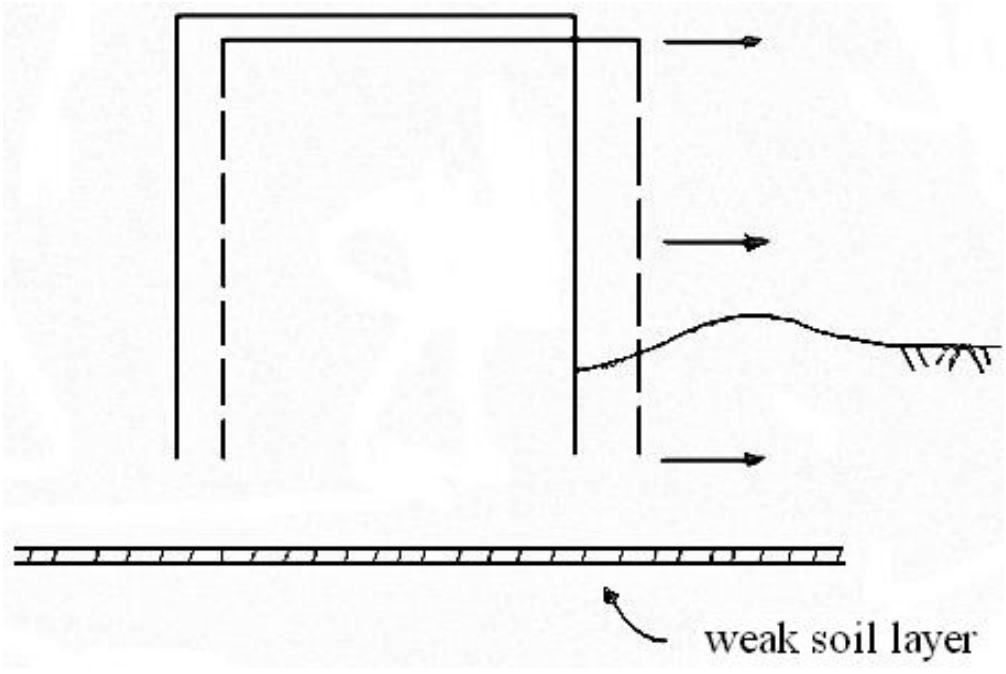

Fig. (4-6): Sliding due to zone of weakness.

Although such settlement may uniform and occur mostly during construction, it can be cause problems of alignment with appurtenant attached structures such as fender pile system.

Along the direction of loading, there are two modes of deformation that taken place; compression (passive) at the front side and expansion (active) at the back side. As stated by many authors **[Terzaghi, (1945)]**, the active failure is soon taken place while the passive failure requires much more displacement to generate. The cell resisting in this respect is mainly dependent on the soil passive resistance. Since the later passive resistance, is strongly dependent on the depth of point under consideration. Thus it may be anticipated that a progressive passive failure is taken place into the soil mass after each load increment. That is; a new location of the passive failure surface is generated after each load increment, therefore, if the sheetpile elements are well connected, and can safely withstand loading the only possible failure will be an external failure that is; sliding, overturning or shear failure in the foundation. Local failure between sheets elements under the influence of hoop tension may also be anticipated when these elements are poorly interlocked. However, the displacement of any point along the cell depth, which consists of translation and rotation, is strongly related to the applied bending moment. That is; when the load is applied at the ground surface (no bending moment) the cell will be subjected to a pure translation. The cell failure in this case will be pure shear failure. **[Schroeder, (1977)]**

4-4: Effect of Loading Height

All the cells were placed on the ground surface. It is worth mentioned that a pure translation failure has taken place for all cells if the load exerted close to the base while an overturning failure was taken place under (300 mm) height of loading. Thus, the results may indicate that the overturning resistance

of cell is generally greater than that of the sliding. The sliding resistance should be:

$$P = W * \tan\emptyset, \quad (4\text{-}1)$$

Where:

P = the lateral load.

W = the weight of the cell,

$\emptyset$ = the angle of friction of the cell fill.

on the other hand, the ultimate load that cause overturning failure may be estimated as:

$$P.y = W * \frac{b}{2}, \quad (4\text{-}2)$$

$$\text{thus, } P = W * \frac{b}{2y}, \quad (4\text{-}3)$$

where:

y = height of lateral load.

b = the cell width.

For the cases under consideration where ($\emptyset$, b and y) are known, a comparison between the values of (P) resulted from eq. (4-1) and eq. (4-3) was listed in table (4-1). This table indicate that the overturning resistance greater than the sliding resistance.

In an attempt to define the critical height above which an overturning failure is taken place, the value of (P) obtained from equation (4-1) is equated to that of equation (4-3).

$$W * \tan\emptyset = W * \frac{b}{2y}, \quad (4\text{-}4)$$

$$\therefore y_{cr} = \frac{b}{2\tan\emptyset}$$

The (y_{cr}) values for all tests are listed in Table (4.2).

Table (4.1): The anticipated values of cellular resistance.

Soil type		$(\frac{b}{H} = 1.0)$	$(\frac{b}{H} = 0.85)$	$(\frac{b}{H} = 0.75)$
Subbase	***Sliding resistance***	0.78*W	0.78*W	0.78*W
	Overturning resistance	1.5*W	1.275*W	1.125*W
Sand passing sieve No.4	***Sliding resistance***	0.661*W	0.661*W	0.661*W
	Overturning resistance	1.5*W	1.275*W	1.125*W
River sand	***sliding resistance***	0.612*W	0.612*W	0.612*W
	Overturning resistance	1.5*W	1.275*W	1.125*W
Sand clay	***Sliding resistance***	0.383*W	0.383*W	0.383*W
	Overturning resistance	1.5*W	1.275*W	1.125*W

Table (4-2): The y_{cr}(mm) values for all tested models.

Type of soil	Angle of friction	$\frac{b}{H} = 1.0$	$\frac{b}{H} = 0.85$	$\frac{b}{H} = 0.75$
Subbase	38	192	163	144
Sand passing sieve No.4	33.5	226.6	192.6	170
River sand	31.5	245	208	183.5
Sand clay	21	390	332	293

4-5: Effect of $(\frac{b}{H})$ Ratio

To understand the effect of $(\frac{b}{H})$ ratio, three diaphragm cells with different ratio (0.75, 0.85, 1.0) were tested under lateral load applied at one third of the cell height, mean while all the cells were placed at the ground surface, the effect of $(\frac{b}{H})$ ratio was illustrated in Fig. (4-7).

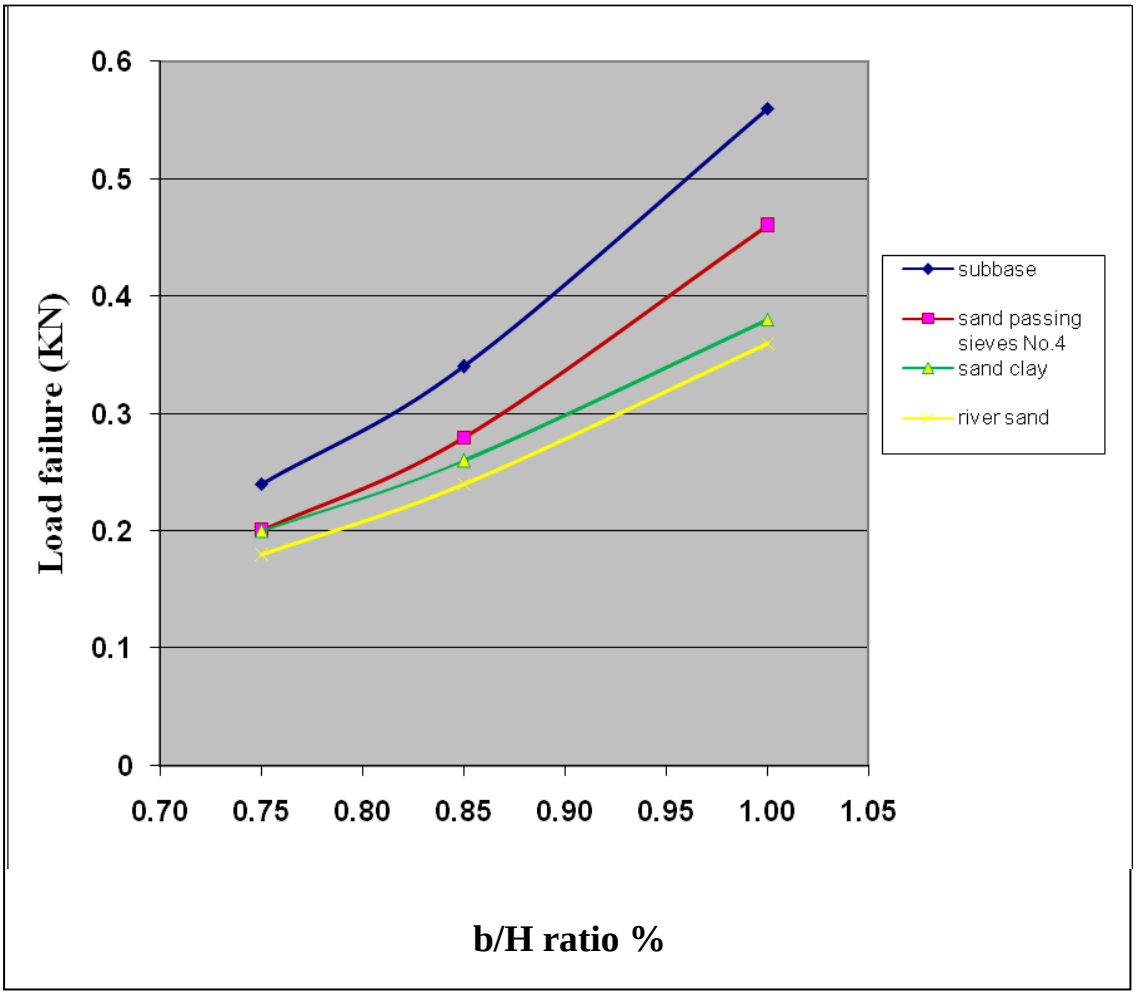

Fig. (4-7): Effect of $(\frac{b}{H})$ ratio on cell filled.

It is clear that the resistance decreases as the $(\frac{b}{H})$ ratio of the cell decreases. This is due to decreasing in the width of cell for the same height leading the weight accordingly the resistance of cell should be decreasing. The ratio of decreasing illustrated in Table (4-3).

Table (4-3): Ratio of decreasing in resistance according to the ($\frac{b}{H}$) ratio.

Type of soil	Decreasing ratio of resistance from $\frac{b}{H} = 1.0$ to 0.85	Decreasing ratio of resistance from $\frac{b}{H} = 0.85$ to 0.75	Decreasing ratio of resistance from $\frac{b}{H} = 1.0$ to 0.75
Subbase	39%	29.4%	57%
Sand passing No.4	38.6%	28.5%	56.4%
Clay	33.3%	25%	50%
River sand	31.5%	23%	47%

4-6: Effect of Soil Type

To show the effect of soil type which be used in the cell fill, the cell resistance along diaphragm cell is drawn against embedment depth (D/H), as shown in Figs. (4-8). It is clear that the cell resistance decreased as the unit weight and the angle of friction of fill decreased, when embedment depth is (0mm and 45mm), so that the cell resistance of the subbase greater than the other soils. But when the embedment was (95mm and 135mm) the effect of angle of friction decreased and the stable of cell was become depending on the unit weight of the soil that was used in the fill, so that the cell resistance of sand passing No.4 was greater than that in the other soils fill because it has a height unit weight.

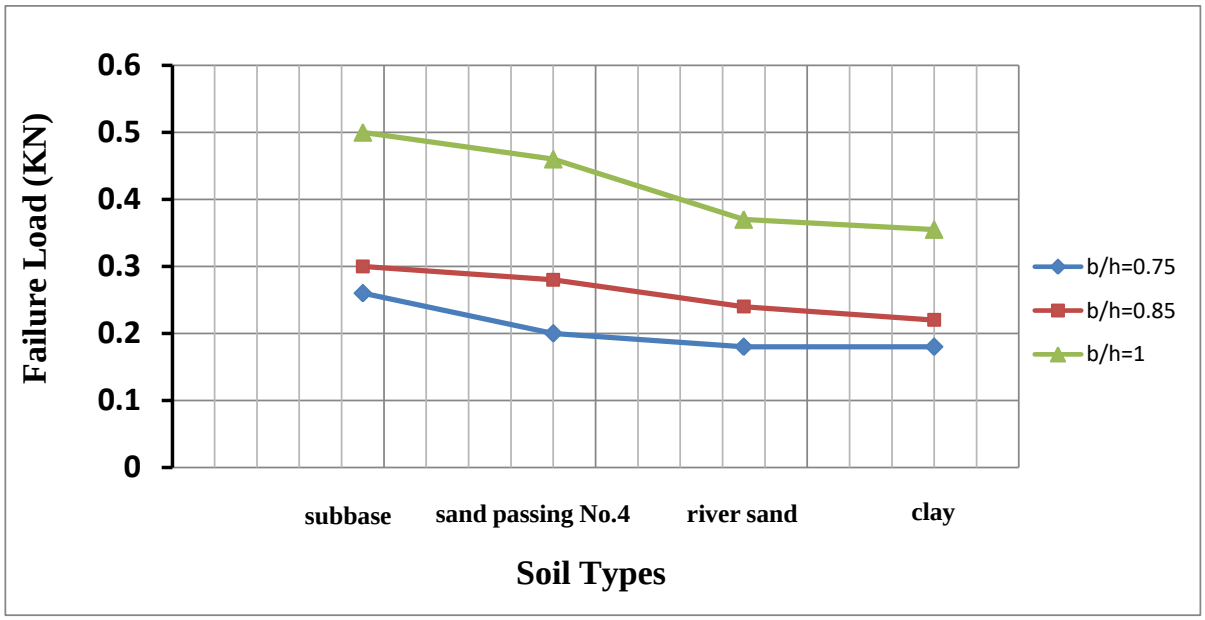

Fig. (4-8): Effect of soil type on cell resistance.

4-7: Effect of Embedment depth

To understand the effects of the embedment depth, a diaphragm cell of 450mm length, 300mm height, 225mm width and subjected to a load applied at one third of the cell height have been tested. The lower end, of the cell considered in study, was placed (0.15, 0.30, 0.45) depth (D) to height (H) ratios below the ground surface. It is worth mention that the curve form vary from cell to others according to the (D/H) ratio and type of soil used in the filling. It was found that the resistance of cell increased and the deformation decreased if compared when the cell was placed on the ground surface. Thus, an embedment of 15% has increase the cell resistance by approximately as much as 8.5%, when used embedment of 30% has increase the cell resistance 25% and the embedment of 45% the cell resistance increased to 32%. The figures from (4-9) to (4-20) is showed the effects of embedment depth on resistance and deformation of the cofferdam. And the tables in the appendix illustrated the effects embedment depth.

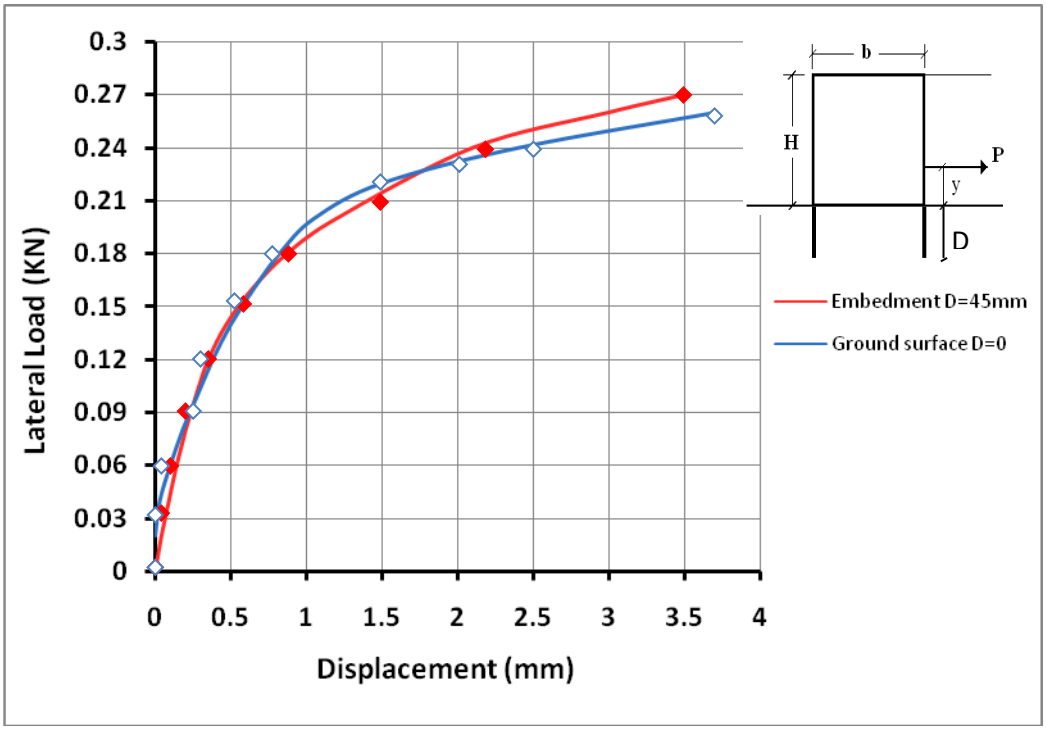

Fig. (4.9): Displacement vs. lateral load for cell filled with subbase, embedment depth D/H=0.15 and y=10 cm.

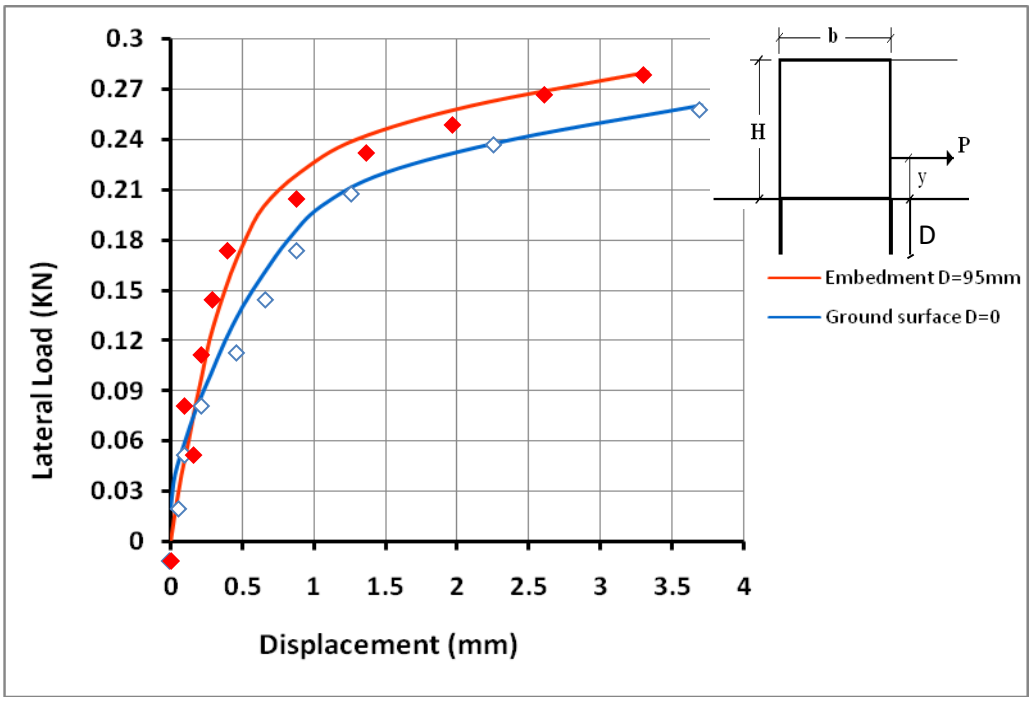

Fig. (4.10): Displacement vs. lateral load for cell filled with subbase, embedment depth D/H=0.3 and y=10 cm .

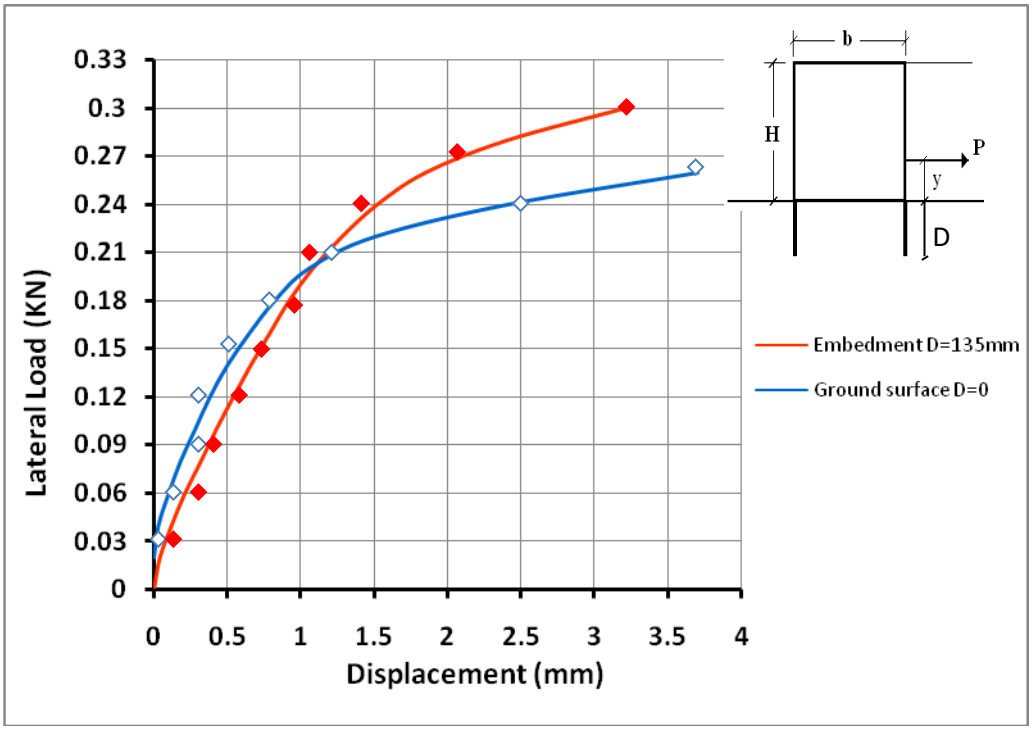

Fig. (4.11): Displacement vs. lateral load for cell filled with subbase, embedment depth D/H=0.45 and y=10 cm

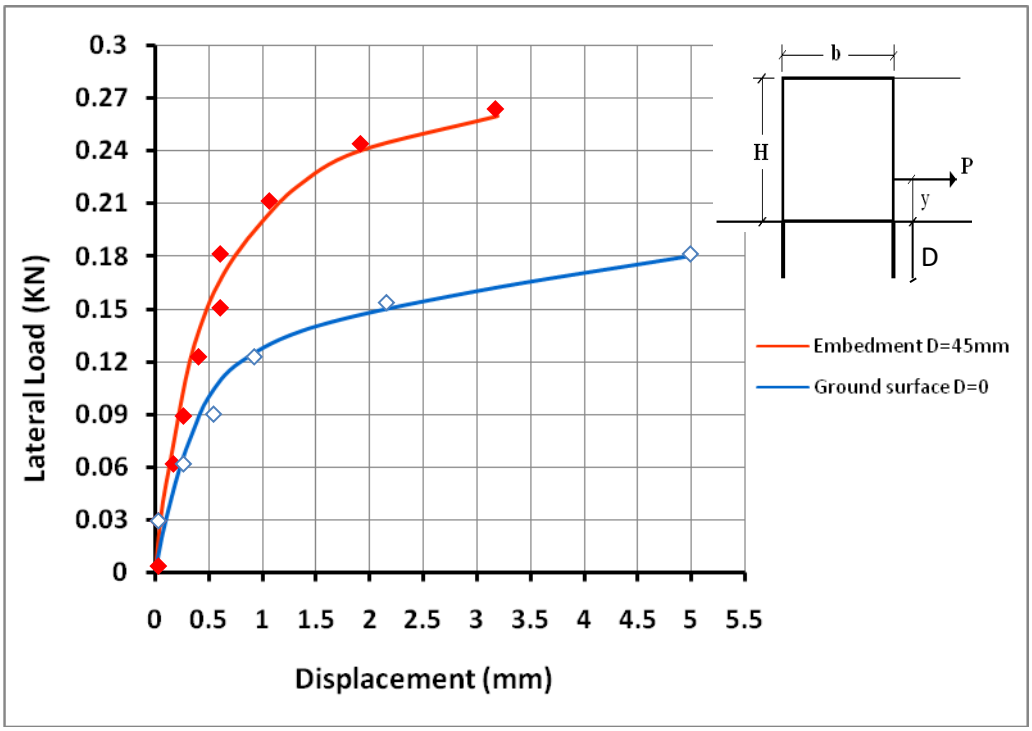

Fig(4-12):Displacement vs. lateral load for cell filled with sand passing sieve No.4, embedment depth D/H=0.15 and y=10 cm .

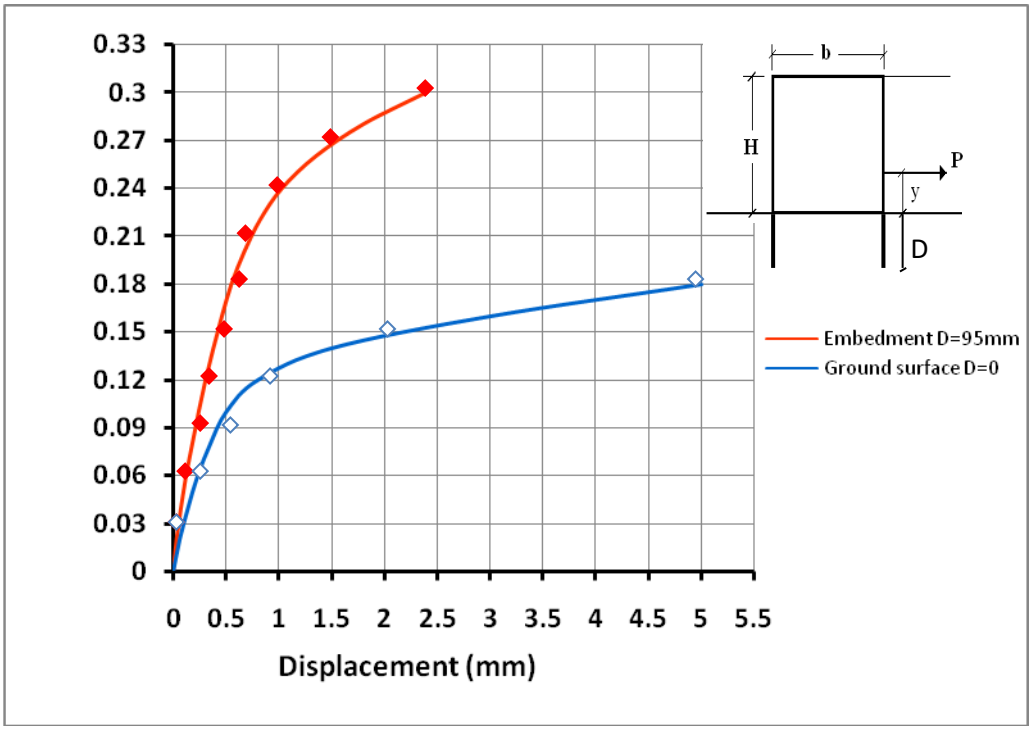

Fig(4-13):Displacement vs. lateral load for cell filled with sand passing sieve No.4, Embedment depth D/H=0.3 and y=10 cm .

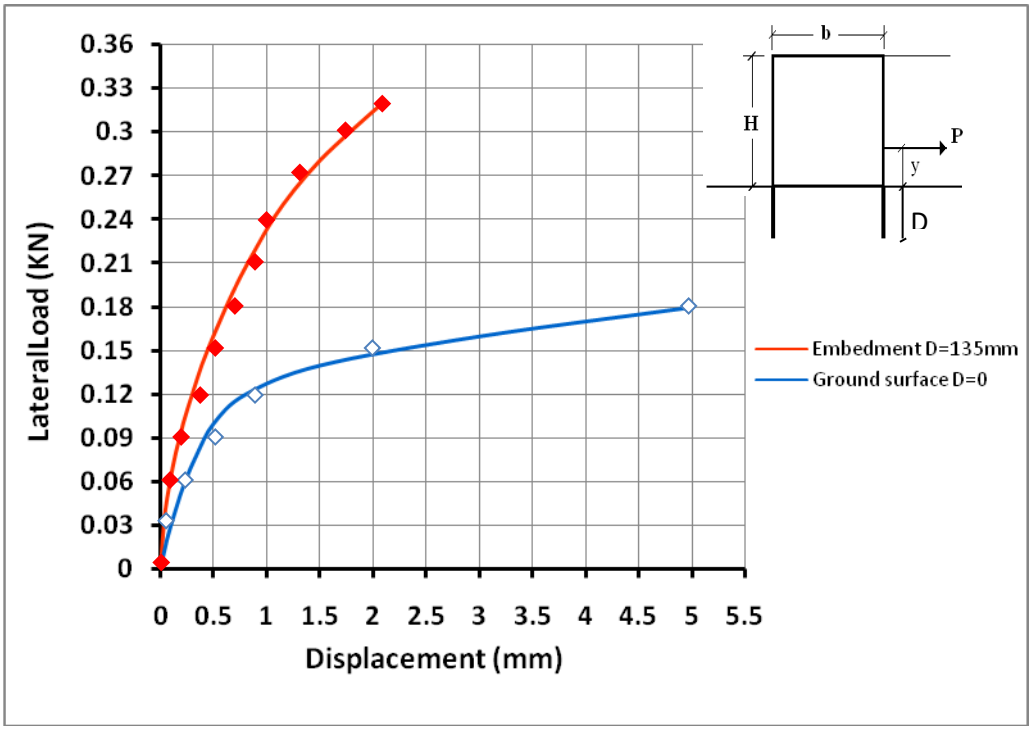

Fig(4-14):Displacement vs. lateral load for cell filled with sand passing sieve No.4, Embedment depth D/H=0.45 and y=10 cm .

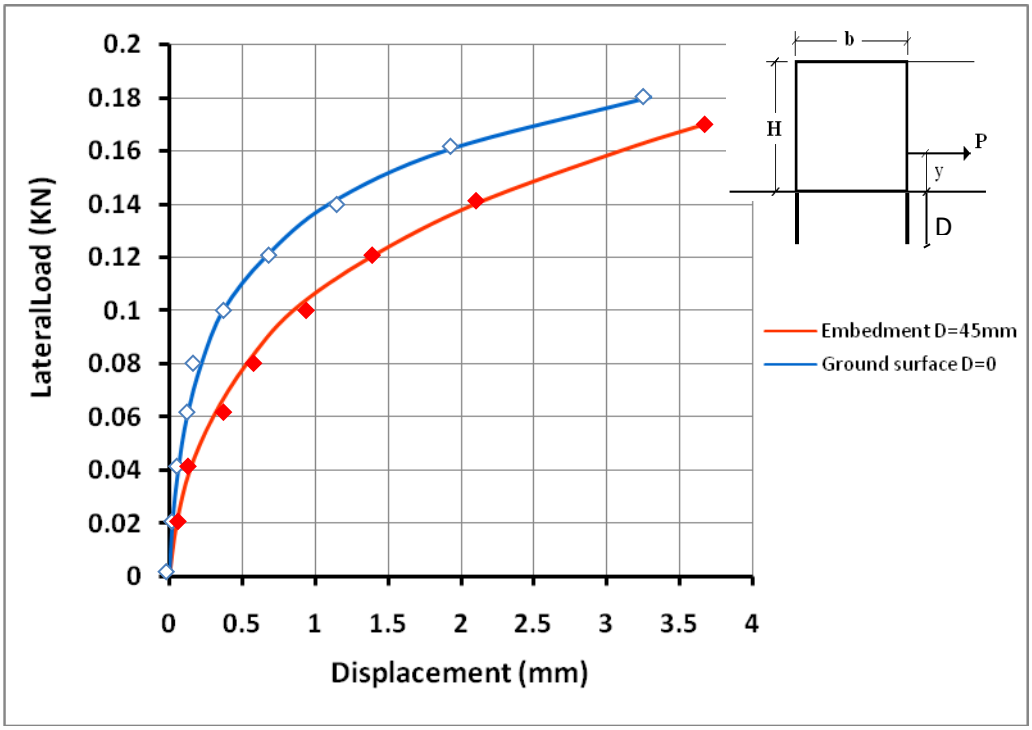

Fig(4-15):Displacement vs. lateral load for cell filled with river sand, Embedment depth D/H=0.15 and y=10 cm .

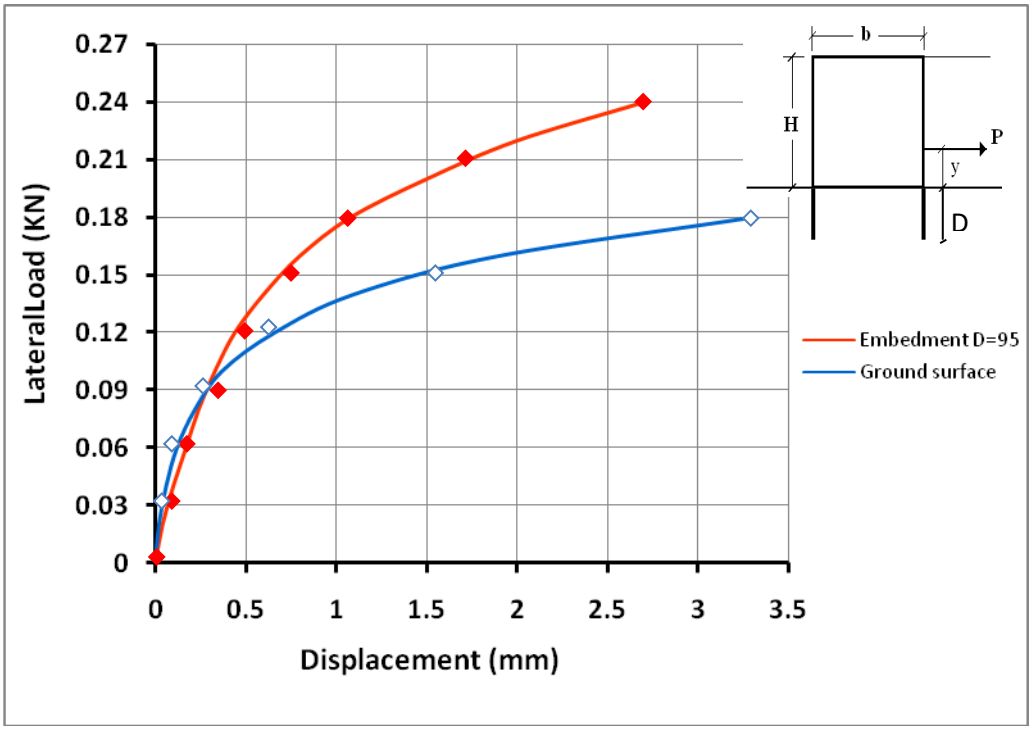

Fig(4-16):Displacement vs. lateral load for cell filled with river sand, Embedment depth D/H=0.3 and y=10 cm .

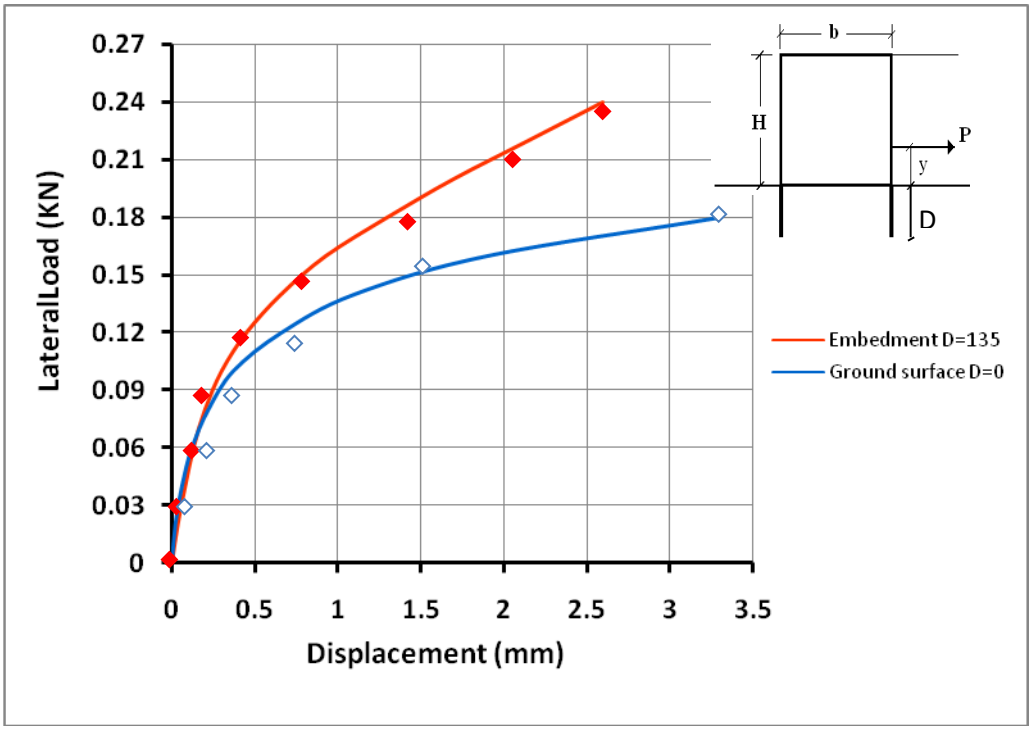

Fig(4-17):Displacement vs. lateral load for cell filled with river sand, Embedment depth D/H=0.45 and y=10 cm .

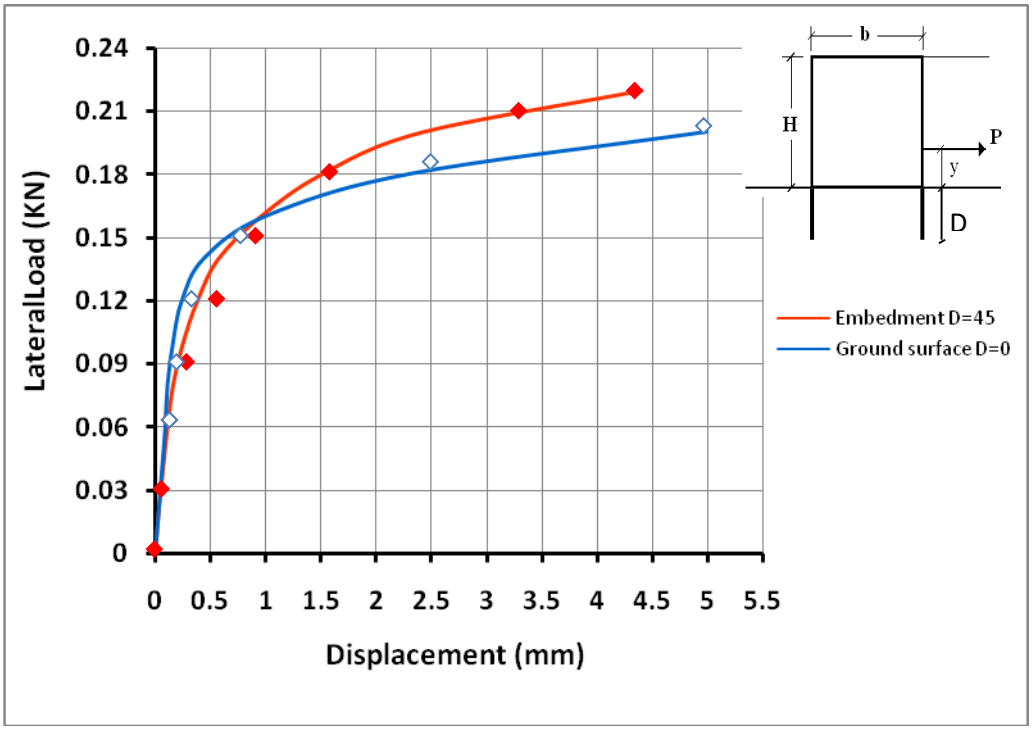

Fig(4-18):Displacement vs. lateral load for cell filled with clay, Embedment depth D/H=0.15 and y=10 cm .

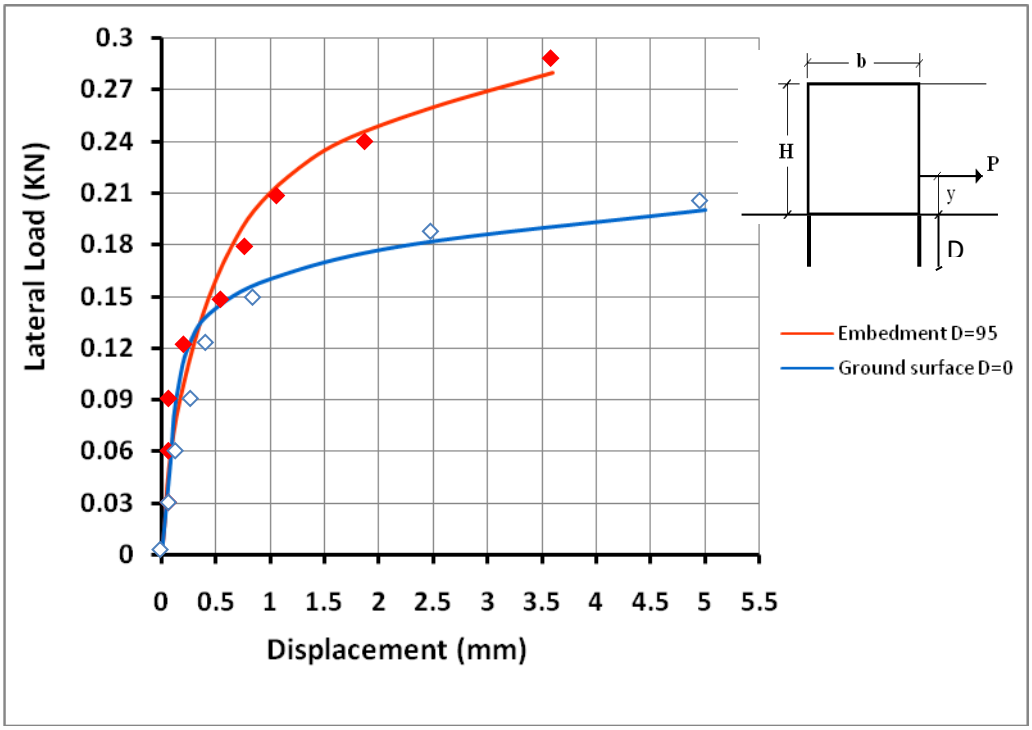

Fig(4-19):Displacement vs. lateral load for cell filled with clay, Embedment depth D/H=0.3 and y=10 cm .

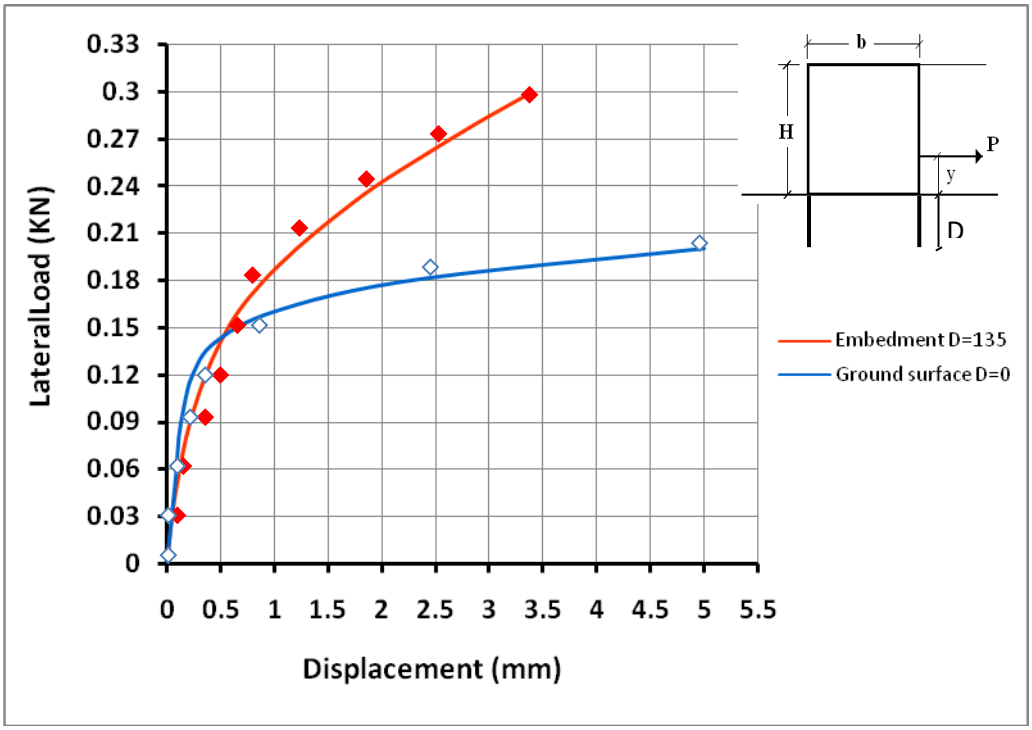

Fig(4-20):Displacement vs. lateral load for cell filled with clay, Embedment depth D/H=0.45 and y=10 cm .

4-8: Brinch Hansen's Equilibrium Method

Where the driving depth of such a cofferdam is shallow (D/H=0.15), the entire dam, at failure, will rotate as one rigid body about a point located below the cofferdam, which getting line rupture, a so-called X-rupture, between the walls, as shown in Figs.(4-21).**[Hansen's, (1953)]**.

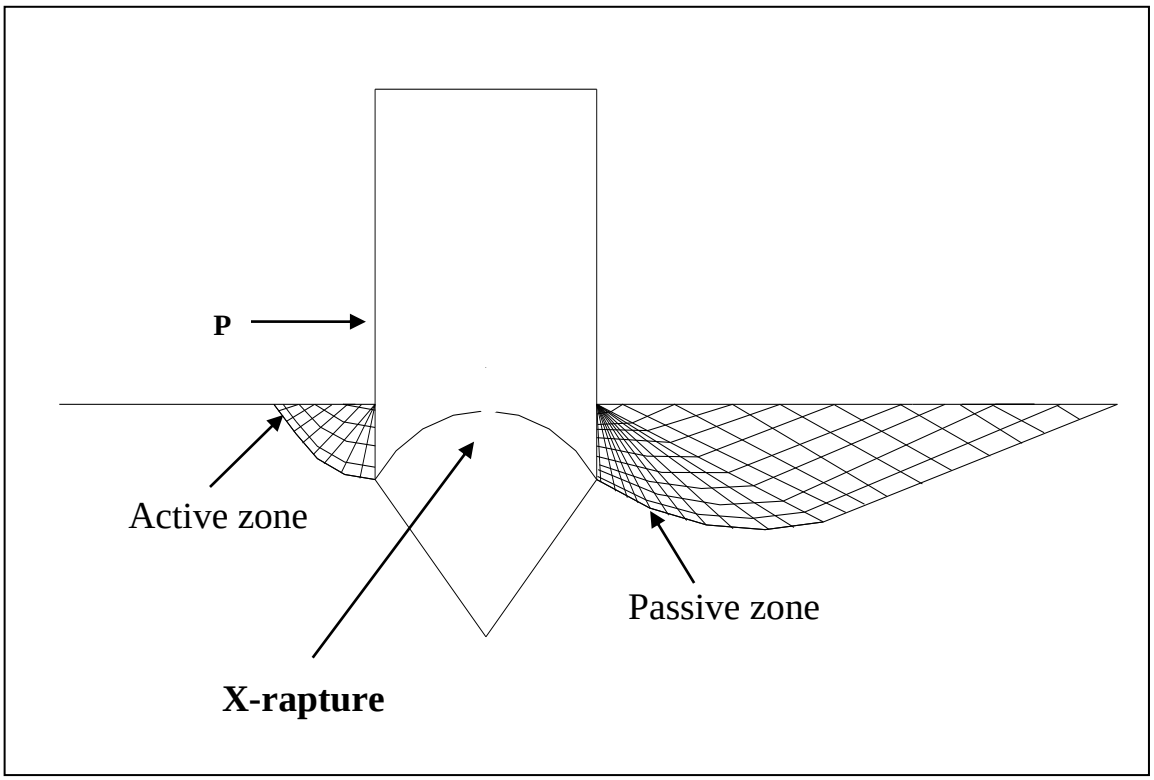

Fig. (4-21): Pattern of rupture for cellular cofferdam on a soil stratum (shallow depth)

Notice that the active zone rupture on the left of the cofferdam's outside and either a passive or composite rupture on the right of the cofferdams outside.

With greater driving depth the cofferdam, when in a state of failure, will rotate about a point located above the foot of the cofferdam, as shown in Fig.(4-22). Between the walls a concave line-rapture, a so-called A-rapture. A composite rupture will appear on the outside of either wall. **[Hansen's, (1953)]**.

.

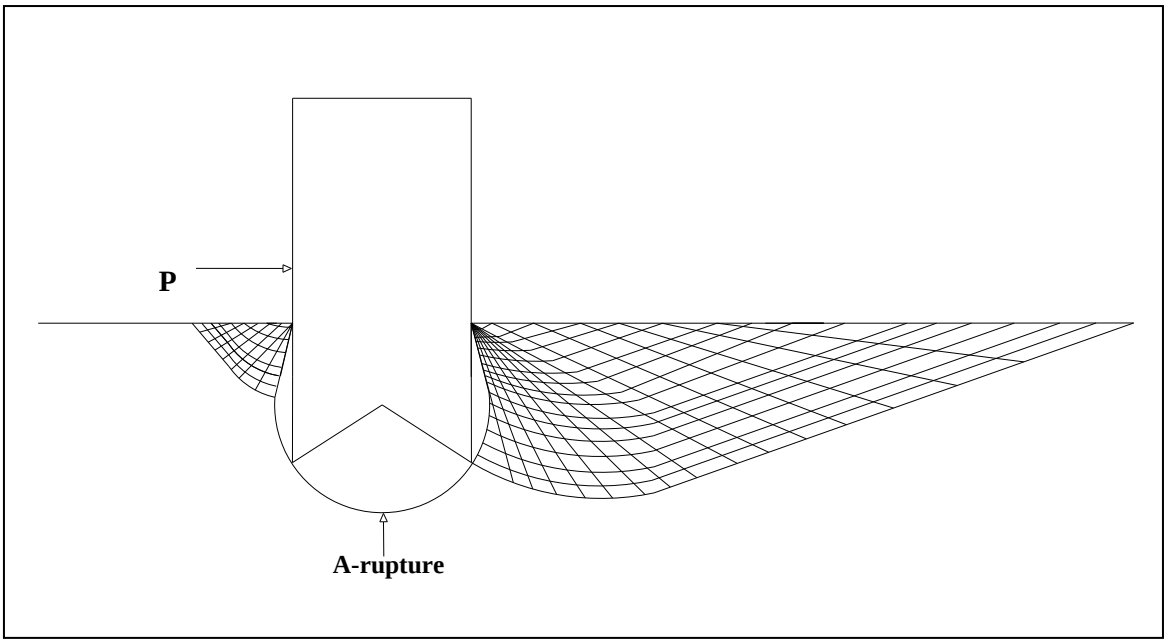

Fig. (4-22): Figure of rupture for cellular cofferdam on a soil stratum

It is noted be that these increase related to passive resistance of soil behind the soil, Fig.(4-23) is shown a resistance forces on cellular cofferdam, the embedment has shallow depth. By projection on the horizontal and vertical, and taking moments about the chord's mid-point the following three equations of equilibrium may be derived:

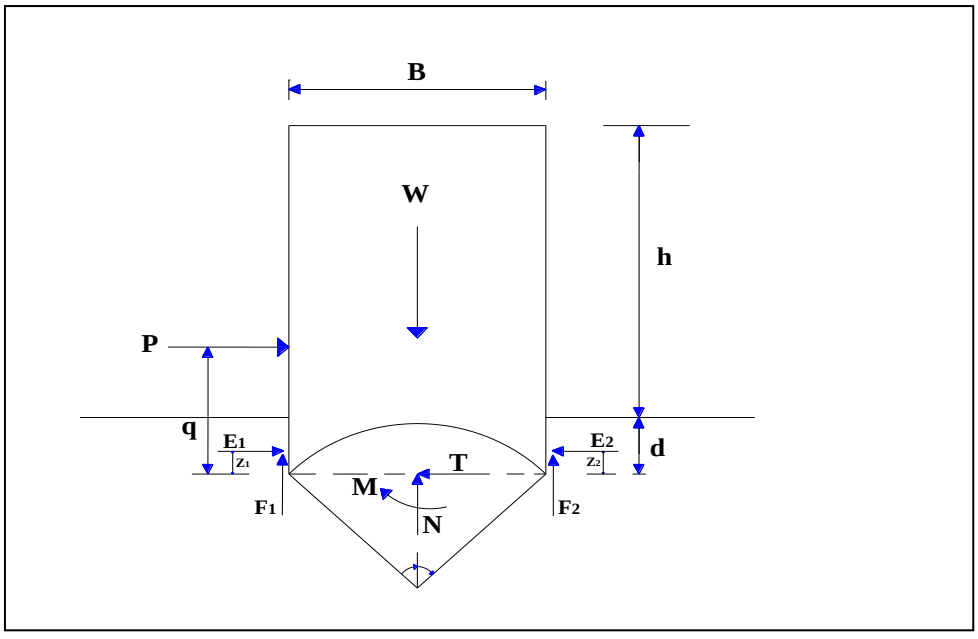

Fig. (4-23): Forces affecting on cellular cofferdam (shallow depth)

$\Sigma F_X=0$

$T=P+E1-E2,$ (4-5)

$\Sigma FY=0$

$N = W – F1 –F2,$ (4-6)

$\Sigma FM=0$

$M = P*q + F1*B/2 + E1*z1 – F2*B/2 – E2*z2,$ (4-7)

In case of very great driving depths (0.45) depth to height ratio as shown in Fig.(4-24). The figure is shows that the affects forcing same forces in previous state, but the difference is the distances from these forces which more stability of cofferdam.

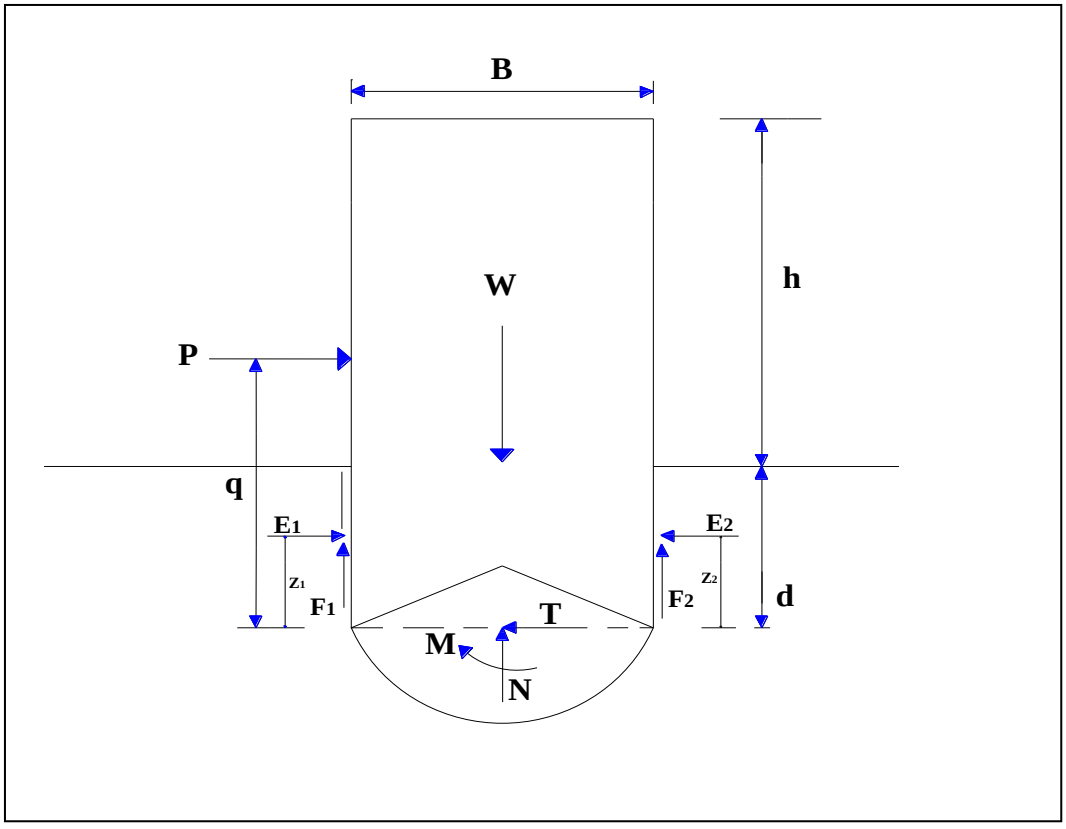

Fig. (4-24): Forces affecting on cellular cofferdam (great depth)

4.9: Evaluation of The Current Design Method

Tables (4-4), (4-5), and (4-6), show comparison between the observed and calculated resistance of different diaphragm cofferdams. The method of calculation has been considered for this purpose, the horizontal shear (Cummings) method. It is clear from the tables, that the Cummings method is overestimating the capacity. The horizontal shear method gives a load capacity which in not good agreement with the observed. And all of tables included the factor of safety (F.S) for each case, a factor of safety for all cases is more than the limited 1.10 to 1.25 that recommended (Bowles 1977) but the factor of safety for the model have been width (b) to height (H) ratios equal to 0.75 is near to limited that show in table (4-4), therefore, the case that the cofferdam have embedment depth based on 0.75 as ratio width (b) to height (H).

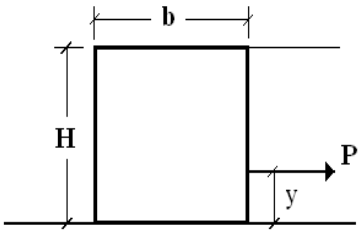

Table (4-4): Comparison of the resistance observed and those calculated by horizontal shear method for cell with (b/H) =0.75

Soil type	H mm	b mm	Resistance KN/m		Difference %	Factor of safety	Remark
			bserved	calculated			
Subbase	300	225	0.57	0.76	-25%	1.21	in all cases, the load applied at one third of the cell height.
Sand passing No.4	300	225	0.45	0.75	-40%	1.23	
River sand	300	225	0.40	0.56	-28%	1.28	
Sand clay	300	225	0.40	0.37	8%	1.31	

Table (4-5): Comparison of the resistance observed and those calculated by horizontal shear method for cell with (b/H)=0.85

soil type	H mm	b mm	resistance KN/m		difference %	Factor 0f safety	remark
			observed	calculated			
subbase	300	255	0.68	0.93	-27%	1.55	in all cases, the load applied at one third of the cell height.
sand passing No.4	300	255	0.55	0.90	-38.8%	1.63	
river sand	300	255	0.43	0.69	-36%	1.71	
Sand clay	300	255	0.47	0.44	+7%	1.67	

Table (4-6): Comparison of the resistance observed and those calculated by horizontal shear method for cell with (b/H)=1.0

soil type	H mm	b mm	resistance KN/m		difference %	Factor 0f safety	remark
			observed	calculated			
subbase	300	300	0.83	1.08	-23%	1.88	in all cases, the load applied at one third of the cell height.
sand passing No.4	300	300	0.76	1.04	-24%	1.81	
river sand	300	300	0.61	0.81	-24%	1.97	
Sand clay	300	300	0.60	0.52	16%	2.11	

Table (4-7): Comparison of the resistance observed and those calculated by horizontal shear method for cell with (D/H) =0.15

soil type	H mm	b mm	resistance KN/m		difference %	Factor 0f safety	remark
			observed	calculated			
subbase	300	225	0.64	0.86	-25%	1.2	in all cases, the load applied at one third of the cell height.
sand passing No.4	300	225	0.63	0.81	-22%	1.23	
river sand	300	225	0.42	0.62	-32%	1.36	
Sand clay	300	225	0.5	0.4	25%	1	

Table (4-8): Comparison of the resistance observed and those calculated by horizontal shear method for cell with (D/H) =0.3

soil type	H mm	b mm	resistance KN/m		difference %	Factor 0f safety	remark
			observed	calculated			
subbase	300	225	0.68	0.90	-24.5%	1.3	in all cases, the load applied at one third of the cell height.
sand passing No.4	300	225	0.71	0.92	-23%	1.25	
river sand	300	225	0.57	0.69	-17.3%	1.22	
Sand clay	300	225	0.64	0.455	40.6%	0.95	

Table (4-9): Comparison of the resistance observed and those calculated by horizontal shear method for cell with (D/H) =0.45

soil type	H mm	b mm	resistance KN/m		difference %	Factor 0f safety	remark
			observed	calculated			
subbase	300	225	0.715	0.99	-27.7%	1.6	in all cases, the load applied at one third of the cell height.
sand passing No.4	300	225	0.79	1	-21%	1.3	
river sand	300	225	0.607	0.75	-19%	1.23	
Sand clay	300	225	0.67	0.49	37%	0.99	

4.10: Reliability of Results by Statistical Analysis

The results that obtained from experimental tests represent the relation between the deformations that occurred after applied load and the embedment depth, beginning from D/H = 0, 0.15, 0.30 and 0.45 the depth is measured from the ground surface. The tables (4-10), (4-11), (4-12) and (4-13) shows the relation between these variables.

Table (4-10): Effect of embedment depth on deformation for cell filled with subbase

D/H (%)	Load Failure (KN)	Deformation (mm)
0	0.261	3.411
0.15	0.27	3.282
0.30	0.285	3.21
0.45	0.3103	3.852

Table (4-11): Effect of embedment depth on deformation for cell filled with sand passing sieve No.4

D/H (%)	Load Failure (KN)	Deformation (mm)
0	0.201	5.11
0.15	0.261	3.299
0.30	0.304	2.706
0.45	0.3304	2.42

Table (4-12): Effect of embedment depth on deformation for cell filled with river sand

D/H (%)	Load Failure (KN)	Deformation (mm)
0.15	0.176	3.71
0.30	0.181	3.521
0.45	0.241	2.923
0.15	0.255	2.71

Table (4-13): Effect of embedment depth on deformation for cell filled with clay

D/H (%)	Load Failure (KN)	Deformation (mm)
0.15	0.191	5.106
0.30	0.213	4.512
0.45	0.271	3.626
0.15	0.312	3.426

Then, the results in table (4-10) above using in statistica nonlinear estimation by using Statistica software to create equation deal with three variables are (D) , (F) and (δ), embedment depth , load failure and deformation respectively. At the first, the regression models have the following form as follows:

dependent variable = expression including independent variables

$$\triangle = C_1F - C_2D + C_3 \qquad (4\text{-}8)$$

the equation (4-8) represents the first specify a regression models and loss function, on the left side of the equation specify the dependent variable, represents by the deformation (△), on the right side specify the expression including independent variables; embedment depth (D) and load failure (F), and parameter (C_1 (unitless), C_2 (unitlss), C_3 (mm/KN)) to be estimated. The maximum number of iteration is used equal to (1000) and convergence criterion equal to(0.000001). The table (4-14) shows the functions and parameters that obtained from statistica nonlinear estimation, in addition, squared regression (R^2) and variance explained (V). Table (4-15) gives comparison between the observed and predicted values of deformation.

Table (4-14): Estimation of functions and parameters for subbase soil

Equations	Parameters			variance explained (V) %	square regression (R^2) %
	C_1	C_2	C_3		
△=C_1F-D^2	12.498	0	0	48.95	69.96
△ =C_1F-C_2SIN(D)+C_3	9.612	0.341	0.838	52.41	72.34
△ =C_1SIN(F)^2+C_2COS(D)^2	28.142	1.358	0	53.69	73.27
△ =C_1F-C_2SIN(D)	12.634	0.592	0	61.32	78.35
△ = C_2D^2- C_1SIN(F)^2 +C_3	134.92	19.70	12.34	68.04	82.48
△ = C_3- C_1SIN(F)-C_2COS(D)	82.189	42.79	67.41	75.68	86.99
△ =C_2√D-C_1F+C_3	21.843	0.817	8.993	87.086	93.33
△ =-C_1COS√F-C_2√D+C_3	164.64	1.174	165.2	88.61	94.13
△ =C_1TAN(F) ^{2}-C_2D/2	47.502	4.941	0	90.76	95.27
△ =C_1SIN(F)^2-C_2D-C_3	82.70	4.009	2.068	96.48	98.22
△ =C_1[TAN(4F)]^3-C_1D-C_3	0.059	1.693	-3.118	99.57	99.78
△ =C_1 [TAN(4*F)]^4-C_2D+C_3	0.016	1.42	3.273	99.80	99.90
△ =C_1[4LOG(4F)]^4-C_2D+C_3	1.646	1.073	3.415	99.89	99.95

Table (4-15): Comparison between the observed and predicted values of deformation for subbase soil.

N0.	Observed values (mm)	Predicted values, D (mm)						
		δ for Equ.1	δ for Equ.2	δ for Equ.3	δ for Equ.4	δ for Equ.5	δ for Equ.6	δ for Equ.7
1	3.411	3.261	3.231	3.232	3.316	3.359	3.400	3.296
2	3.282	3.352	3.326	3.330	3.336	3.188	3.167	3.416
3	3.210	3.472	3.471	3.464	3.439	3.451	3.412	3.219
4	3.852	3.675	3.7I6	3.725	3.677	3.754	3.773	3.822

Predicted values, D (mm)					
δ for Equ.8	δ for Equ.9	δ for Equ.10	δ for Equ.11	δ for Equ.12	δ for Equ.13
3.433	3.388	3.438	3.422	3.419	3.416
3.176	3.267	3.213	3.256	3.264	3.269
3.332	3.336	3.265	3.226	3.220	3.217
3.812	3.772	3.837	3.849	3.850	3.851

then, It is clear from the table (4-14) the best function is in the thirteen raw, where the raw is shaded in red colour. and this function has a good squared regression (R^2) equal to 99.95 % and variance explained (V) equal to 99.89 % if comparison with other function is done, so the table (4-15) gives a good predicted values of deformation; therefore, these functions will be depending it in the design of cellular cofferdam and soil material for cell filled is subbase. And so on the function in the final form is:

△=1.64[4LOG (4F)] ^4-1.07D+3.41 (4-9)

The whole previous works as well as the data that used in statistica nonlinear estimation and the final equation were be found for the cells filled with subbase, to return to table (4-11) to treatment these data and create function dependent on embedment depth and soil material; soil in this case is sand passing sieve No.4.

At the first checking the function (4-9), however, use this equation by means of the data in table (4-11), the results can be summarized in the table (4-16)

Table (4-16): Estimation of functions and parameters for sand passing sieve No.4 soil

Equations	Parameters			variance explained (V) %	square regression (R^2) %
	C1	C2	C3		
$\triangle = C_1[4LOG(4F)]^4 - C_2D + C_3$	0.019	3.024	3.703	99.67	99.83
$\triangle = C_1[2LOG(2F))^2 - C_2D + C_3$	0.237	2.118	3.175	99.827	99.913
$\triangle = C_1[LOG(2F)]^2 - C_2D + C_3$	0.951	2.118	3.175	99.827	99.913
$\triangle = C_1[TAN(2F)]^2 + C_2*D + C_3$	-10.14	6.31	5.717	99.995	99.997
$\triangle = C_1[SIN(2F)]^2 + C_2D + C_3$	-10.74	1.66	5.718	99.999	99.999

It can be seen from the table (4-16) the function that used with subbase soil, equation (4-9) is a good function with sand passing sieve No.4 soil but if this

equation is modified it will be obtained more confidence function and it represents in the raw has red color in table (4-16), and the function has a good squared regression (R^2) which is equal to 99.999 % and variance explained (V) equal to 99.999 %. The formulation of this function is:

$$\triangle = C_1[SIN(2F)]^2 + C_2D + C_3 \quad (4\text{-}10)$$

then, substitute the parameters that getting from table (4-16) in equation (4-11) to obtain final form for sand soil:

$$\triangle = -10.74[SIN(2F)]^2 + 1.66D + 5.71 \quad (4\text{-}11)$$

the table (4-17) shows the predicted values of (△) for the data that concerning with sand soil, the column has red color represents the predicted values is very close if it is compared with the column has green color which it represents the observed values.

Table (4-17): Comparison between the observed and predicted values for deformation.

N0.	Observed values (mm)	Predicted values, D (mm)				
		δ for Equ.1	δ for Equ.2	δ for Equ.3	δ for Equ.4	δ for Equ.5
1	5.110	5.110	5.112	5.112	5.108	5.110
2	3.299	3.249	3.260	3.260	3.306	3.296
3	2.706	2.803	2.776	2.776	2.695	2.710
4	2.420	2.371	2.386	2.386	2.424	2.418

After formulation of subbase and sand by functions, these functions is taked and checked with sand river which is using the equation (4-9) for the first case and using the equation (4-11) for the two case for the data in table (4-11), and the results of nonlinear estimation in this case represented by equations

which is shown in table (4-17). Therefore, the best square regression (R^2) equal to 99.999 % and the variance explained (V) equal to 99.999 %.

Table (4-18): Estimation of functions and parameters for river sand soil

Equations	Parameters			variance explained (V) %	square regression (R^2) %
	C_1	C_2	C_3		
△ =C_1 [4LOG(4F)]^4-C_2D+C_3	5.624	2.987	0	76.442	87.431
△ =C_1[4*LOG(4F)]^4-C_2D+C_3	-9.113	3.925	0	94.733	97.331
△ =C_1SIN(F)-C_2COS(D)	-6.768	-4.83	0	97.663	98.824
△ =C_1[4LOG(4F)]^4-C_2D+C_3	0.131	1.134	3.252	98.640	99.318
△=C]SIN(2F)^2+C_2COS(2D)^2+ C_3	-6.237	0.348	4.044	98.884	99.440
△=C_1[TAN(2F)])^2+C_2D+C_3	-3.452	0.870	4.158	99.726	99.863
△ =C_1[LOG(2F)]^2-C_2]D+C_3	0.920	0.918	2.707	99.999	99.999

The seven raw in the table (4-18) shows good function for the river sand; this function is as follows:

△ =C1[LOG (2F)] ^2-C2D+C3 (4-12)

If the parameters (C_1, C_2, C_3) are substituted, the final function will be obtained the following form:

△ =0.92[LOG (2F)] ^2-0.91D+2.7 (4-13)

Table (4-19) shows predicted values of (△) for the data that concerning with river sand.

Table (4-19): Comparisons between the observed and predicted values for deformation.

N0.	Observed values (mm)	Predicted values, D (mm)							
		δ for Equ.1	δ for Equ.2	δ for Equ.3	δ for Equ.4	δ for Equ.5	δ for Equ.6	δ for Equ.7	δ for Equ.8
1	3.71	3.656	3.646	3.649	3.762	3.650	3.692	3.696	3.710
2	3.521	3.431	3.542	3.562	3.447	3.579	3.532	3.531	3.521
3	2.923	3.243	3.063	3.003	2.911	2.941	2.952	2.943	2.923
4	2.71	2.494	2.603	2.646	2.741	2.692	2.686	2.692	2.71

After obtaining the final function for subbase at function (4-9), sand passing sieve No.4 at function (4-11) and river sand soil at function (4-13), using these functions for checking the deformation that concerning with model has fill clay soil as shown in table (4-20).

Table (4-20): Estimation of functions and parameters for clay soil

Equations	Parameters			variance explained (V) %	square regression (R^2) %
	C_1	C_2	C_3		
△ =C_1 [SIN (2F)] ^2-C_2D+C_3	0.238	4.062	5.026	95.301	97.622
△ =C_1[4LOG(4F)]^4-C_2D+C_3	0.204	3.631	4.875	97.108	98.543
△ =C_1[4LOG(4F)]^4-C_2D+C_3	3.198	1.303	2.073	99.088	99.543
△ =C_1 [LOG(2F)]^2-C_2√D+C_3	1.976	0.518	3.263	99.225	99.612
△ =C_1[LOG(2F)]^4-C_2√D+C_3	2.541	0.773	2.933	99.952	99.976

Then, from table (4-20) noted the best function has more proportion of variance, which square regression (R^2) equal to 99.976 % and variance explained (V) equal to 99.952 % and has a good parameters values (C1, C2, C3); therefore, choice the function in the five raw that shaded by light red color takes the following form:

△=C_1[LOG (2F)] ^4-C_2√D+C_3 **(4-14)**

After substitute the parameters in the equation above are:

△=2.541[LOG (2F)] ^4-0.773√D+2.933 **(4-15)**

The table (4-21) represents the comparison between observed and predicted deformation values. Then, the five column in this table has an approximated magnitude which is equal to observed value.

Table (4-21): comparison between the observed and predicted values for deformation.

N0.	Observed values (mm)	Predicted values, D (mm)				
		δ for Equ.1	δ for Equ.2	δ for Equ.3	δ for Equ.4	δ for Equ.5
1	5.106	5.059	5.150	5.035	5.093	5.112
2	4.512	4.458	4.364	4.598	4.501	4.504
3	3.626	3.871	3.787	3.664	3.720	3.606
4	3.426	3.280	3.367	3.371	3.354	3.446